FAST kinase domain-containing protein 1 in mitochondrial function, cell death and cardiovascular disease

---

A Dissertation Presented to

The Faculty of the Graduate School

At the University of Missouri

In Partial Fulfillment

Of the Requirement for the Degree

Doctor of Philosophy

By

Kurt Daniel Marshall

Dr. Christopher P. Baines, Thesis Supervisor

July 2016

The undersigned, appointed by the dean of the Graduate School have examined the dissertation entitled

FAST kinase domain-containing protein 1 in mitochondrial function, cell death and cardiovascular disease

Presented by Kurt Daniel Marshall

A candidate for the degree of doctor of philosophy
And hereby certify that, in their opinion, it is worthy of acceptance

_____
Christopher P. Baines, PhD

_____
Douglas K. Bowles, PhD

_____
Salman Hyder, PhD

_____
Maike Krenz, MD

Acknowledgements

I would like to thank my mentor, Dr. Christopher Baines, for his support throughout my time here at the University of Missouri. His insistence on producing high quality science using multiple experimental models has made me a better scientist. Without his help, support and guidance, this project would not have been possible and I would not be writing this dissertation today.

I would also like to thank the members of my committee, Drs. Douglas Bowles, Salman Hyder and Maike Krenz. Their support and input has guided this project and me.

I would also like to thank the members of the Baines and Krenz labs both past and present. From bouncing ideas off one another to technical discussions, your support has been immeasurable. Without you, I would never have been able to complete the work required to finish this project.

Finally, I would like to thank my wife Jenni for her patience and support throughout my studies. Without her, I never would have made it.

Table of Contents

List of Figures

Abbreviations

ANT, adenine nucleotide translocase

APAF -1, apoptotic peptidase activating factor 1

Atg, autophagy related protein

ATP, adenosine triphosphate

βGal, β-galactosidase

BAK, BCL-2-like protein 4

BAX, BCL-2 homologous antagonist/killer

BCL-2, B-cell lymphoma 2

BCL-X_L, B-cell lymphoma-extra large

cIAP1/cIAP2, cellular inhibitor of apoptosis proteins

CCCP, carbonylcyanide m-chlorophenylhydrazone

CONsi, control siRNA

CYLD, cylindromatosis

CypD, cyclophilin-D

$\Delta\Psi_m$, mitochondrial transmembrane potential

DISC, death-inducing signaling complex

DNA, deoxyribonucleic acid

Drp1, dynamin-related protein 1

ETC, electron transport chain

FADD, Fas-associated protein with death domain

$FADH_2$, flavin adenine dinucleotide

FasL, Fas ligand

FASTK, Fas-activated Serine/Threonine Kinase

FASTKD1, Fas-activated serine/threonine phosphoprotein kinase domain-containing protein 1

FASTKD2, Fas-activated serine/threonine phosphoprotein kinase domain-containing protein 2

FASTKD3, Fas-activated serine/threonine phosphoprotein kinase domain-containing protein 3

FASTKD4, Fas-activated serine/threonine phosphoprotein kinase domain-containing protein 4

FASTKD5, Fas-activated serine/threonine phosphoprotein kinase domain-containing protein 5

FUNDC1, FUN14 domain containing protein 1

GAPDH, glyceraldehyde 3-phosphate dehydrogenase

GTP, guanasine triphosphate

GLUD1, glutamate dehydrogenase 1

GSH, glutathione

GSK-3β, glycogen synthase kinase-3β

H_2O_2, hydrogen peroxide

hFis1, human mitochondrial fission protein 1

LC3, microtubule-associated protein light chain 3

LVFWR, left ventricular free wall rupture

mdivi-1, mitochondrial division inhibitor 1

MEF, mouse embryonic fibroblast

MI, myocardial infarction

Mff, mitochondrial fission factor

MFN, mitofusin

MLKL, mixed lineage kinase domain-like

MMP, matrix metalloproteinase

MnSOD, Mn-superoxide dismutase

MOMP, mitochondrial outer membrane permeabolization

MPT, mitochondrial permeability transition

mtDNA, mitochondrial DNA

NADH, nicotinamide adenine dinucleotide

NIX, BCL-2/adenovirus E1B interacting protein 3-like

NOX4, NADPH Oxidase 4

NRVM, neonatal rat ventricular myocytes

O_2, oxygen

O_2^-, superoxide

OPA1, optic atrophy-1

OSCP, oligomycin sensitivity conferral protein

P53, tumor protein p53

PGAM5, phosphoglycerate mutase family member 5

PINK1, PTEN-induced putative kinase 1

PiC, mitochondrial phosphate carrier

PIPs, phosphatidylinositides

Prx3, peroxiredoxin-3

Reg3β, regenerating islet-derived protein III beta

RIP, receptor interacting protein

RNA, ribonucleic acid

ROS, reactive oxygen species

SOD, superoxide dismutase

SPG7, spastic paraplegia 7

TGFβ, transforming growth factor β

TIA-1, t-cell intracellular antigen

TMRE, tetramethylrhodamine

TNFα, tumor necrosis factor - alpha

TNFR, tumor necrosis factor - alpha receptor

TRADD, TNFR1-associated death domain protein

TRAF2/5, TNFR-associated factor 2/5

Trx2, thioredoxin-2

VDAC, voltage dependent anion channel

VPS34, vacuolar protein sorting-associated protein 34

FAST kinase domain-containing protein 1 in mitochondrial function, cell death and cardiovascular disease

Kurt D. Marshall

Dr. Christopher P. Baines, Thesis Supervisor

Abstract

Cell death occurs during myriad circumstances and varied physiological and pathological conditions. Identifying novel modulators of cell death pathways is crucial to understanding and controlling cell death. Therefore, we explored and identified Fas-activated serine/threonine phosphoprotein kinase domain-containing protein 1 (FASTKD1) as a novel modulator of cell death via its interaction with the known mitochondrial permeability transition (MPT) pore sensitizer, Cyclophilin D (CypD). In Aim 1, data indicate that FASTKD1 protects cells from oxidative stress-induced cell death. This protection is independent of the MPT pore, CypD and modulation of cellular antioxidant capacity. FASTKD1 is also shown to be a potent modulator of mitochondrial morphology. In Aim 2, we show that cardiac myocyte specific overexpression of FASTKD1 *in vivo* protects mice from myocardial infarction induced left ventricular free wall rupture. This protection is associated with modulation of inflammatory cell recruitment and extracellular matrix composition. Taken together, these data indicate that FASTKD1 presents a novel target for modulation of oxidative stress induced cell death and post-myocardial infarction healing.

Chapter 1: Introduction

This dissertation is focused on the mitochondrial protein, Fas-activated Serine/Threonine Kinase Domain Containing Protein 1 (FASTKD1). We initially identified this protein as a potential modulator of mitochondrial cell death pathways, and translated these findings to an *in vivo* model. Therefore, cell death pathways, mitochondrial function and Myocardial Infarction (MI) will be covered in this chapter.

1. Mechanisms of Cell Death

Cells die for a variety of reasons and under myriad circumstances. Cells are thought to undergo three major forms of regulated cell death: apoptosis, autophagy, and necrosis. While these three mechanisms of cell death progress via distinct mechanisms, there is crosstalk and overlap between the three modalities of regulated cell death [1]. Mechanisms of regulated cell death will be discussed in this section of the introduction.

1.1 Apoptosis

Apoptosis was first described as having different morphologic features than necrosis in 1972 by Kerr et al [2]. Apoptosis was originally characterized by the presence of small "spheroid or ovoid cytoplasmic fragments" some of which contained condensed chromatin and was recognized to occur under both physiological and pathological conditions [2]. Since its initial description, the role of apoptosis as a mechanism of cell death has been extensively characterized. Currently, apoptosis is defined by

condensation of the nucleus, caspase activation and membrane blebbing/fragmentation followed by phagocytosis by nearby cells [3]. Apoptosis is considered a "clean" form of cell death in which the immune system is not activated [4]. Two molecular pathways are known to lead to apoptotic cell death: the intrinsic and extrinsic apoptotic pathways [1,3,5,6]. These pathways require either an internal or an external stimulus, respectively, and converge at multiple points including the effector caspases 3 and 7 [3].

The intrinsic apoptotic pathway is initiated by signals from within the cell and was classically described in *caenordabditis elegens* during development [3]. In mammals, the intrinsic pathway can be activated by cellular insults leading to mitochondrial outer membrane permeabilization (MOMP) by B-cell lymphoma 2 (BCL-2) protein family members and release of apoptotic factors including cytochrome c [3,7]. The proteins BCL-2-like protein 4 (BAX) and BCL-2 homologous antagonist/killer (BAK) are critical to MOMP in a process distinct from mitochondrial permeability transition (MPT), which will be discussed later in this chapter [8-10]. However BAX and BAK have been implicated in the rupture of the outer mitochondrial membrane following MPT pore opening [9]. Cytochrome c then binds to apoptotic peptidase activating factor 1 (APAF-1), resulting in pro-caspase-9 binding and activation in an adenosine triphosphate (ATP) dependent process [11,12]. Oligomerized structures of these proteins comprising the apoptosome then cleave and activate pro-caspases 3 and 7 [13].

Extrinsic apoptosis is triggered by signaling from outside the cell and is classically mediated by tumor necrosis factor α (TNFα), Fas ligand (FasL) or transforming growth factor β (TGFβ) binding to their respective receptors resulting in the formation of the multi-protein death-inducing signaling complex (DISC) [3]. At this point, procaspase-8 is

activated which can cleave and activate procaspase-3 or act on BCL-2 family proteins [3]. Caspases are proteolytic enzymes that can mediate apoptosis and are responsible for orchestrating the complex series of events that make up apoptosis [14]. Upon caspase activation, a coordinated deconstruction of the cell begins including translational shutdown, golgi and endoplasmic reticulum fragmentation, chromatin cleavage and cytoskeletal changes [14].

These processes can occur during development or during pathological processes in many tissues including the heart, kidney and brain [15-17].

1.2 Autophagy

Autophagy, or "self eating", is a process by which organelles and cytosolic components are engulfed by membranes and subjected to degradation [1]. Physiologically, autophagy takes place during times of energy starvation, removes damaged organelles, protein aggregates and intracellular pathogens [7]. This process utilizes lysosomes to "recycle" cellular material in either a general mechanism or by targeting specific organelles [7]. Autophagy can be both protective and detrimental; with its over activation resulting in cell death [18]. Autophagy is observed in cells dying from a variety of insults and during certain instances its inhibition can protect cells from death [1]. It has been shown that reactive oxygen species (ROS) play a critical role in autophagy dependent cell death as ROS scavengers can limit this form of cell death [19]. Recently, an autophagy dependent mechanism of cell death termed autosis was characterized [20]. Autosis is characterized by the absence of other cell death mechanisms (apoptosis, necroptosis), morphological features including enhanced cell adherence, fragmentation and eventual

loss of the endoplasmic reticulum and nuclear membrane involution followed by swelling of the perinuclear space and dependence on the sodium-potassium ATPase [13]. This form of cell death takes place both *in vitro* and *in vivo* [13].

In the case of either autophagic mechanism, an extension of intracellular membranes is initiated by recruitment of the kinase vacuolar protein sorting-associated protein 34 (VPS34) that converts phosphatidylinositol to phosphatidylinositol 3-phosphate in a Beclin-1 dependent manner. This results in the formation of a double membrane structure called the initiation complex, which contains a variety of autophagy related (Atg) proteins [7,8,13,21]. Next, this membrane is elongated, isolating any enclosed cytosolic components. This process utilizes the conjugation of the protein Atg5 to Atg12 and the conversion of microtubule-associated protein light chain 3-I (LC3-I) to LC3-II via the conjugation of phosphatidylethanolamine [22]. Eventually, this autophagosome fuses with a lysosome forming an autolysosome, and the enclosed contents are degraded [7].

In a specific form of autophagy, dubbed mitophagy, mitochondria are specifically targeted and degraded by the autophagic machinery [23,24]. The mitochondrial outer membrane proteins BCL-2/adenovirus E1B interacting protein 3-like (NIX) and FUN14 domain containing protein 1 (FUNDC1) are known to interact with autophagic machinery including LC3 to induce mitophagy of mitochondria [25]. The Ubiquitin ligase Parkin and the mitochondrial serine/threonine-protein kinase PTEN-induced putative kinase 1 (Pink1) are involved in targeting mitochondria for degradation [25-27]. In damaged mitochondria, Pink1 is stabilized on the outer mitochondrial membrane, which results in Parkin recruitment to the mitochondria [28,29]. In addition to Pink1, Parkin also ubiquitinates the GTPases mitofusins (Mfn) 1 and 2, leading to mitochondrial

fragmentation, discussed later, which is a process that is important for mitophagy [29]. Mfn-2 is known to be the receptor for Parkin on damaged mitochondria and targets them for degradation [30]. Low levels of ROS that are not sufficient to damage cells have also been shown to initiate the culling of damaged mitochondria in a process requiring Dynamin related protein 1 (Drp-1) mediated mitochondrial fragmentation [31].

Autophagy presents an interesting case in which mild activation can be protective, whereas over activation can lead to irreversible cell damage and eventual death.

1.3 Programmed Necrosis

In contrast to apoptosis and autophagy, necrosis was once thought of as a random uncontrolled form of cell death. However, research has established that necrosis can proceed via a controlled and varied series of events. The most studied and defined molecular necrotic pathway is traditionally mediated by signaling via the TNFR through receptor interacting proteins (RIPs) 1 and 3 and subsequently the pseudokinase mixed lineage kinase-like (MLKL) and is called necroptosis [32-34].

The pro-inflammatory cytokine TNFα plays an important role in inducing cell death [34,35]. In response to TNFα stimulation, TNFR recruits proteins to the plasma membrane [32,34,35]. When TNFR trimerizes in response to ligand binding, TNFR1-associated death domain protein (TRADD) is recruited to the cytoplasmic domain of this receptor [36]. The TNFR/TRADD complex then recruits RIP1 and TNFR-associated factor 2/5 (TRAF2/5) to the plasma membrane [37-40]. Next, cellular inhibitor of apoptosis proteins (cIAP1/cIAP2) are recruited to the TNFR which are involved in inhibition of RIP1 and RIP3 signaling [41]. Together with the TNFR, this assemblage of proteins is known as

complex I, and is responsible for signaling a variety of cell behaviors including proliferation and survival[32]. Complex I can transition from a membrane associated protein assembly to the cytosol. This cytosolic collection of proteins is known as complex IIa and in place of TNFR from complex I contains caspase 8 and adaptor protein FADD [32,34]. Formation of complex IIa can yield two cell fates, apoptosis or necrosis, and when caspase 8 is inhibited, necrosis prevails.

Through the interaction of RIP1 and RIP3, necroptotic signaling is induced [42-44]. RIP1 and RIP3 comprise the necrosome, on which the remainder of this section will be focused. Post-translational modifications of RIP1 and RIP3 are crucial steps for the initiation of necrosome formation and signaling [42-44]. Initially, cylindromatosis (CYLD) a deubiquinase has been shown to deubiquinate RIP1 after complex I dissociates from the TNFR and facilitate necrosome signaling (Moquin et al., 2013). This deubiquitination activates RIP1 so that it can bind to and phosphorylate RIP3. This activates RIP3, whose kinase activity is required for necroptotic signaling [42,43,45]. RIP3 then phosphorylates the pseudokinase mixed lineage kinase domain-like protein (MLKL) that is essential for RIP1/RIP3-dependent necroptosis [46-48]. However, at this point the sequence of events downstream of RIP1/RIP3/MLKL that ultimately lead to cell rupture becomes muddled.

The interaction of RIP3 with MLKL has been reported to induce translocation of the RIP1/RIP3/MLKL complex to the mitochondrial membrane as TNFα induced necroptosis results in enriched levels of RIP1/RIP3/MLKL in the mitochondrial associated membrane fraction of cells [49]. Upon translocation to the mitochondria, the necrosome interacts with and activates the mitochondrial phosphatase phosphoglycerate mutase family member 5

(PGAM5) [50], resulting in mitochondrial fragmentation in a Drp1 manner [50]. However recent work indicates that necroptosis can occur independently of PGAM5 [51].

Recent studies have emerged indicating that MLKL may bypass the mitochondria altogether, instead translocating to the plasma membrane upon homo-oligomerization [49,52], where MLKL complexes then induce either calcium [52] or sodium [49] overload of the cell. However, new studies from Wang's and Vandenabeele's groups have demonstrated that MLKL can bind to phosphatidylinositides (PIPs) and can directly permeabilize liposomes containing these phospholipids [53,54]. A recent study by Green's group indicated that mitochondria are entirely dispensable for necroptosis used cells depleted of mitochondria via the induction of mitophagy by the uncoupler carbonylcyanide m-chlorophenylhydrazone (CCCP) [55]. This study demonstrated that although TNFα-induced ROS was lost in the absence of mitochondria, necroptosis was still very much functional. However, a recent study showed mitochondria are involved in necroptosis [56].

2. The Mitochondrial Permeability Transition Pore

The mitochondrial permeability transition (MPT) pore is a large conductance, non-specific pore in the inner mitochondrial membrane [57]. Calcium overload and ROS among other triggers are known to induce opening of the MPT pore [58,59]. Upon opening, the MPT pore allows ions and metabolites to flow down their concentration gradients, dissipating the mitochondrial transmembrane potential ($\Delta\Psi_m$) and ceasing mitochondrial ATP production [60,61]. In addition, the mitochondria swell, disrupting the architecture of the cristae and further impairing mitochondrial function [57]. This detrimental process has

been shown to be involved in mediating cell death and dysfunction in a variety of pathological states including: ischemia/reperfusion injury in a variety of organs [62-65], diabetic cardiomyopathy [66], doxorubicin cardiotoxicity [67], and muscular dystrophy [68,69]. Thus there is a need to understand the molecular makeup of the MPT pore and the proteins that regulate it.

2.1 Proposed Molecular Componentry

Many proteins have been hypothesized to compose the channel forming unit of the MPT pore including the voltage dependent anion channel (VDAC), adenine nucleotide translocase (ANT) and the mitochondrial phosphate carrier (PiC), but they have either been ruled out completely as a MPT pore component or shown to have a more regulatory function [70-73]. However, multiple recent studies have hypothesized that the pore may in fact be composed of either subunits or dimers of the ATP synthase [74-77]. Until this discovery, the only agreed upon component of the MPT pore was the mitochondrial matrix protein, Cyclophilin D (CypD). Although not the pore itself, CypD is known to sensitize the MPT pore to calcium induced opening [63,65,78,79]. Other proteins have been hypothesized to modulate the MPT pore as well. Some of this modulation is thought to be due to direct post-translational modification of CypD. For example, cysteine-203 of CypD undergoes S-nitrosylation, and this promotes MPT in response to oxidative stress [80]. A fraction of the glycogen synthase kinase-3β (GSK-3β) pool is thought to translocate to the mitochondria where it also acts as a positive MPT pore regulator in response to oxidative stress, possibly through phosphorylation of CypD [81,82]. The tumor suppressor tumor protein p53 (p53) has also been proposed to trigger MPT by interacting with

CypD, however the mechanism by which this protein translocates to the mitochondria remains unclear [83]. Identification of novel MPT pore modulatory proteins is more crucial than ever, as inhibiting ATP synthase function *in vivo* is most likely not a viable therapeutic option.

Currently, it is thought that the MPT pore is composed of either subunits or dimers of the mitochondrial F_1F_0 APT synthase [57]. Importantly, the MPT pore sensitizer, CypD, has been shown to interact with the oligomycin sensitive subunit (OSCP) of ATP synthase [74]. Dimers of APT synthase have been proposed to form a calcium sensitive channel [74,76]. In addition to dimers of ATP synthase, it has been proposed that the c-subunit of ATP synthase can form the mitochondrial permeability transition pore [77]. In this model, the MPT pore itself is formed by the c-subunit containing F_0 component of ATP synthase, while the major regulatory components of the MPT pore are located on the F_1 subunit of ATP synthase. However, it has recently been proposed that mitochondrial protein spastic paraplegia 7 (SPG7) is a core component of the MPT pore [84]. This study used an *in vitro* approach to knock down and later completely deplete proteins of interest and test the sensitivity of cells to ROS and calcium induced MPT. However, the main finding of this study has already been called into question because cells lacking SPG7 were still able to undergo MPT, indicating the presence of a functional pore [85].

2.2 Mechanism of Action

Mitochondria act as a major calcium sink in the cell, and can take up excess cytosolic calcium via the recently identified calcium uniporter [86]. Under conditions including high

levels of ROS, matrix calcium, adenine nucleotide depletion or high pH, the MPT pore can open in the inner-mitochondrial membrane [57]. Upon accumulation of high levels of calcium, or ROS in the presence of calcium, a pore of about 2.3 nm in diameter can open in the inner-mitochondrial membrane in a process that can be reversed by the chelation of calcium [87-89]. Decreasing mitochondrial matrix ROS with a mitochondrially targeted antioxidant can decrease MPT pore opening and cell death in the context of ischemia-reperfusion injury [58]. An important aspect of MPT mediated cell death is mitochondrial swelling and rupture. This process is mediated by the proteins BAX/BAK on the outer mitochondrial membrane, as cells lacking BAX/BAK are more resistant to mitochondrial swelling and necrotic cell death [9].

It has also been hypothesized that the MPT pore can function in a physiological role in contrast to its role in pathological cell death [57]. Mice lacking the MPT pore sensitizer CypD are more sensitive to pressure overload than their wild type counterparts [90]. These mice had elevated levels of mitochondrial matrix calcium, and decreased calcium efflux. It has been shown that asynchronous opening of the MPT pore is important for low levels of ROS production in the heart that is important for cardioprotection [91]. Pharmacological inhibition of the MPT pore is sufficient to inhibit the cardioprotective effects of ROS in model of ischemia-reperfusion injury [92]. These studies indicate that the MPT pore may play an important role in normal mitochondrial calcium homeostasis and physiological mitochondrial ROS production.

The MPT pore may also provide a link to necroptosis. Genetic experiments where a critical regulator of the MPT pore, CypD, was knocked out revealed a role for the MPT pore primarily in necrotic cell death as opposed to apoptosis [63,65,78]. TNFα-induced

necroptosis was found to be partially attenuated by the loss of CypD in mouse embryonic fibroblasts [43,56]. Similarly, TNFα-induced zebrafish macrophage ROS production and necrosis was blocked by the CypD inhibitor alisporivir [93]. In the myocardium, protection against ischemia/reperfusion by the RIP1 inhibitor necrostatin was not additive to that conferred by CypD ablation, also suggesting that the two components were part of the same genetic pathway [94].

However, whether the MPT pore plays a role in necroptosis has also been questioned. Specifically, the embryonic lethality caused by caspase-8 deletion, and is due to RIP3-dependent necroptosis [95], cannot be rescued by CypD ablation [55]. Similarly, necroptosis in caspase-8 deficient macrophages could be blocked by depletion of RIP1 and RIP3 but not by depletion of CypD [96]. Finally, a recent paper examining ischemia/reperfusion injury in the kidney found that ablation of RIP3 and CypD was protective but that double knockout mice exhibited even greater protection [97], suggesting that the necrosome and the MPT pore are distinct.

3. Mitochondrial Dynamics

Mitochondria are dynamic organelles that are constantly undergoing fission and fusion to maintain their function and cellular homeostasis, with fission resulting in a fragmented mitochondrial morphology and fusion causing an elongated mitochondrial morphology [98]. The processes of mitochondrial fission and fusion have been shown to be involved in processes ranging from cell death to control of the cell cycle and maintenance

of mitochondrial function [99-101]. Mitochondrial dynamics are critical for cellular function and will be discussed in the following section.

3.1 Molecular Mechanisms of Mitochondrial Fission and Fusion

Mitochondrial fission and fusion are accomplished by a set of pro-fusion and pro-fission proteins dispersed between the mitochondria and cytosol. Mitochondrial fusion is accomplished by the profusion proteins optic atrophy-1 (OPA-1), mfn1 and mfn2. Mitochondrial fission is primarily accomplished by the proteins Drp-1 and human mitochondrial fission protein 1 (hFis1) [98]. These proteins work together to maintain mitochondrial morphology, function and meet metabolic demands.

Mfn1 and Mfn2 are guanosine triphosphate (GTP) -ases that anchor to the outer mitochondrial membrane via c-terminal transmembrane domains [98]. These pro-fusion proteins were first identified in mammalian cells in 2001 and were shown to be regulators of mitochondrial fusion [102]. In this initial study, it was shown that Mfn1 and Mfn2 are GTPases that target to the mitochondria, whose catalytic activity is important for their function. Overexpression of Mfn2 was shown to result in hyper-fused mitochondrial architecture. Further studies revealed that Mfn1 and Mfn2 are required for normal embryonic development and form homotypic and heterotypic interactions [26,27]. In fact, the deletion of either Mfn1 or Mfn2 is embryonically lethal [27]. These early studies investigating the role of Mfn1 and Mfn2 in mammalian mitochondrial biology indicated that the two mitofusin proteins have distinct but redundant functions yet both are required for normal development. Interestingly, while cells deficient for both Mfn proteins showed normal levels of mitochondrial deoxyribonucleic acid (DNA) and coupled

respiration, the same individual cells contained both functional and abnormal mitochondria [27]. There is also a critical role for mitochondrial fusion in normal cellular division and function. During cell division, mitochondria are known to be fragmented at G_2/M, phase, and this is mediated by degradation of Mfn-1 [103].

Similar to the outer mitochondrial membrane, the inner mitochondrial membrane is home to a GTPase involved in the maintenance of mitochondrial morphology. OPA-1 is a GTPase that is anchored to the mitochondrial inner membrane that protrudes into the inner membrane space [28]. OPA-1 is critically involved in mitochondrial dynamics as its siRNA mediated knockdown results in mitochondrial fragmentation and apoptosis [28]. While Mfn1 and Mfn2 are necessary for mitochondrial outer-membrane fusion, OPA-1 is required for mitochondrial inner membrane fusion. Knockout of OPA-1 results in large mitochondria with one outer membrane surrounding a number of inner membrane enclosed vesicles [104]. Also of note, maintenance of the mitochondrial membrane potential ($\Delta\Psi_m$) is required for proper OPA-1 function, as treatment of cells with a mitochondrial uncoupler limits inner mitochondrial membrane fusion due to proteolytic cleavage of OPA-1. A large molecular weight OPA-1 (L-OPA-1) is cleaved to a small molecular weight OPA-1 (S-OPA-1) isoform, resulting in mitochondrial fragmentation in a process that can be rescued by overexpression of L-OPA-1 [24].

In addition to defects in mitochondrial fusion machinery, mitochondrial fission can be regulated by its own set of specific proteins. Drp-1 is a cytosolic GTPase that is critical for mitochondrial fission. Upon post-translational modification, Drp-1 translocates to the mitochondria where it can act to induce mitochondrial fission [105]. Upon recruitment to the outer mitochondrial membrane, Drp-1 monomers self-assemble to form large

oligomeric structures that mediate mitochondrial fission through a GTPase dependent mechanism [105]. In yeast, the mitochondrial outer membrane protein, hFis-1, is required for the recruitment of Drp-1 from the cytosol to the mitochondria, but this is not the case in mammals, which instead utilize mitochondrial fission factor (Mff) as the Drp-1 receptor on the outer mitochondrial membrane [106]. Similar to the mitochondrial fusion associated GTPases Mfn-1 and Mfn-2, Drp-1 is required for normal development, as its deletion results in embryonic lethality [107]. Drp-1 can be inhibited by the compound mitochondrial division inhibitor 1 (mdivi-1), which acts by stabilizing Drp-1 in a non-oligomeric form, preventing its aggregation and action [108].

Clearly, mitochondrial fission and fusion are important processes for the development and maintenance of cells and their functions. Mitochondrial dynamics are also involved in cell death, and this function will be discussed in the following section.

3.2 Mitochondrial Dynamics and Cell Death

As discussed earlier, it is evident that mitochondria are critically involved in cell death. Mitochondrial fission and fusion have been noted accompanying cell death [109]. Mitochondrial morphology and changes therein are known to be involved in apoptosis, MPT and necroptosis and these processes will be discussed below.

During apoptosis, Drp-1 translocates from the cytosol to the outer mitochondrial membrane where it facilitates permeabilization of the outer mitochondrial membrane by BAX/BAK [110]. This process is actually independent of Drp-1's GTPase activity [111]. Of note, the mitochondrial outer membrane can rupture during apoptosis without Drp-1, however, the absence of this important fission protein results in a slowed rate of

cytochrome c release [107]. SiRNA mediated silencing of Drp-1 yields cells that are less susceptible to apoptosis and contain mitochondria exhibiting an elongated phenotype [112]. An important part of apoptosis is DNA fragmentation; depletion of Drp-1 results in decreased DNA fragmentation in apoptotic cells [99]. In addition to Drp-1, the GTPases Mfn-1 and Mfn-2 play a role in apoptosis. Silencing of Mfn-1 and Mfn-2 results in increased susceptibility of cells to apoptotic stimuli, and results in fragmented mitochondrial morphology [112]. Fusion of the inner mitochondrial membrane is also involved in apoptosis. In addition to its effects on mitochondrial morphology, siRNA mediated knockdown of OPA-1 results in apoptosis in HeLa cells [28]. Conversely, overexpression of OPA-1 can protect cells from multiple inducers of apoptosis in a process independent of Mfn-1 and Mfn-2 [113]. Cells lacking Mfn-1 and Mfn-2 contain fragmented mitochondria, and overexpression of OPA-1 did not alter this phenotype, indicating that the cytoprotective effects of OPA-1 are independent of its effects on mitochondrial morphology. Taken together, these data indicate that in addition to their role in regulating mitochondrial morphology, mitochondrial fission and fusion machinery are involved in apoptosis.

Drp-1 was shown to have an important role in mediating necroptosis. Wang et al. showed that the mitochondrial phosphatase PGAM5 recruited Drp-1 to the mitochondria, activated it via dephosphorylation, which resulted in necroptosis [50]. However, the role of the mitochondrial PGAM5-Drp1 axis has also been questioned by several recent studies. Silencing of PGAM5 was found to have no effect on necroptosis induced by TNFα or RIP3 dimerization in a variety of cell lines [46,55,114]. Similar results have been obtained

when Drp-1 was either silenced or knocked out [114,115]. Taken together, these data call into question Drp-1's role in necroptosis.

The mitochondrial fusion proteins Mfn-1 and Mfn-2 are also known to be involved in cell death. While possessing fragmented mitochondria, cells lacking either Mfn-1 or Mfn-2 are not grossly dysfunctional [100]. However, in this same study, it was shown that cells lacking both Mfn-1 and Mfn-2 exhibited defects in $\Delta\Psi_m$, mitochondrial respiration and cell growth [100]. Based on the data showing that inhibition of mitochondrial fission protects cells against death, one would expect any manipulation that limits mitochondrial fusion to sensitize cells to death. Heart specific deletion of Mfn-1 confers resistance to myocytes against ROS induced MPT pore opening [116]. As seen in myocytes from Mfn-1 knock out mice, specific myocyte Mfn-2 deletion delays calcium induced MPT pore opening [117].

Taken together, it is clear that both mitochondrial dynamics and the molecular machinery of this process are involved in cell death. It is interesting to note that inhibition of both mitochondrial fission and fusion can modulate cell death. Additionally, it may not be changes in mitochondrial morphology that mediate all of the cytoprotective effects of altering mitochondrial dynamics, as Drp-1's pro-death properties seem to be independent from its GTPase activity.

4. Fas-activated Serine/Threonine Kinase

The Fas-activated Serine/Threonine Kinase (FASTK) family of proteins consists of its founding member, FASTK, and five additional proteins, FASTKD1-FASTKD5 [118].

The five FASTKD proteins all share two FAST domains, a ribonucleic acid (RNA) binding domain and an N-terminal mitochondrial targeting sequence. This family of proteins has a broad range of functions that will be discussed in the following section.

4.1 Mechanism of Action and Signaling

Tian et al. first identified FASTK, in 1995 [119]. In this initial study, FASTK was identified as a novel T-cell intracellular antigen (TIA-1) interacting protein, and dubbed a kinase because it contained a domain related to the kinase domain of the herpes simplex virus ICP10 gene. This kinase activity was confirmed using a cell free system with TIA-1 as a target. During Fas-mediated apoptosis, FASTK is dephosphorylated, and then associates with TIA-1, which becomes phosphorylated. However, FASTK mediated phosphorylation of TIA-1 was never shown directly *in vivo*. It took almost a decade before research provided more insight into FASTK signaling. In non-apoptotic cells, FATSK is tethered to the mitochondrial outer membrane where it interacts with B-cell lymphoma-extra large (BCL-X_L) [120]. At this same time, it was also reported that FASTK overexpression inhibits whereas knockdown of FASTK increases apoptosis to a variety of stimuli [121]. FASTK was shown to act as an antagonist of TIA-1 in response to apoptotic stimuli, limiting the decrease in translation of anti-apoptotic proteins normally associated with apoptosis [121]. In addition to its role in regulating apoptotic protein translation, FASTK is also known to modulate alternative splicing of certain genes in the nucleus [122]. Interestingly, FASTK actually promotes apoptosis via its involvement in the alternative splicing of a pro-apoptotic form of the Fas receptor [123]. This finding runs counter to the commonly held idea that FASTK is an anti-apoptotic protein. FASTK is

also hypothesized to bind RNA [124]. In accordance with its hypothesized RNA binding ability, it was recently shown that FASTK can translocate to the mitochondria where it is required for the processing of a mitochondrial mRNA [125]. Finally, FASTK is also known to be a pro-inflammatory protein involved in neutrophil recruitment [126]. FASTK performs a plethora of roles in multiple cellular compartments and its physiological roles will continue to be elucidated.

4.2 FAST Kinase Family Members

The roles of the other five members of the FASTK family have only recently been explored, and little is known of their functions in both physiology and pathology. There have been very few studies investigating the roles of FASTKD1-5 in health and disease. Besides its mitochondrial localization and RNA binding ability, FASTKD1 is up regulated in aspirates from endometrial carcinoma [118,124,127]. Additionally, enhanced expression of FASTKD1 expression in lymphoblastic leukemia is associated with a poor disease prognosis [128]. A nonsense mutation in FASTKD2 is associated with a mitochondrial encephalomyopathy involving mitochondrial respiratory chain complex IV defects [129]. Recently, along with two helicases, FASTKD2 was implicated in mitochondrial ribosome assembly [130]. As with FASTK, another member of this protein family is associated with cell death. In addition to its role in mitochondrial ribosome assembly, FASTKD2 is also a pro-apoptotic protein involved in triggering death in breast cancer cells [131]. FASTKD3 localizes to the mitochondria where it interacts with respiratory chain and translational machinery and is required for mitochondrial respiration [118]. FASTKD4 localizes to the mitochondria where it interacts with

mitochondrial mRNAs and prevents their degradation [132]. The final member of the FASTK family of proteins is FASTKD5. It was only recently ascribed a role in the processing of mitochondrial mRNAs[130]. It is only in the last few years that the FASTK family of proteins received limited attention. It is clear that the FASTK family of proteins plays critical roles in the cell. Further efforts need to be made to better understand this family of proteins and their diverse and important actions.

5. Oxidative Stress and the Mitochondria

Mitochondria are the powerhouses of the cell and generate ATP via the electron transport chain (ETC). The ETC is also a major source of ROS production and mitochondria contain a well developed antioxidant system to handle this stressor [133]. This section will focus on the generation and elimination of ROS in the mitochondria and the physiological implications of this process especially in the context of cell death.

5.1 Mitochondrial Respiration and the Production/Elimination of Oxidative Stress

A discussion of mitochondrial ROS generation must include at least a brief description of the mitochondrial respiratory chain and its actions. The electron donors nicotinamide adenine dinucleotide (NADH) and flavin adenine dinucleotide ($FADH_2$) are produced by the Krebs cycle, which takes place in the mitochondrial matrix. Upon donation to the ETC, electrons are passed sequentially down the ETC by complexes I-IV, and this energy is used to pump protons out of the mitochondrial matrix to generate the proton motive force and to create an electrical gradient across the inner-mitochondrial

membrane (IMM)[134]. This separation of charges and ions forms the force required for the F_1F_0-ATP synthase to form ATP from ADP [133]. The components of the mitochondrial respiratory chain and their roles in ROS production will be discussed in the following paragraphs.

Complex I, or NADH dehydrogenase, binds NADH, is reduced, and then pumps four protons from the mitochondrial matrix into the inner membrane space and transfers its two donated electrons to ubiquinone forming ubiquinol [135,136]. This respiratory chain complex contains subunits encoded by both the nuclear and mitochondrial genomes [134]. Of note, Complex I of the respiratory chain has been hypothesized to be involved in MPT in tissues with low levels of CypD expression [137]. Here the authors showed that the Complex I inhibitor, rotenone, is able to inhibit MPT in a phosphate dependent mechanism. Next, the electron is passed to Complex II, or succinate dehydrogenase, which can also act as the initial electron receptor when succinate is acting as the electron donor resulting in the reduction of FAD [135,138]. Complex II transfers electrons to ubiquinone in a process that does not result in the pumping of protons out of the mitochondrial matrix [135]. Complex II subunits are encoded by nuclear genes and this enzyme is also involved in the Krebs cycle [134]. Complex III, or cytochrome c oxidoreductase, receives electrons from ubiquinol, and in the process oxidizes it to ubiquinone, resulting in the pumping of two protons from the mitochondrial matrix to the inner membrane space [135]. Complex III donates its electrons to cytochrome c, reducing this protein [134]. Finally, electrons are passed to Complex IV, or cytochrome c oxidase, which passes the electrons to the final electron acceptor, oxygen, and pumps four protons out of the mitochondrial matrix into the inner membrane space [135]. All of these redox

reactions provide the energy for Complex V of the respiratory chain, or F_1F_0-ATP synthase to form ATP.

In addition to its central role in ATP production, the mitochondrial ETC is also a major source of ROS, and this will be discussed later. In fact, complexes I – IV of the mitochondrial respiratory chain are capable of producing ROS under various conditions [139]. Mitochondrial ROS production, elimination and the role of these processes in cell death will be described in this section.

Under physiological conditions, Complex I of the ETC is a major source of ROS production through three primary mechanisms [139]. Complex I can generate ROS during both forward and reverse electron flow. In the first mechanism, flavin mononucleotide in Complex I that is reduced by donor electrons is capable of reducing oxygen (O_2) to Superoxide (O_2^-), the major type of ROS generated by Complex I [140]. Secondly, Complex I is capable of incomplete reduction of ubiquinone to an ubisemiquinone radical which can then result in reduction of O_2 to O_2^- [141-143]. Finally, Complex I contains 8 iron-sulfur clusters that are critical for enzymatic function, however, electrons can "leak" during this process and reduce O_2 to O_2^- [139].

While not as significant a contributor mitochondrial ROS production as Complex I or Complex III, Complex II of the mitochondrial respiratory chain is also capable of ROS production. Two mechanisms are responsible for the O_2^- produced by Complex II. In the first mechanism, reduced FAD auto-oxidizes from $FADH_2$ to $FADH^-$ which can auto-oxidize again [139]. This was shown by inhibiting electron transfer from Complex II to Complex III, resulting in the accumulation of electrons in Complex II and O_2^- production [138]. Like Complex I, Complex II reduces ubiquinone. Complex II can incompletely

reduce ubiquinone to ubisemiquinone and result in ROS production when its structure is altered [139,144].

Complex III of the mitochondrial respiratory chain is a major source of endogenous ROS production in the cell primarily through the oxidation of ubiquinol to ubiquinone [139]. ROS production can occur primarily at two points during this process. Complex III accepts electrons from ubiquinol and transfers one electron to the Rieske iron-sulfur protein, which in turn reduces cytochrome c. However, during this process, an unstable semiquinone is generated that can produce O_2^- because it is highly unstable and can reduce O_2 [139]. The second potential sites of O_2^- production are the heme groups located in Complex III. If it does not spontaneously oxidize, the semiquinone formed by Complex III donates one electron to a heme group, which then reduces another heme group, and it is during this process that O_2 can be reduced to O_2^- [139].

It has recently been shown that Complex IV of the mitochondrial respiratory chain is also a source of oxidative stress in the cell. Under physiological conditions, electron leakage from Complex IV is minimal [139]. However, during ischemia, Protein Kinase A (PKA) phosphorylates Complex IV, resulting in electron leakage and reduction of O_2 to O_2^- [145]. This final finding implicates Complexes I-IV of the mitochondrial respiratory chain in ROS generation.

ROS generation in the mitochondria is not limited to the ETC. Indeed, there are additional sources of ROS production in the mitochondria. While the ETC primarily generates ROS on the IMM, proteins on the outer-mitochondrial membrane (OMM) are also capable of ROS production. Monoamine oxidases A and B are enzymes present on the OMM that deaminate neurotransmitters and other amines generating hydrogen

peroxide (H_2O_2) as a byproduct of their reaction [146]. NADPH Oxidase 4 (NOX4) is also present in the mitochondrial matrix and can produce H_2O_2 [147].

In addition to its remarkable ROS generating abilities, mitochondria contain an extensive and well-developed anti-oxidant system to remove these potentially harmful substances. O_2 that has been reduced to highly reactive O_2^- is converted to less reactive H_2O_2 by CuZn-Superoxide dismutase (SOD) in the inner membrane space or Mn-SOD in the mitochondrial matrix [148]. O_2^- is also able to leave the mitochondrial inner membrane space via the voltage dependent anion channel (VDAC) [149]. H_2O_2 then either diffuses out of the mitochondria through the membrane or via aquaporins, or is further detoxified in the mitochondrial matrix [148,150]. In the mitochondrial matrix, H_2O_2 can be converted to H_2O and O_2 by catalase, which can be detected in the mitochondria [151]. Additionally, H_2O_2 can be detoxified to H_2O by the peroxiredoxin system or the thioredoxin system [148]. Interestingly, excess antioxidant capacity can also be harmful, as the reducing capacity of these enzymes can induce cellular damage [152]. The mitochondrial antioxidant system is an efficient mechanism for the elimination of ROS.

5.2 The Consequences of Excessive Mitochondrial Oxidative Stress

Mitochondrial oxidative stress has been implicated in mediating cell damage and even death through a variety of mechanisms under various pathological conditions. Under physiological conditions, O_2^- is rapidly dismutated to H_2O_2, which is known to have a physiological function as a pro-survival signaling molecule [153,154]. In the mitochondria, excessive ROS can have dire consequences not just for organelle function, but also for cellular survival. Overproduction of mitochondrial ROS can severely

damage mitochondria by inactivating ETC proteins, exhausting antioxidant enzymes, damaging mitochondrial DNA (mtDNA) and peroxidizing lipids [139].

Excessive mitochondrial ROS production can initiate apoptosis. Multiple perturbations of mitochondria by ROS are known to result in apoptosis. First, depletion of the mitochondrial pool of glutathione (GSH) is a known prerequisite for initiation of mitochondrial apoptotic signaling [155]. Next, oxidative damage to mitochondrial DNA results in increased superoxide production by the mitochondria, which can eventually trigger cytochrome c release and apoptosis [156]. Additionally, oxidation of cardiolipin, a mitochondrial membrane lipid, is critical for release of cytochrome c, a major step in the execution of apoptosis [157].

As discussed previously, the mitochondrial respiratory chain is a major source of ROS. Under basal conditions, low levels of ROS are produced, however this can change upon exposure to stressors. A link between mitochondrial ROS and necroptosis has been proposed. The Complex II and necrosome proteins RIP, TRAFF and Fas-associated protein with death domain (FADD) have been shown to be critical for the accumulation of ROS in TNF signaling [158]. TNF mediated ROS generation has been shown to be dependent on RIP1 and mitochondrially derived in L929 cells [159]. In support of this finding, mitochondrial, but not cytosolic ROS is critical in mediating TNF induced cell death in L929 and RAW 264.7 cells [160]. Studies have indicated that Complex I of the electron transport chain is responsible for the ROS production seen during TNFα-induced necroptosis [161,162]. This coupled with the fact that RIP1, RIP3 and/or MLKL have been reported to translocate to the mitochondrial fraction of cell lysates upon stimulation in a

variety of cell types [44,50,163,164], indicates that ROS production could indeed be a key step in the execution of the necroptotic process.

Additionally, mitochondrial ROS have been proposed as a mediator of MPT pore opening. Early studies showed that in addition to calcium, the MPT pore could be opened by exposure of mitochondria to oxidants [165,166]. Additional evidence supporting this phenomenon comes from studies in which mitochondrially targeted antioxidant treatment partially blocked MPT pore opening [58].

These studies indicate that in addition to damaging mitochondria and altering their function, ROS can trigger multiple mechanisms of cell death including possible activation of necroptosis, initiation of apoptosis and opening of the MPT pore. ROS are produced in the mitochondria by many processes and are implicated in multiple mechanisms of cell damage and death.

6. Myocardial Infarction and Left Ventricular Rupture

Myocardial infarction (MI) is a major cause of death around the world and is characterized pathologically by death of the myocardium due to ischemia [167]. After the cessation of blood flow to a portion of the heart, cells begin to die. Cell death primarily occurs via necrotic mechanisms, however both apoptotic and autophagic cell death are known to occur in the heart following MI [168]. Following MI, the heart undergoes remodeling encompassing myocytes, non-myocytes and the interstitium, which can lead to heart failure and/or other consequences [169]. MI is associated with elevations in myocardial ROS with mitochondrial respiratory chain, including complex IV, being a

potential mitochondrial contributor during ischemia [145]. Elevated ROS during ischemia is also involved in recruitment of immune cells and activation of the inflammatory response [170].

Although increasingly rare in humans in the post-reperfusion era, left ventricular free wall rupture remains an important sequelae to acute MI with a high rate of mortality [171]. Rupture of the left ventricle normally occurs between three and ten days post MI in humans [172]. Whereas in mice, left ventricular free wall rupture (LVFWR) generally occurs from day two to six post-experimental MI, and is highly dependent on mouse strain and sex [173]. Reported rates of ventricular rupture vary widely in the literature based on strain, and even within one strain, with rates of rupture in FVB/N mice ranging from 3% to nearly 60% during the first ten days post MI [173,174].

Following initial occlusion of a coronary artery and onset of tissue ischemia, a complex series of events is initiated. Because the heart has a limited ability to regenerate muscle cells, a scar is formed to replace the lost myocardium [175]. This process functions as a wound healing response and includes many cell types and process [176]. Cell death usually begins in the endocardium, then spreads outward and laterally to encompass the entire area at risk and the epicardium. However in mice, diffusion of oxygen can occur from the lumen sparing the inner part of the endocardium from death [177]. This accumulation of dead cells results in the recruitment of immune cells to the region of tissue injury. Cells dying of necrosis (as is the case for many cells in the ischemic region) release intracellular components that act as “alarmins”, activating the innate immune system [170]. A variety of inflammatory cells are recruited to the site of injury with neutrophils being the initial responders, peaking in their abundance in the border

zone of the infarct 24-48 hours post MI [175,178]. In the case of ischemia-reperfusion injury, these neutrophils are thought to be deleterious, as their depletion results in decreased infarct size [179]. Another major effector of the innate immune system, macrophages, also accumulate in the infarct and border zone. Macrophages reach their peak tissue numbers about four days post injury, but their levels remain elevated in the myocardium for up to four weeks after the initial injury [180]. In addition to their role in clearing necrotic tissue, leukocytes are important mediators of wound healing, release cytokines and growth factors and regulate extracellular matrix homoeostasis post-MI [175]. The initial inflammatory cells in the infarct are known to secrete signals involved in the healing process. Neutrophils and activated T-cells secrete the cytokine oncostatin-m, which causes cardiomyocytes to secrete regenerating islet-derived protein III beta (Reg3β), resulting in the accumulation of macrophages and proper healing and scar formation [181]. After the initial inflammatory phase, myofibroblasts are recruited to the infarct where they reconstruct the heart's collagen network and are critical for scar formation [175,182]. Initially, these fibroblasts secrete matrix-degrading enzymes until dead cells and debris can be removed from the infarct area [170]. Once a stable scar is formed, a majority of the myofibroblasts in the infarct die via apoptosis, leaving a mostly acellular scar behind [170]. In fact, changes in the heart's collagen structure can be detected within 24 hours of MI and it continues to change during infarct healing [183]. There is some cross talk between inflammatory cells and collagen depositing cells. It has been hypothesized that T-cells may regulate collagen deposition in the healing myocardium with their depletion leading to higher rates of ventricular rupture and improper scar formation [184]. It is clear that

myocardial healing after MI is a multifaceted process encompassing multiple cell types and molecular processes.

Aberrations in infarct healing can result in complications such as ventricular rupture. One mechanism known to influence rupture involves the interplay between collagen deposition and collagen degradation, wherein excessive degradation by matrix metalloproteinases (MMPs) and/or decreased deposition can predispose a heart to rupture [180]. The proteinases MMP-2 and MMP-9, which both degrade collagen and are plentiful in the myocardium, are implicated in the process of wound healing and scar formation [180,185]. Changes in cell recruitment to the infarct site can have disastrous implications for scar formation. In the absence of Reg3β, insufficient macrophages are recruited to the damaged myocardium, resulting in insufficient clearance of neutrophils, increased matrix degradation and increased incidence of left ventricular rupture [181]. Additionally, reducing cardiomycyte apoptosis following MI is a powerful tool in decreasing the risk of LVFWR [186]. In fact, strategies that reduce cardiomyocyte death without altering the inflammatory response are effective at preventing LVFWR [187]. Clearly, many factors can lead to improper scar formation in the myocardium from inflammation to matrix degradation to factors secreted by cardiomyocytes.

7. Study Hypothesis and Aims

The overarching hypothesis for the studies described herein is that FASTKD1 represents a novel target for cytoprotection with its overexpression decreasing the susceptibility of cells to ROS induced cell death, and abrogating the effects of MI using

an *in vivo* mouse model. These studies may both be related as MI progression has a ROS component. In Aim 1, we will investigate FASTKD1's potential as a novel cytoprotective target and attempt to identify its mechanism of action. In Aim 2, we will assess the ability of cardiac specific FASTKD1 overexpression to protect the myocardium from experimental MI in a mouse model *in vivo*.

This study has two major aims:

Aim 1: Identify FASTKD1 as a novel cytoprotective target due to its interaction with the MPT pore sensitizer CypD, and assess its ability to modulate this process and cell death.

Hypothesis: Given its ability to bind CypD, we hypothesized that FASTKD1 is a regulator of mitochondrial-dependent cell death and survival.

Rationale: FASTKD1 interacts with a known regulator of the MPT pore and has been shown to localize to the mitochondria. Consequently, we designed this study to test whether FASTKD1 is a positive or negative regulator of the MPT pore, and to which extent FASTKD1 protects cells against oxidative stress-induced death. Employing gain- and loss-of-function approaches in cultured mouse embryonic fibroblasts and neonatal rat cardiomyocytes, we also characterized the role of FASTKD1 for maintaining mitochondrial and/or cellular antioxidant capacity, mitochondrial respiration, and $\Delta\Psi_m$, as well as mitochondrial morphology.

Aim 2: Determine whether cardiac-specific FASTKD1 overexpression protects mice against MI induced cardiac dysfunction.

Hypothesis: Mice overexpressing FASTKD1 will show decreased functional impairment and reduced markers of injury following experimental MI.

Rationale: The pathogenesis of MI is a complex process involving cell death, inflammation and wound healing. Additionally, ROS is known to be elevated during ischemic injury. Therefore, we believe that strategies to reduce cell loss in the face of excess ROS may provide a novel target for reducing MI associated cardiac injury. Overexpression of FASTKD1 may represent a novel mechanism to reduce cardiac injury in response to MI. We have developed an inducible, cardiac-specific FASTKD1 overexpressing mouse to test this hypothesis.

Chaper 2: The Novel Cyclophilin-D Interacting Protein FASTKD1 Protects Cells Against Oxidative Stress-Induced Death

1. Abstract

We identified Fas-activated serine/threonine phosphoprotein kinase domain-containing protein 1 (FASTKD1) as a novel cyclophilin D (CypD) interacting protein. Overexpression of FASTKD1 protected whereas depletion of FASTKD1 sensitized cells to oxidative stress-induced cell death. However, manipulation of FASTKD1 levels did not alter mitochondrial Ca^{2+}-retention capacity nor affect Ca^{2+}-ionophore-induced cell death, indicating that FASTKD1 does not modulate the mitochondrial permeability transition pore. Consistent with this, FASTKD1 still protected CypD-deficient cells against oxidative stress. Additionally, overexpression of FASTKD1 induced mitochondrial fragmentation whereas knockdown of FASTKD1 had the opposite effect. This suggests that FASTKD1 could be part of a novel cytoprotective mechanism.

2. Introduction

Mitochondria sit at the nexus of multiple cell death mechanisms, and are known to be critical mediators of both apoptotic and necrotic cell death [61]. This is nowhere more apparent than in the heart. Following injury, cardiac myocytes are known to die by multiple mechanisms, many of them critically involving mitochondria [15]. However the precise molecular mechanisms by which this occurs are still being defined. Therefore, the goal of the experiments described herein was to identify and then characterize so far unknown mitochondrial modulators of cell death. To accomplish this, we searched for

novel proteins that interact with one of the known regulators of mitochondrial-dependent cell death, cyclophilin D (CypD). CypD regulates the mitochondrial permeability transition (MPT) pore by sensitizing it to calcium-induced opening [63,65,78,79]. Calcium overload and reactive oxygen species (ROS) among other triggers induce opening of the MPT pore [58,59], resulting in dissipation of the mitochondrial transmembrane potential ($\Delta\Psi_m$) [60,61] and subsequent mitochondrial swelling. This detrimental process has been shown to be involved in mediating cell death and dysfunction in a variety of pathological states including: ischemia/reperfusion injury in a variety of organs [62-65], diabetic cardiomyopathy [66], doxorubicin cardiotoxicity [67], and muscular dystrophy [68,69].

Given the critical role of CypD for cell death and survival, we therefore performed a yeast two-hybrid screen with CypD as bait, which led to the identification of Fas-activated serine/threonine phosphoprotein kinase domain containing protein 1 (FASTKD1) as a novel CypD interacting protein. FASTKD1 belongs to a family of 5 mitochondrial proteins, the members of which have been proposed to play roles in apoptosis (FASTKD2), mitochondrial respiration (FASTKD3), and mitochondrial RNA processing (FASTKD4) [118,131,188]. However, other than localizing to the mitochondria [118], nothing is known regarding the specific function of the FASTKD1 isoform.

Given its CypD binding capacity, we hypothesized that FASTKD1 is a regulator of mitochondrial-dependent cell death and survival. Consequently, we designed this study to test whether FASTKD1 is a positive or negative regulator of the MPT pore, and to which extent FASTKD1 protects cells against oxidative stress-induced death. Employing gain- and loss-of-function approaches in cultured mouse embryonic fibroblasts and neonatal rat cardiomyocytes, we also characterized the role of FASTKD1 for maintaining

mitochondrial and/or cellular antioxidant capacity, mitochondrial respiration, and $\Delta\Psi_m$, as well as mitochondrial morphology.

3. Results

3.1 FASTKD1 interacts with CypD and Localizes to the mitochondria

Using a yeast-two hybrid screen we identified 18 known proteins that interacted with the mature form of CypD (Supplementary Table 1). However, of these only one, FASTKD1, has been reported to localize exclusively to the mitochondria [118]. To confirm the interaction between FASTKD1 and CypD, we first generated a Myc-tagged FASTKD1 adenovirus and a FLAG-tagged CypD adenovirus. Infection of NRVMs with the CypD or FASTKD1 viruses alone, or in combination, resulted in a robust expression of the respective protein (**Figure 1A**). FLAG immunoprecipitation from NRVM infected with CypD and/or FASTKD1 resulted in the pull down of the FASTKD1-Myc only in samples co-infected with both the CypD-FLAG and FASTKD1-Myc (**Figure 1B**). Together, these data indicate that FASTKD1 associates with the known mitochondrial cell death modulator CypD.

In order to determine the function of FASTKD1 we overexpressed the FASTKD1-Myc protein in MEFs, which resulted in a robust expression of the FASTKD1 protein (**Figure 1C**). Unfortunately, the Myc antibody also recognized a non-specific band in the β-galactosidase-infected MEFs that ran at the exact same molecular weight as the FASTKD1-Myc (**Figure 1C**). However, this band was not seen in the NRVMs (see **Figure 1A**). To confirm that FASTKD1 localizes to the mitochondria, MEFs were infected with an adenovirus expressing either β-galactosidase or FASTKD1-Myc and

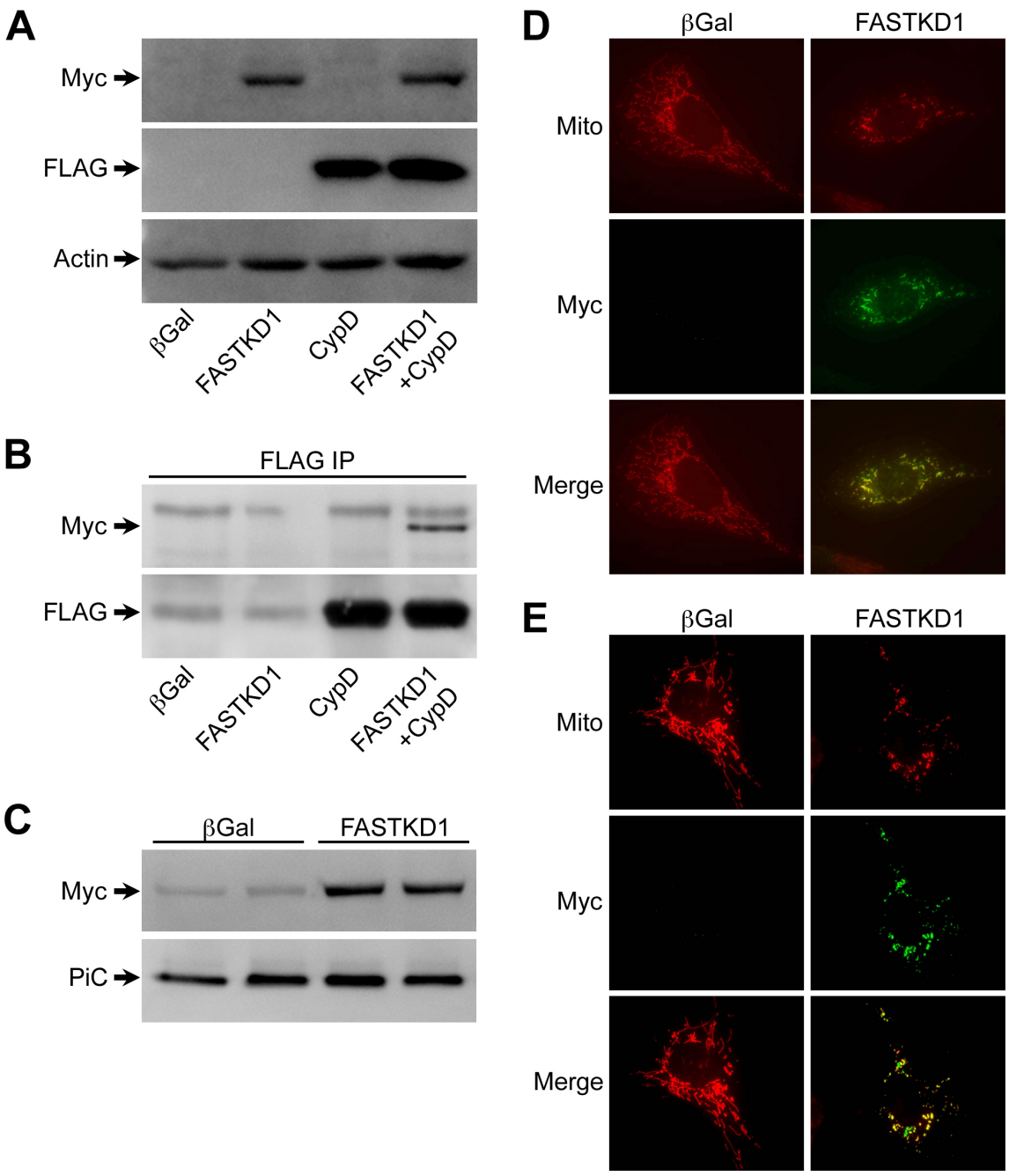

Figure 1. FASTKD1 interacts with the mitochondrial protein cyclophilin-D and localizes to mitochondria. (A) Neonatal rat ventricular myocytes (NRVMs) were infected with β-galactosidase (βGal), FASTKD1-Myc, or cyclophilin-D (CypD)-FLAG adenoviruses for 48 hours and the lysates blotted for either Myc or FLAG. Actin was used as a loading control. (B) NRVMs were infected with βGal, FASTKD1-Myc, CypD-

FLAG, or FASTKD1-Myc plus CypD FLAG adenoviruses for 48 hours. The lysates were then subjected to immunoprecipitation using a FLAG antibody and the resultant complexes blotted for Myc and FLAG. (C) Mouse embryonic fibroblasts (MEFs) were infected with βGal or FASTKD1-Myc for 48 hours and the lysates blotted for Myc. The mitochondrial phosphate carrier (PiC) was used as a loading control. (D) Representative images of immunocytochemistry performed on MEFs infected with either βGal or FASTKD1-Myc adenoviruses and then stained for Myc tag. Mitotracker Red was used to stain mitochondria. (E) Representative images of immunocytochemistry performed on neonatal rat ventricular myocytes (NRVMs) infected with either βGal or FASTKD1-Myc adenoviruses and then stained for Myc tag. Mitotracker Red was used to identify mitochondria.

subjected to immunocytochemistry. The mitochondrial dye Mitotracker Red was used to stain mitochondria while overexpressed FASTKD1 was stained using an anti-Myc antibody. Overlaying the two fluorescences revealed significant overlap, indicating that FASTKD1-Myc was localized to the mitochondria (**Figure 1D**). As in MEFs, we performed immunocytochemistry to confirm that FASTKD1-Myc localizes to the mitochondria in NRVMs (**Figure 1E**). Mitochondria were labeled with the dye, Mitotracker Red, and FASTKD1-Myc was identified with an anti-Myc primary antibody. Both fluorescences showed significant overlap indicating that FASTKD1-Myc localizes to the mitochondria in NRVMs.

3.2 FASTKD1 protects MEFs against oxidative stress-induced cell death

We first wanted to investigate the role of FASTKD1 in oxidative stress-induced cell death, which is CypD-dependent. MEFs expressing β-galactosidase or FASTKD1-Myc adenovirus were treated with increasing concentrations of H_2O_2 for four hours followed by analysis of cell death by Sytox staining. In β-galactosidase-infected cells, H_2O_2 induced a dose-dependent increase in Sytox positive cells (**Figure 2A**). However, the number of dead cells was significantly reduced at all concentrations of H_2O_2 by FASTKD1 overexpression (**Figure 2A**). We next tested the effects of FASTKD1 depletion on H_2O_2-induced death. Because we were not able to detect FASTKD1 with commercially available antibodies, we first confirmed siRNA-mediated knockdown of FASTKD1 using NRVMs expressing FASTKD1-Myc that were also transfected with a mouse specific FASTKD1 siRNA. Western blotting for Myc demonstrated that the FASTKD1 protein was significantly reduced following 48 hours of siRNA treatment

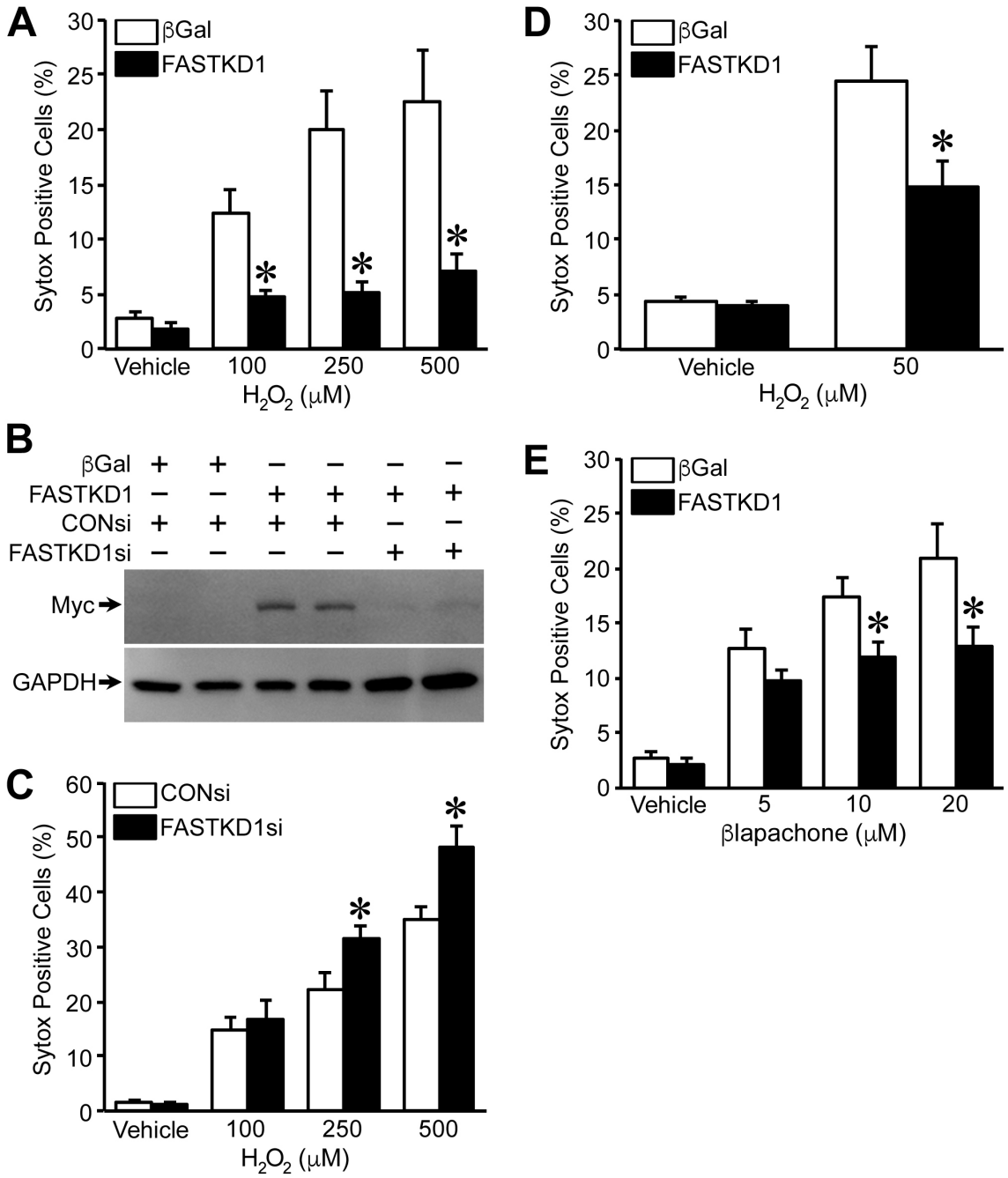

Figure 2. FASTKD1 protects mouse embryonic fibroblasts and neonatal rat myocytes against oxidative stress-induced cell death. (A) Cell death as measured by Sytox staining in β-galactosidase (βGal) or FASTKD1-Myc infected mouse embryonic fibroblasts (MEFs) treated with increasing concentrations of H_2O_2 for 4 hours. (B) Neonatal rat ventricular myocytes (NRVMs) were transfected with 100nM control siRNA

(CONsi) or mouse specific FASTKD1 siRNA (FASTKD1si) followed by infection with βGal or FASTKD1-Myc adenoviruses. The lysates were then blotted for Myc. GAPDH was used as a loading control. (C) Cell death as measured by Sytox staining in control siRNA (CONsi) or FASTKD1 (FASTKD1si) siRNA-transfected MEFs treated with increasing concentrations of H_2O_2 for 4 hours. (D) Cell death as measured by Sytox staining in βGal or FASTKD1-Myc infected NRVMs treated with 50μM H_2O_2 for 1 hour. (E) Cell death as measured by Sytox staining in βGal or FASTKD1-Myc infected MEFs treated with increasing concentrations of β-lapachone for 4 hours. Results are representative of 3-4 independent experiments performed in duplicate. Error bars indicate s.e.m. with $*P<0.05$ vs. βGal or CONsi.

(**Figure 2B**). In contrast to the FASTKD1-overexpressing cells, MEFs transfected with FASTKD1 siRNA exhibited an exacerbation in the degree of H_2O_2-induced cell death at the 250μM and 500μM concentrations (**Figure 2C**). We then examined whether FASTKD1 could also protect against oxidant-induced cell mortality in NRVMs. NRVMs expressing β-galactosidase or FASTKD1-Myc were treated with H_2O_2 for one hour at a concentration of 50μM followed by analysis of cell death by Sytox staining (**Figure 2D**). FASTKD1-Myc overexpression significantly attenuated death in NRVMs compared with β-galactosidase-infected control cells. To confirm that the cytoprotective effect of FASTKD1 was not H_2O_2 specific, β-Lapachone, which induces cell death through ROS production [189,190], was examined (**Figure 2E**). As seen with the H_2O_2, FASTKD1 overexpression significantly protected MEFs from all doses of β-Lapachone tested. Taken together, these results indicate that FASTKD1 protects cells from ROS induced death.

3.3 FASTKD1 does not modulate the MPT pore

We then wanted to determine if FASTKD1 exerts its protective effects via inhibition of the MPT pore. First, Western blotting was performed on cell lysates from MEFs overexpressing β-galactosidase or FASTKD1-Myc adenovirus (**Figure 3A**). Blots were probed for purported MPT pore components and modulators including: PiC, CypD, ANT, and key components of respiratory complexes I, II, and V. There were no significant changes seen at the level of protein expression between control β-galactosidase infected cells and those overexpressing FASTKD1-Myc. Similarly, there were no changes in these proteins in MEFs transfected with either control or FASTKD1 siRNAs (**Figure 3B**).

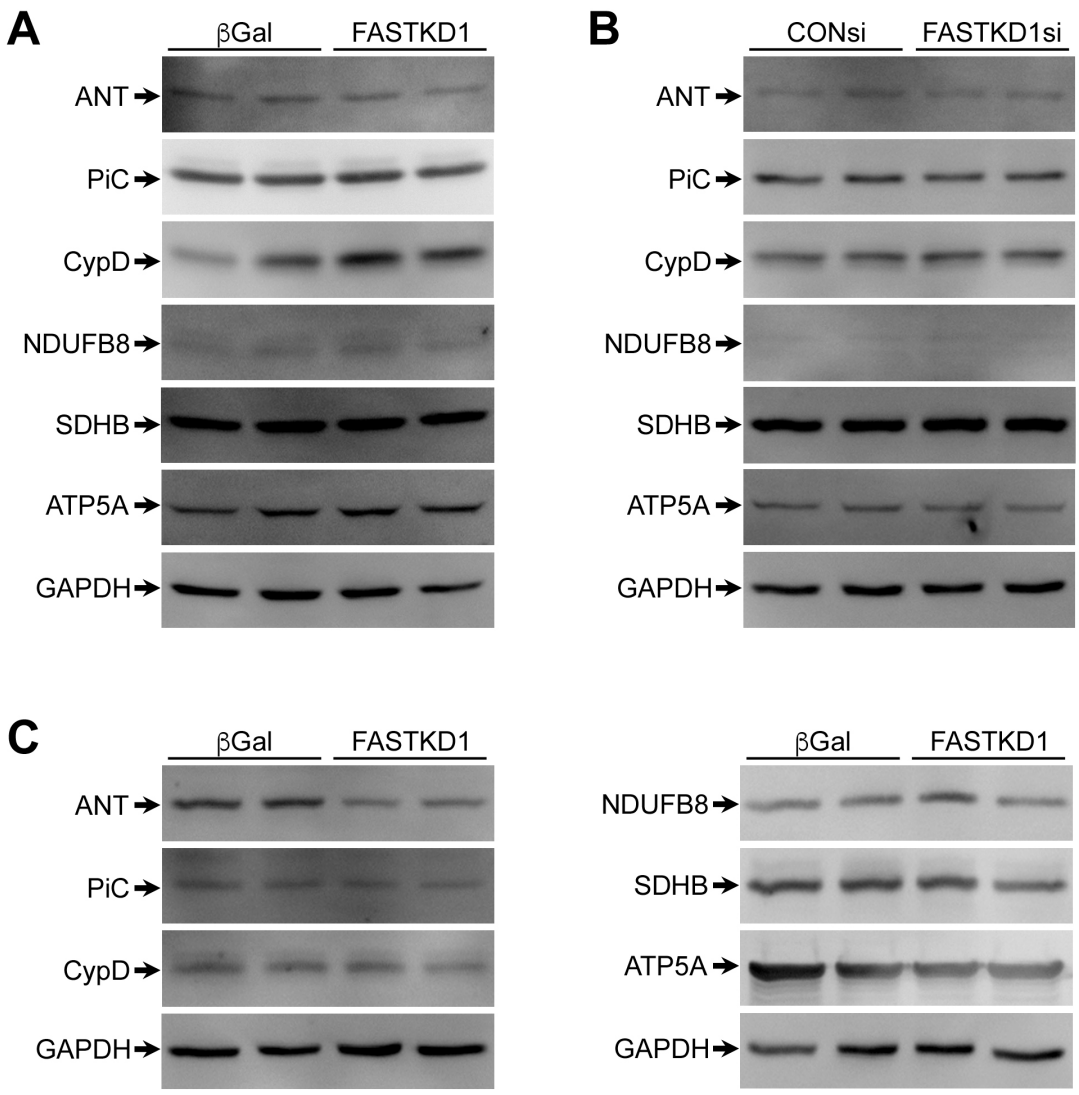

Figure 3. FASTKD1 does not significantly affect expression of mitochondrial permeability transition pore and respiratory chain components. (A) Western blotting for adenine nucleotide translocase (ANT), mitochondrial phosphate carrier (PiC), cyclophilin-D (CypD), NADH dehydrogenase β subcomplex 8 (NDUFB8, complex I), succinate dehydrogenase B (SDHB, complex II), and ATP synthase (ATP5A, complex V) in β-galactosidase (βGal) or FASTKD1-Myc infected mouse embryonic fibroblasts (MEFs). GAPDH was used as a loading control. (B) Western blotting for ANT, PiC, CypD, NDUFB8, SDHB, and ATP5A in control (CONsi) or FASTKD1 (FASTKD1si)

siRNA-transfected MEFs. GAPDH was used as a loading control. (C) Western blotting for ANT, PiC, CypD, NDUFB8, SDHB, and ATP5A in βGal or FASTKD1-Myc infected NRVMs. GAPDH was used as a loading control. Results are representative of 3-4 independent experiments performed in duplicate.

Blotting in NRVMs overexpressing β-galactosidase or FASTKD1-Myc adenovirus also revealed no significant changes in PiC, CypD, and Complex I, II, and V proteins (**Figure 3C**). However, unlike the MEFs, the mitochondrial inner-membrane protein, ANT, was reduced to 0.55 ± 0.05-fold of normal levels in the FASTKD1-Myc overexpressing NRVMs (**Figure 3C**).

To assess MPT, Ca^{2+} retention capacity (CRC) experiments were performed on MEFs overexpressing FASTKD1. **Figure 4A** depicts representative CRC traces from β-galactosidase- and FASTKD1-infected MEFs. Calcium spikes can be monitored by an increase in fluorescence every minute followed by a decrease in fluorescence as the mitochondria take up the Ca^{2+}. Upon opening of the MPT pore, Ca^{2+} is released resulting in a large increase in fluorescence. The total number of Ca^{2+} spikes required to induce pore opening can be used to deduce the CRC of the sample. There was no significant difference in the CRC of β-galactosidase infected cells and those overexpressing FASTKD1-Myc when energized with the complex I substrates glutamate and malate (**Figure 4B**). Similar results were obtained when the mitochondria were energized with the complex II substrate succinate (**Figure 4B**).

To confirm the CRC results, cell death assays were performed in MEFs using the Ca^{2+} ionophore ionomycin to simulate Ca^{2+} overload-induced, MPT-dependent death. MEFs expressing β-galactosidase or FASTKD1-Myc were treated with ionomycin for eighteen hours followed by analysis of cell death using Sytox exclusion dye staining (**Figure 4C**). FASTKD1-Myc overexpression did not protect MEFs from ionomycin induced cell death. Finally, MEFs generated from *Ppif*$^{-/-}$ mice were infected with β-galactosidase or FASTKD1-Myc adenovirus, and treated with increasing doses of H_2O_2

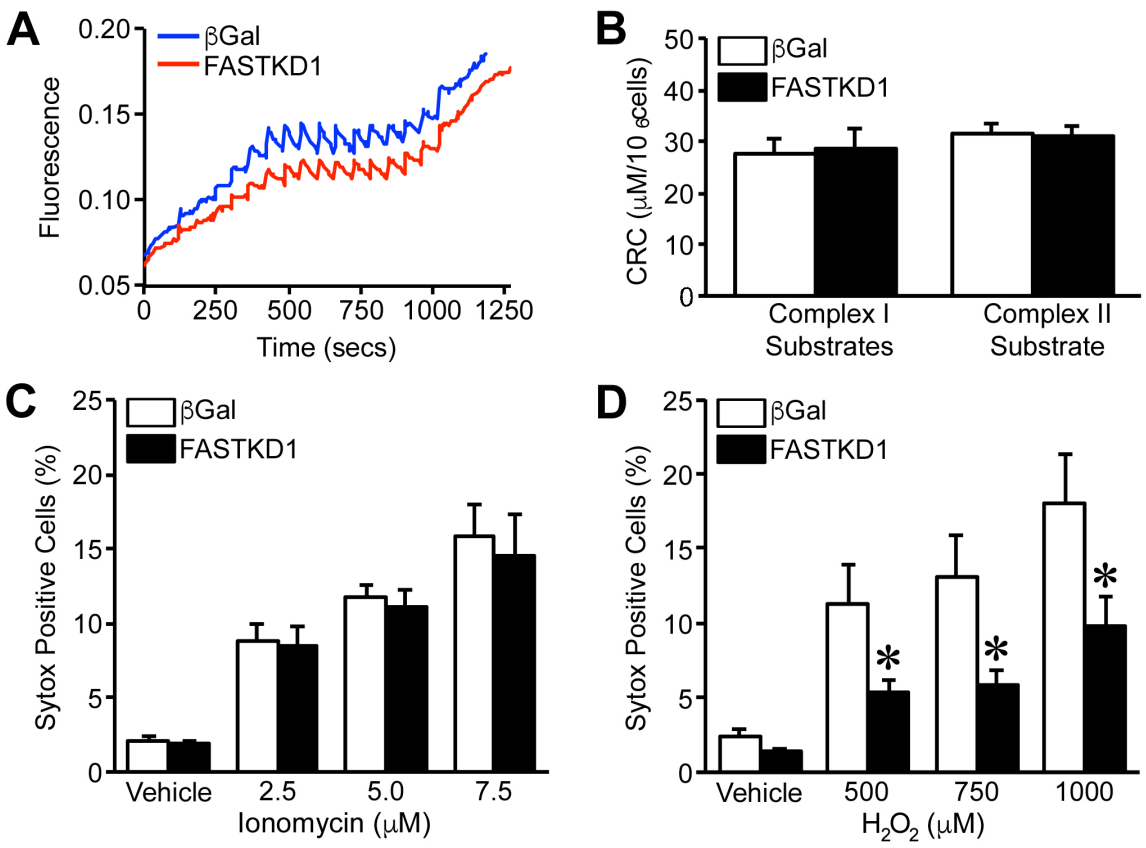

Figure 4. FASTKD1 does not modulate mitochondrial permeability transition. (A). Representative Ca^{2+} retention capacity (CRC) traces from digitonin permeabilized mouse embryonic fibroblasts (MEFs) infected with either β-galactosidase (βGal) or FASTKD1-Myc adenoviruses and exposed to 2.5μM pulses of Ca^{2+}. (B) Quantification of CRC data from βGal or FASTKD1-Myc infected MEFs energized with either the complex I substrates glutamate and malate or the complex II substrate succinate. (C) Cell death as measured by Sytox staining in βGal or FASTKD1-Myc infected MEFs treated with increasing concentrations of ionomycin for 18 hours. (D) Cell death as measured by Sytox staining in βGal or FASTKD1-Myc infected *Ppif*$^{-/-}$ MEFs treated with increasing concentrations of H_2O_2 for 4 hours. Results are representative of 3-4 independent experiments performed in duplicate. Error bars indicate s.e.m. with **P*<0.05 vs. βGal.

for four hours. As *Ppif*$^{-/-}$ MEFs are significantly resistant to H_2O_2-induced death, higher concentrations of H_2O_2 had to be used to generate meaningful levels of cell mortality (**Figure 4D**). However, FASTKD1-Myc overexpression was still able to significantly protect *Ppif*$^{-/-}$ MEFs from H_2O_2 induced cell death, further indicating that FASTKD1's protective effects are independent of the MPT pore.

3.4 FASTKD1 does not alter mitochondrial antioxidant proteins or cellular antioxidant capacity

Because FASTKD1 only protects cells from oxidative stress and not Ca^{2+} overload-induced death, we measured mitochondrial antioxidant protein expression in MEFs both over and underexpressing FASTKD1 and in NRVMs overexpressing FASTKD1. Additionally, we measured total cellular antioxidant capacity and GSH content in MEFs and NRVMs overexpressing FASTKD1. Overexpression of FASTKD1-Myc in MEFs did not alter expression of the mitochondrial antioxidants thioredoxin-2 (Trx2), peroxiredoxin-3 (Prx3), and Mn-superoxide dismutase (MnSOD) (**Figure 5A**). SiRNA-mediated knockdown of FASTKD1 did not alter expression of the same panel of antioxidant proteins either (**Figure 5B**). To assess the ability of cells to remove ROS, we performed a total antioxidant capacity experiment on MEFs overexpressing FASTKD1-Myc (**Figure 5C**). There was no statistically significant difference between cells infected β-galactosidase or FASTKD-Myc adenovirus, indicating that FASTKD1 does not modulate total antioxidant capacity in MEFs. Total GSH content was similarly unaltered (**Figure 5C**). Next, we measured the expression of mitochondrial antioxidant proteins in NRVMs infected with a β-galactosidase control or FASTKD1-Myc

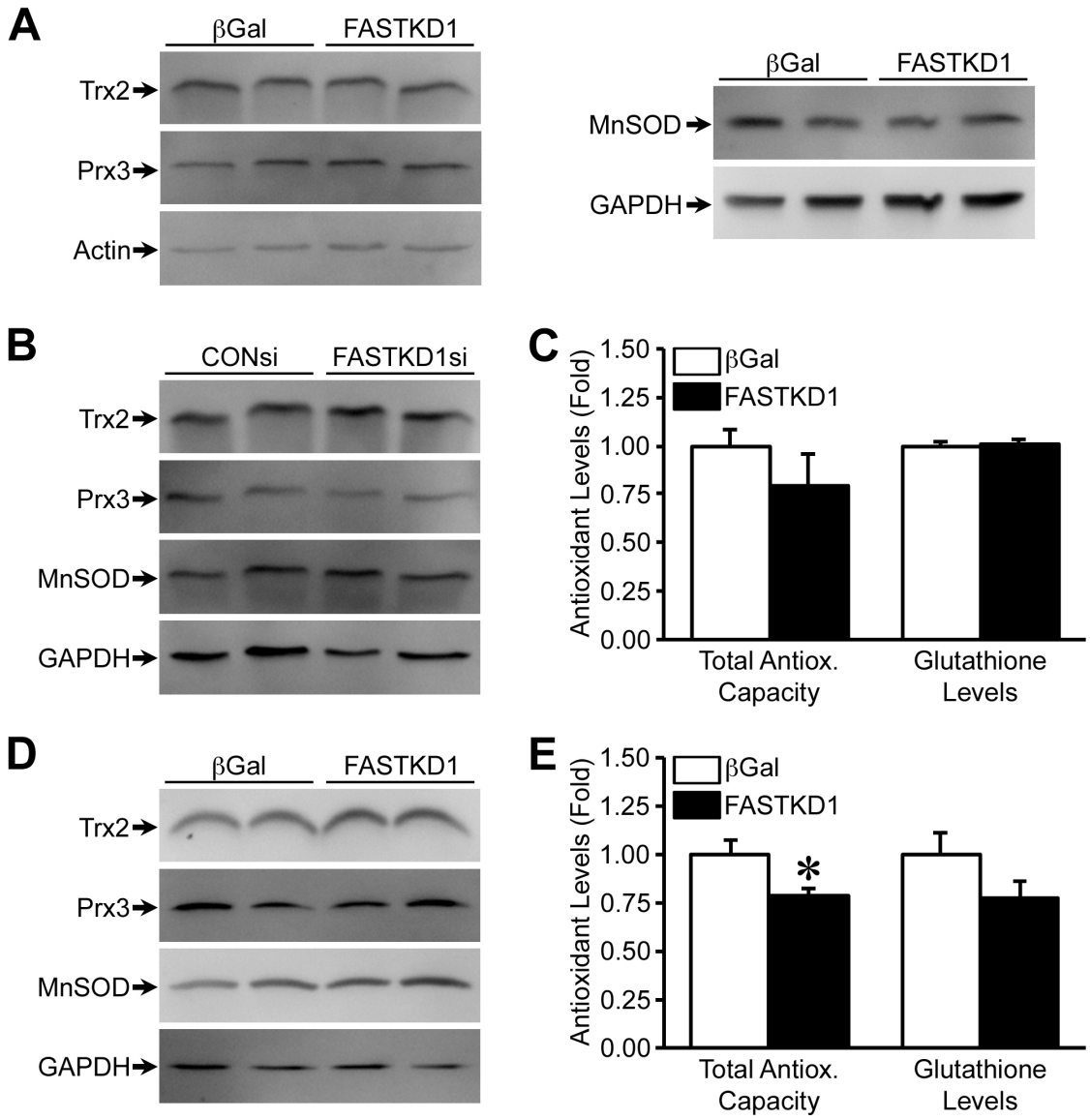

Figure 5. FASTKD1 does not alter mitochondrial antioxidant protein expression or cellular antioxidant capacity. (A) Western blotting for thioredoxin-2 (Trx2), peroxiredoxin-3 (Prx3) and Mn-superoxide dismutase (MnSOD) in β-galactosidase (βGal) or FASTKD1-Myc infected mouse embryonic fibroblasts (MEFs). Actin and GAPDH were used as loading controls. (B) Western blotting for Trx2, Prx3, and MnSOD in control (CONsi) or FASTKD1 (FASTKD1si) siRNA-transfected MEFs. GAPDH was used as a loading control. (C) Quantification of total antioxidant capacity

and glutathione levels in βGal or FASTKD1-Myc infected MEFs. (D) Western blotting for Trx2, Prx3, and MnSOD in βGal or FASTKD1-Myc infected neonatal rat ventricular myocytes (NRVMs). GAPDH was used as a loading control. (E) Quantification of total antioxidant capacity and glutathione levels in βGal or FASTKD1-Myc infected NRVMs. Results are representative of 3-4 independent experiments performed in duplicate. Error bars indicate s.e.m. with *P<0.05 vs. βGal.

adenovirus, and did not detect any change in expression of Trx2, Prx3, or MnSOD (**Figure 5D**). Next, to confirm that this lack of change in expression correlated with no changes in activity we measured total antioxidant capacity and GSH content in NRVMs as well (**Figure 5E**). A small but statistically significant decrease in antioxidant capacity was measured in FASTKD1-Myc overexpressing cells compared to β-galactosidase expressing control cells. However, no difference was seen between the groups with regards to GSH content. These data show that cells do not up-regulate their antioxidant systems in response to FASTKD1-Myc overexpression, and NRVMs actually have decreased total antioxidant capacity with FASTKD1-Myc overexpression.

3.5 FASTKD1 modulates mitochondrial respiration and $\Delta\Psi_m$ in MEFs and NRVMs

MEFs were infected with β-galactosidase or FASTKD1-Myc adenovirus and subjected to analysis of mitochondrial respiration (**Figure 6A**). When provided with the Complex I substrates glutamate/malate, FASTKD1-Myc overexpressing cells showed a decrease in state 3 and an increase in state 4 oxygen consumption. Complex II activity as measured by oxygen consumption of MEFs in the presence of succinate was not significantly different between β-galactosidase and FASTKD1-Myc-infected cells (**Figure 6B**). When the respiratory control (RC) ratio was calculated, FASTKD1-Myc overexpressing MEFs displayed a significant decrease in this measure of mitochondrial coupling during Complex I stimulated respiration (**Figure 6C**). Mitochondrial respiration and RC ratio were determined for cells transfected with a control non-targeting siRNA or FASTKD1 siRNA and were not significantly different when measured using substrates for either

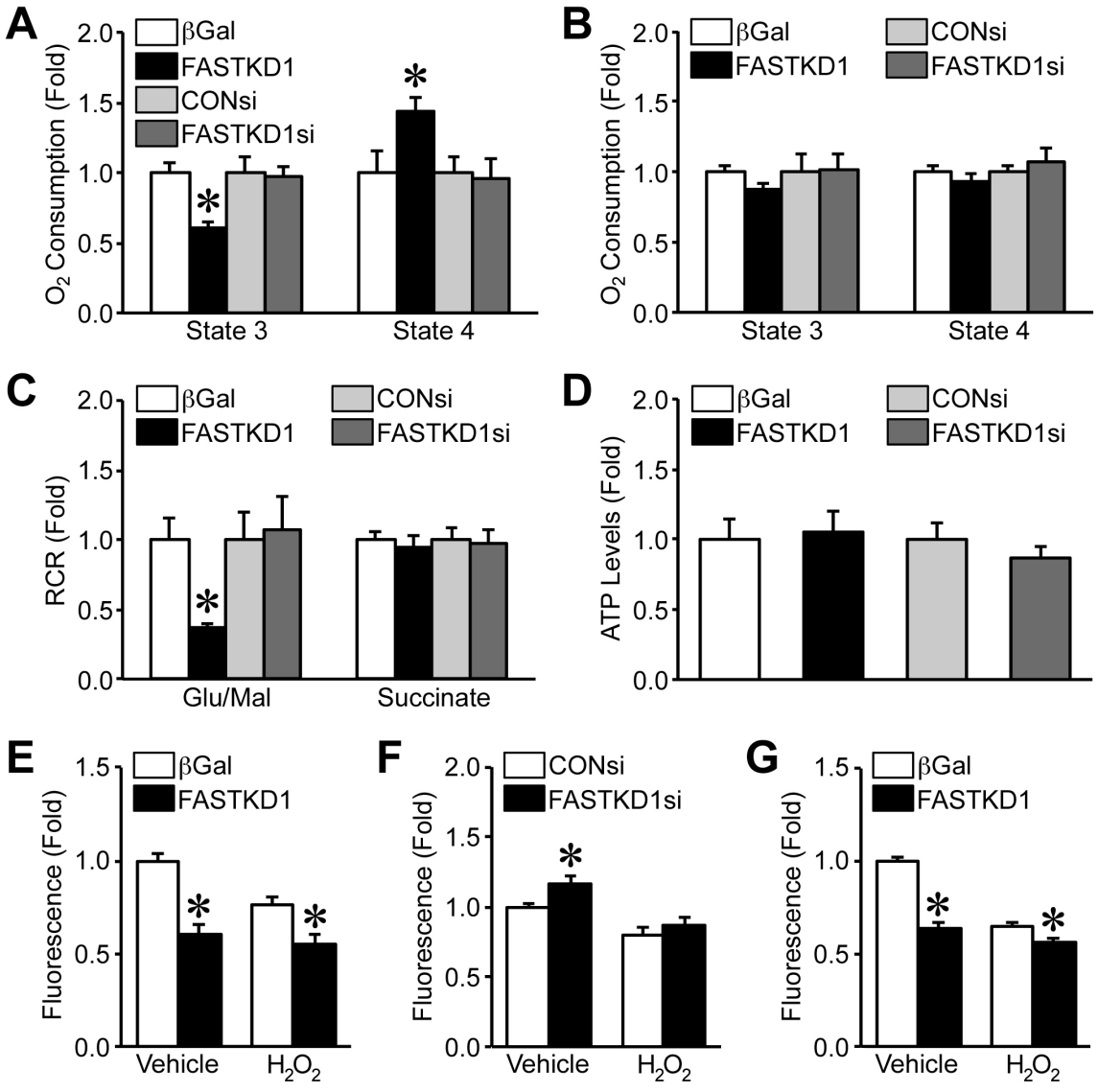

Figure 6. FASTKD1 modulates mitochondrial respiration and mitochondrial potential ($\Delta\Psi_m$). (A) Glutamate/malate-energized State 3 and State 4 respiration in mouse embryonic fibroblasts (MEFs) either infected with β-galactosidase (βGal) or FASTKD1-Myc adenoviruses or transfected with control (CONsi) or FASTKD1 (FASTKD1si) siRNAs. (B) Succinate-energized State 3 and State 4 respiration in MEFs either infected with βGal or FASTKD1-Myc adenoviruses or transfected with CONsi or FASTKD1si. (C) Respiratory control ratio (RCR) of Glutamate/malate-energized MEFs

either infected with βGal or FASTKD1-Myc adenoviruses or transfected with CONsi or FASTKD1si. (D) Cellular ATP levels in MEFs either infected with βGal or FASTKD1-Myc adenoviruses or transfected with CONsi or FASTKD1si. (E) Relative $\Delta\Psi_m$ as measured by TMRE fluorescence in βGal or FASTKD1-Myc infected MEFs treated with vehicle or 100μM H_2O_2 for 2 hours. (F) Relative $\Delta\Psi_m$ as measured by TMRE fluorescence in CONsi or FASTKD1si-transfected MEFs treated with vehicle or 100μM H_2O_2 for 2 hours. (G) Relative $\Delta\Psi_m$ as measured by TMRE fluorescence in βGal or FASTKD1-Myc infected neonatal rat ventricular myocytes treated with vehicle or 50μM H_2O_2 for 0.5 hours. Results are representative of 3-4 independent experiments performed in duplicate. Error bars indicate s.e.m. with *P<0.05 vs. βGal or CONsi.

Complex I or Complex II (**Figure 6A-C)**. These changes in mitochondrial respiration were not accompanied by any changes in total cellular ATP content (**Figure 6D**).

Next, $\Delta\Psi_m$ was measured in the infected/transfected MEFs and NRVMs. Overexpression of FASTKD1 resulted in a decrease in $\Delta\Psi_m$ compared to β-galactosidase infected MEFs at baseline (**Figure 6E**). H_2O_2 treatment resulted in a decrease in $\Delta\Psi_m$ in β-galactosidase infected cells while the decreased $\Delta\Psi_m$ seen at baseline was maintained in FASTKD1-Myc overexpressing cells. Knockdown of FASTKD1 in MEFs resulted in an increase in relative $\Delta\Psi_m$ at baseline compared to control siRNA-transfected cells (**Figure 6F**). Treatment of MEFs with H_2O_2 resulted in a decrease in the relative TMRE fluorescence with no difference detected between FASTKD1 siRNA and Control siRNA treated cells. In NRVMs, TMRE fluorescence was decreased at baseline in FASTKD1-Myc overexpressing cells compared to β-galactosidase infected cells (**Figure 6G**). β-galactosidase infected NRVMs showed a significant decrease in $\Delta\Psi_m$ following H_2O_2 treatment, whereas the FASTKD1 overexpressing did not exhibit a further decrease upon H_2O_2 stimulation. These data show that FASTKD1 can modulate mitochondrial respiration and mitochondrial $\Delta\Psi$.

3.6 FASTKD1 modulates mitochondrial morphology in MEFs and NRVMs

Mitochondria are dynamic organelles that undergo fission and fusion within a cell [98]. In our initial studies examining the mitochondrial localization of FASTKD1 we observed that the FASTKD1 overexpressing cells exhibited a considerably fragmented pattern of mitochondria, both in the MEFs (**Figure 1D**) and NRVMs (**Figure 1E**). To better assess this, FASTKD1-Myc-infected and siRNA-transfected MEFs were stained with an

antibody to ANT to delineate the mitochondrial network, and then mitochondrial morphology was determined by calculation of a mitochondrial fragmentation score (**Figure 7A,B**). Overexpression of FASTKD1-Myc resulted in increased mitochondrial fragmentation compared to β-galactosidase infected MEFs. Conversely, knockdown of FASTKD1 via siRNA transfection resulted in decreased mitochondrial fragmentation compared to control siRNA-transfected cells. Because alterations were seen in mitochondrial morphology with manipulation of FASTKD1 levels, expression of proteins involved in mitochondrial fission and fusion were measured via Western blotting. Overexpression of FASTKD1-Myc resulted in a significant decrease in mitofusin-1 (Mfn1) compared to β-galactosidase-infected controls while mitofusin-2 (Mfn2), optic atrophy-1 (OPA1), and dynamin-related protein-1 (Drp1) levels remained unchanged (**Figure 7C,D**). However, mitochondrial content, as assessed by measurement of mtDNA by real time PCR, was not affected by FASTKD1-Myc overexpression (**Figure 7E**). Finally, in MEFs siRNA mediated knockdown of FASTKD1 did not alter levels of any of the fusion/fission proteins (**Figure 7F**).

Because FASTKD1 modulated mitochondrial morphology in MEFs, we aimed to repeat these experiments in NRVMs. A mitochondrial fragmentation score was used to determine mitochondrial morphology in NRVMs (**Figure 8A,B**). NRVMs were stained with an antibody to the mitochondrial PiC for delineation of the mitochondrial network. Co-staining for Myc was used to identify cells infected with FASTKD1-Myc. FASTKD1-Myc positive NRVMs displayed a significantly higher level of mitochondrial fragmentation than β-galactosidase infected control NRVMs. As seen in MEFs, overexpression of FASTKD1-Myc resulted in decreased Mfn1 levels as measured by

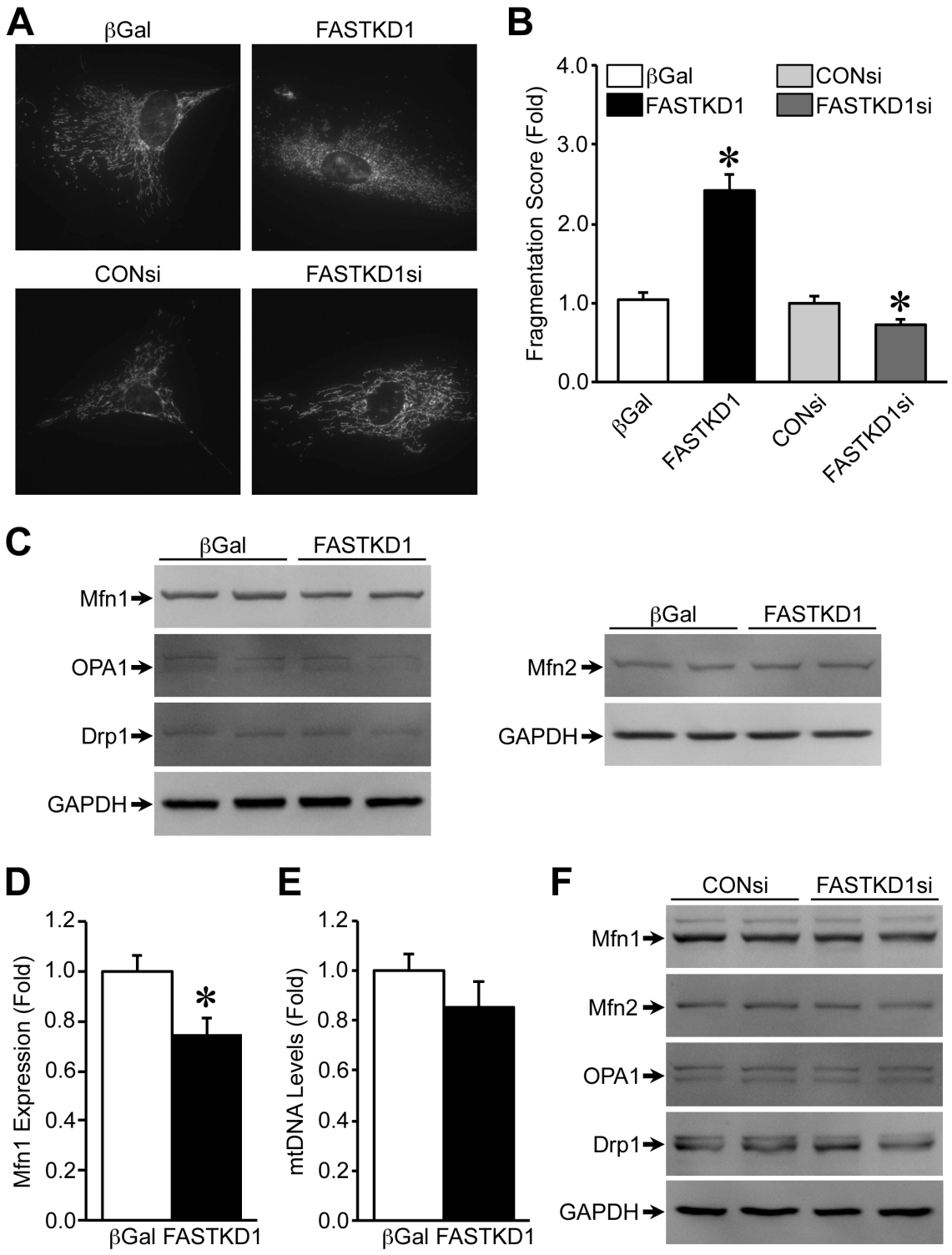

Figure 7. FASTKD1 modulates mitochondrial morphology in mouse embryonic fibroblasts. (A) Representative fluorescent images of mouse embryonic fibroblasts (MEFs) either infected with β-galactosidase (βGal) or FASTKD1-Myc adenoviruses or

transfected with control (CONsi) or FASTKD1 (FASTKD1si) siRNAs and then immunostained for the adenine nucleotide translocase. (B) Quantification of mitochondrial fragmentation scores from MEFs either infected with βGal or FASTKD1-Myc adenoviruses or transfected with CONsi or FASTKD1si. (C) Western blotting for mitofusin-1 (Mfn1), mitofusin-2 (Mfn2), optic atrophy-1 (OPA1), and dynamin-related protein-1 (Drp1) in βGal or FASTKD1-Myc infected MEFs. GAPDH was used as a loading control. (D) Densitometric analysis of Mfn1 expression blotting in βGal or FASTKD1-Myc infected MEFs. (E) Relative mitochondrial content as assessed by mtDNA in βGal or FASTKD1-Myc infected MEFs. (F) Western blotting for Mfn1, Mfn2, OPA1, and Drp1 in CONsi or FASTKD1si-transfected MEFs. GAPDH was used as a loading control. Results are representative of 3-4 independent experiments performed in duplicate. Error bars indicate s.e.m. with $*P<0.05$ vs. βGal or CONsi.

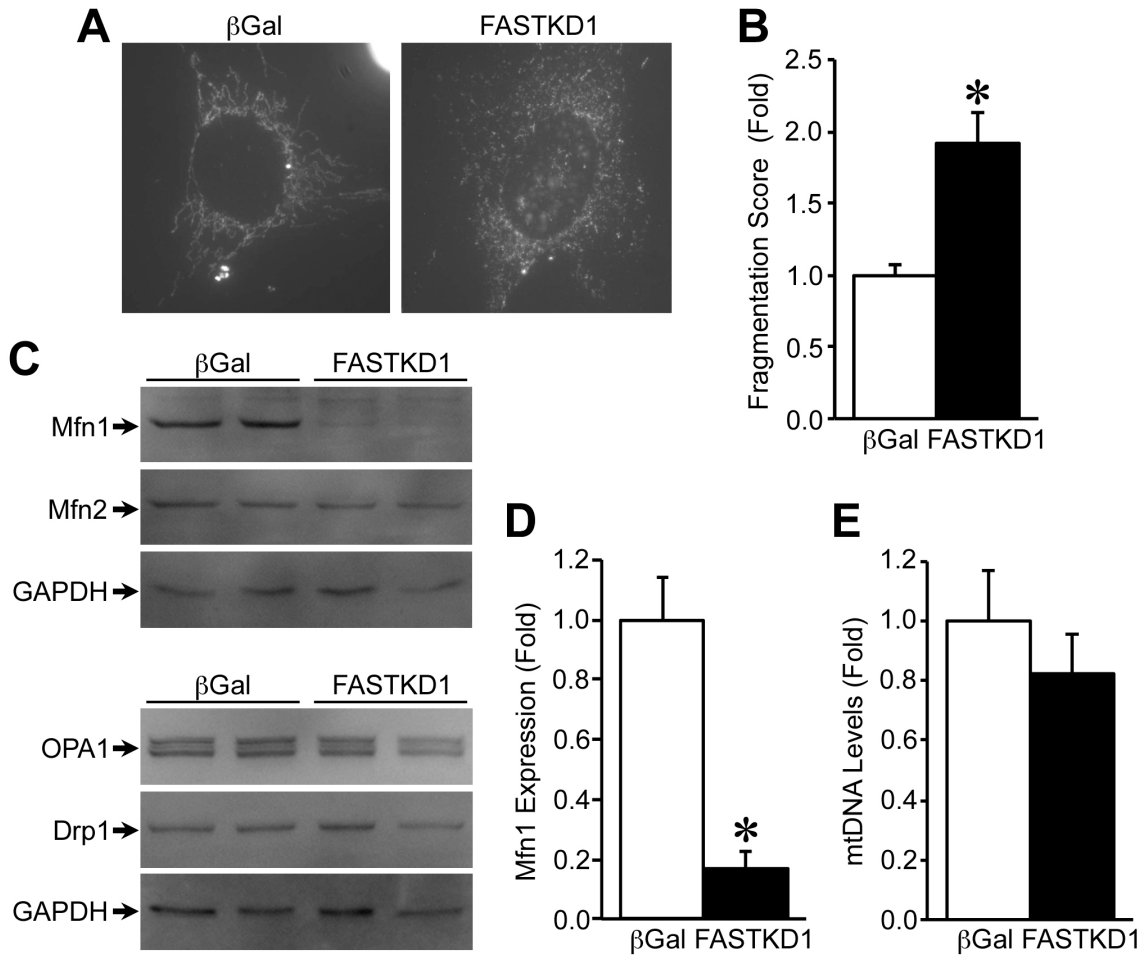

Figure 8. FASTKD1 modulates mitochondrial morphology in neonatal rat myocytes. (A) Representative fluorescent images of neonatal rat ventricular myocytes (NRVMs) infected with either β-galactosidase (βGal) or FASTKD1-Myc adenovirus and immunostained for the mitochondrial phosphate carrier. (B) Quantification of mitochondrial fragmentation scores from βGal or FASTKD1-Myc infected NRVMs. (C) Western blotting for mitofusin-1 (Mfn1), mitofusin-2 (Mfn2), optic atrophy-1 (OPA1), and dynamin-related protein-1 (Drp1) in βGal or FASTKD1-Myc infected NRVMs. GAPDH was used as a loading control. (D) Densitometric analysis of Mfn1 expression in βGal or FASTKD1-Myc infected NRVMs. (E) Relative mitochondrial content as assessed by mtDNA in βGal or FASTKD1-Myc infected MEFs. Results are

representative of 3-4 independent experiments performed in duplicate. Error bars indicate s.e.m. with *P<0.05 vs. βGal.

Western blotting compared to β-galactosidase infected control cells (**Figure 8C,D**). Expression levels of other mitochondrial fusion proteins Mfn2 and OPA1 and the mitochondrial fission protein Drp1 did not change with FASTKD1-Myc overexpression. As seen in MEFs, FASTKD1-Myc overexpression did not alter mitochondrial content in NRVMs (**Figure 8E**). Taken together, these data indicate that FASTKD1 modulates mitochondrial morphology in cells without changing total mitochondrial content.

4. Discussion

Here we describe for the first time that FASTKD1 is a novel CypD-binding protein. Based upon this observation, we hypothesized that FASTKD1 would modulate cell death via this interaction. Surprisingly, FASTKD1 did not modulate MPT responsiveness. We show that FASTKD1 is both necessary and sufficient to protect cells from oxidative stress-induced cell death, and could still protect cells lacking CypD. Moreover, we found that FASTKD1 modulates mitochondrial respiration and $\Delta\Psi_m$. In addition, manipulation of FASTKD1 levels alters mitochondrial morphology. These data indicate that FASTKD1 may play an important protective role against mitochondrial-dependent cell death and supports mitochondrial homeostasis.

Although FASTKD1 had been identified as a mitochondrial protein, [118] its function had not been explored. In fact, little is known about all members of the FASTKD protein family. Knockdown of FASTKD3 was shown to decrease basal as well as ATP stimulated mitochondrial respiration without altering respiratory chain assembly [118]. FASTKD2 has been reported to promote apoptosis [131] and a loss of function mutation in FASTKD2 is associated with a mitochondrial encephalomyopathy [129]. Recently,

FASTKD4 has been reported to act as a modulator of mitochondrial RNA processing [188], and a translational variant of FASTK was shown to localize to the mitochondria where it stabilizes the mRNA of a complex I subunit [125].

Specifically regarding FASTKD1's role in the cell, little information is available although it is elevated at the mRNA and protein level in aspirates from endometrial cancer [127]. Like FASTKD3, we found that FASTKD1 could modulate mitochondrial respiratory chain activity and $\Delta\Psi_m$. However, FASTKD1 appears to have the opposite effect in that FASTKD1 overexpression uncouples respiration and knockdown does not affect basal activity. The uncoupling effect was only observed when substrates for complex I were utilized, as succinate-driven respiration was normal, indicating that FASTKD1 acts at the level of complex I and does not seem to interfere with the rest of the respiratory chain's activity. Expression of a key complex I protein was unaltered however, suggesting that this is not simply due to reduced complex I component levels. Thus the mechanism by which FASTKD1 modulates respiration is not entirely clear and whether FASTKD1 can directly interact with complex I is something we are currently investigating.

The major finding of the study was that FASTKD1 could protect cells against oxidant-induced death, both in MEFs and in NRVMs. Given that ROS induce cell mortality at least in part through MPT [57], and that FASTKD1 interacted with CypD, we first investigated whether FASTKD1 could modulate cell death via the MPT pore. Many proteins have been hypothesized to comprise the channel forming unit of the MPT pore including the voltage dependent anion channel (VDAC), adenine nucleotide translocase (ANT) and the mitochondrial phosphate carrier (PiC), but they have either been ruled out

completely as a MPT pore component or shown to have a more regulatory function [70-73]. However, multiple recent studies have hypothesized that the pore may in fact be composed of either components or dimers of the ATP synthase [74-77]. Until this discovery, the only agreed upon component of the MPT pore was the mitochondrial matrix protein, Cyclophilin D (CypD). Thus, it was an obvious first step to investigate whether FASTKD1 modulates the MPT pore via its interaction with CypD. However, when we measured MPT responsiveness using the CRC assay we found that overexpression of FASTKD1 did not appreciably affect MPT pore opening. Further evidence demonstrating a dissociation between FASTKD1 and the MPT pore was the fact that ionomycin, which causes MPT-dependent death due to Ca^{2+} overload [77], was just as effective in killing FASTKD1 overexpressing cells as it was the control cells. Finally, because FASTKD1 further protects MEFs generated from *Ppif*$^{-/-}$ mice from ROS-induced cell death, it would appear that the interaction between FASTKD1 and CypD is dispensable for FASTKD1-elicited cytoprotection. Thus, FASTKD1's ability to protect against cell death appears to be limited to oxidative stress-induced injury, does not extend to Ca^{2+}-induced cytotoxicity, and is independent of any effect on the MPT pore.

Because we found that FASTKD1-mediated cytoprotection was limited to oxidative stress, we examined the mitochondrial antioxidant system to determine if this is the mechanism by which FASTKD1 exerts its protective effects. Mitochondria are a major source of cellular ROS, and thus contain an efficient antioxidant system [133,191]. We did not detect any differences in mitochondrial antioxidant protein levels with FASTKD1 knockdown or overexpression. Additionally cells did not increase their antioxidant capacity in response to FASTKD1-Myc overexpression. From this, we can conclude that

simply increasing the antioxidant capacity of cells is not the mechanism by which FASTKD1 protects cells from oxidative stress induced cell death. Of note, we actually saw a decrease in total antioxidant capacity in NRVMs overexpressing FASTKD1-Myc. While we did not measure reductive capacity of cells, antioxidants have been shown to be toxic in some cases [152]. Maintaining the balance between ROS and antioxidant capacity is critical, and if this equilibrium becomes unbalanced and antioxidant capacity becomes too great, cells can be damaged [192]. It is conceivable that ROS production, rather than ROS scavenging is altered by FASTKD1. Indeed, the uncoupling effect of FASTKD1 would be expected to reduce mitochondrial ROS production, and it is feasible that the modulation of complex I by FASTKD1 may prevent ROS release from this complex.

Mitochondria are dynamic organelles with their morphology under the control of a variety of pro-fusion proteins including Mfn1, Mfn2, OPA1 and pro-fission proteins including Fis1 and Drp1 [193]. Interestingly we found that FASTKD1 overexpression resulted in an increased mitochondrial fragmentation phenotype, whereas FASTKD1 depletion had the opposite effect. One possibility was that the decrease in $\Delta\Psi_m$ caused by increased FASTKD1 levels would drive mitophagy, which involves the fragmentation of the mitochondrial network [31,194]. The hyperpolarization induced by FASTKD1 depletion would have the opposite effect. However, enhanced levels of mitophagy would be expected to reduce mitochondrial content [195], and we observed no changes in mtDNA, an index of mitochondrial content. When we examined the levels of the major fission and fusion proteins we found no changes in their expression in most cases. The one exception was a reduction of Mfn1, which we observed in both MEFs and NRVMs overexpressing FASTKD1. Reductions in Mfn1 could certainly lead to the fragmented phenotype we see

in the FASTKD1 overexpressing cells, and are of interest as Mfn1 deletion has been reported to protect adult cardiomyocytes from oxidative stress-induced death [116]. However, while FASTKD1 knockdown lead to a hyperfused state, it did so independently of any changes in Mfn1 expression, suggesting an alternative mechanism. Moreover, while Mfn1 has been shown to be targeted for degradation by the mitochondrial ubiquitin ligase March5 [103], it is not clear how this is modulated by FASTKD1.

In conclusion, FASTKD1 presents a novel target to prevent cell loss in the face of oxidative stress. While the precise mechanism by which FASTKD1 protects cells from ROS induced death remains elusive, we have been able to rule out MPT pore modulation as a possible mechanism. Additionally, we have shown that FASTKD1 modulates mitochondrial dynamics, with its overexpression resulting in enhanced mitochondrial fragmentation and its knockdown decreasing mitochondrial fragmentation. We conclude that FASTKD1 protects cells against oxidative stress-induced cell death via a potentially novel mechanism that is independent of CypD and the MPT pore. Future studies are required to determine how FASTKD1 protects cells from oxidative stress-induced death and to which extent this is connected to mechanisms governing mitochondrial fission and fusion.

5. Methods

5.1 Yeast Two-Hybrid

The yeast-2-hybrid screen using mature cyclophilin-D (aa41-206) as bait was performed by Hybrigenics Services (Paris, France). The cDNA encoding the mature form of mouse CypD was cloned into the pB27 (N-LexA-bait-C fusion) plasmid. This construct was

then screened against a human ventricle and embryonic heart RP1 library. From this 62 clones were identified, with 50 of these representing in-frame clones. Sequencing of the clones identified 18 known proteins (Table S1), of which FASTKD1 was one.

5.2 Cell Culture

Experiments involving the isolation of mouse embryonic fibroblasts (MEFs) and neonatal rat ventricular myocytes (NRVMs) were approved by the University of Missouri Animal Care and Usage Committee and were in accordance with the Guidelines for the Care and Use of Laboratory Animals published by the National Institutes of Health. MEFs were generated from embryonic day 15.5 wildtype and CypD-deficient (*Ppif*$^{-/-}$) mice as previously described [63,70]. Embryos were excised, the head and internal organs removed, and the trunks digested in 0.05% trypsin/1mM EDTA (Hyclone) for 30 minutes at 37°C. Cell suspensions were plated in DMEM (Hyclone) containing 10% fetal bovine serum (Atlanta Biologicals) and 100U/mL penicillin/0.1mg/mL streptomycin (Hyclone). NRVMs were isolated and maintained as previously described [196,197]. Ventricles from 1 to 3 day old rats were subjected to trypsin followed by collagenase digestions per the manufacturer's instructions (Worthington). Cells were pre-plated on uncoated plates for 30min at 37°C to remove cardiac fibroblasts. Ventricular myocytes were then plated on gelatin-coated plates for 24 hours in M199 (Hyclone) supplemented with 10% bovine growth serum (Hyclone) and 100U/mL penicillin/0.1mg/mL streptomycin (Hyclone). After washing with PBS cells were maintained in serum free M199.

5.3 Adenoviruses and siRNA Transfection

Replication deficient adenoviruses encoding β-galactosidase, mouse CypD (C-terminal FLAG tag) or mouse FASTKD1 (C-terminal Myc tag) were generated using the AdEasy-XL kit (Agilent Technologies). MEFs and NRVMs were infected with adenovirus at an MOI of 100-200 48 hours before experimentation. For knockdown experiments, MEFs were transfected with a pool of 4 mouse-specific FASTKD1 targeting siRNAs (M-053232-01, Dharmacon; #1 5'-gcagaaguguacaaacgaa-3', #2 5'-gggcugugcguuuaaugua-3', #3 5'-cuacgaagcaucucuuuac-3', #4 5'-ggagaauggcuucacgaau-3') at a concentration of 10nM using Lipofectamine RNAiMax (Life Technologies) for 48 hours before experimentation. A pool of 4 non-targeting siRNAs (D-001206-14, Dharmacon) was used as a control.

5.4 Western Blotting

MEFs and NRVMs were solubilized and sonicated in lysis buffer containing 150mM NaCl, 10mM Tris pH 7.4, 1% Triton-X100, and protease/phosphatase inhibitor (Halt, Thermo Scientific) then centrifuged at 17,000g for 10min at 4°C to remove cell debris. Equal amounts of protein, as determined by Bradford assay (Bio-Rad), in SDS loading buffer were run on 10% SDS/PAGE gels before transfer to PVDF membranes. After blocking in 10% non-fat milk in TBS-T, primary antibodies: Myc (Cell Signaling, 2276S, 1:1000), FLAG (Sigma, F7425, 1:2000), PiC (Custom made by YenZym, 1:1000), Cyclophilin F (Abcam, ab110324, 1:1000), OxPhos antibody cocktail (Mitosciences, MS604, 1:1000), ANT1/2 (Santa Cruz, Sc-9299, 1:100), GAPDH (Millipore, MAB374, 1:1000), Mfn1 (Santa Cruz, Sc-50330, 1:100-1000), Mfn2 (Abcam, ab56889, 1:1000), OPA1 (BD Biosciences, 612606, 1:1000), Drp1 (Santa Cruz, Sc-101270, 1:100), TRX2

(Santa Cruz, Sc-50336, 1:100), PRX3 (Santa Cruz, Sc-59661, 1:1000), and MnSOD (Millipore, 06-984, 1:1000) were applied to the membranes overnight at 4°C in blocking buffer. After washing in TBS-T, the appropriate alkaline phosphatase-conjugated secondary antibodies (Cell Signaling, 1:1000) were applied to the membrane for 2 hours at RT in blocking buffer. Membranes were then washed in TBS-T prior to imaging on a Bio-Rad Gel Doc XR using chemifluorescence (ECF, GE Healthcare Life Sciences).

5.5 Immunoprecipitation

NRVMs were infected with β-galactosidase, CypD-FLAG and/or FASTKD1-Myc for 48 hours. Cells were scraped into a microfuge tube, washed twice with cold PBS then lysed for 30min on ice in 1mL of immunoprecipitation buffer containing: 150mM NaCl, 20mM Tris pH 7.4, 1mM EDTA, 10% glycerol, 0.2% NP40, and protease/phosphatase inhibitor. Lysates were clarified by centrifuging at 17,000g for 20min at 4°C. One mg of each sample was then incubated overnight with 25μL of anti-FLAG-conjugated agarose (A2220, Sigma) in a final volume of 1mL. After washing 3 times with Immunoprecipitation buffer the beads were resuspended in 30μL SDS loading buffer and subjected to immunoblotting with anti-Myc and anti-FLAG antibodies.

5.6 Immunocytochemistry

Immunocytochemistry was performed as described previously [198]. MEFs or NRVMs in chamber slides (Nunc) were infected with the β-galactosidase or FASTKD1-Myc adenoviruses or transfected with control or FASTKD1 siRNAs. After 48 hrs cells were incubated with 100nM Mitotracker-CMXRos (Life Technologies) in media for 30min at

37°C, washed with PBS, then fixed with 4% paraformaldehyde. Cells were permeabilized/blocked with PBS containing 1% bovine serum albumin, 0.1% cold water fish skin gelatin, and 0.1% Tween-20 for 1 hour at RT then incubated overnight with anti-Myc antibody (Santa Cruz, Sc-40, 1:100) in the permeabilization/blocking buffer. After washing 3 times with PBS/0.1% NP-40, cells were incubated with an anti-mouse fluorophore-conjugated secondary antibody (Alexa, Life Technologies, 1:500) for 2 hours at RT. The cells were washed 3 more times with PBS/0.1% NP-40 before imaging using an inverted fluorescence microscope (Olympus IX51).

5.7 Analysis of Mitochondrial Morphology

Mitochondrial morphology was measured as described previously [101]. Briefly, MEFs and NRVMs were stained for ANT (Santa Cruz, Sc-9299, 1:100) or PiC (Custom made by YenZym, 1:1000) respectively, as described above with co-staining for Myc (Santa Cruz, Sc-40, 1:100) to identify FASTKD1-Myc overexpressing cells. Images were acquired using an inverted fluorescence microscope (Olympus IX51) then subjected to the following analysis using ImageJ (NIH): background subtraction, filtering (median), thresholding, binarization and particle counting.

5.8 Measurement of Cell Death

MEFs and NRVMs were treated with H_2O_2 for 4 hours or 1 hour, respectively, at the indicated concentration. MEFs were treated with β-lapachone (Axxora) or ionomycin (LKT Laboratories) for 4 hours or 18 hours, respectively, at the indicated concentrations. Cell death was measured as previously described [197]. Briefly, cells were co-stained with

Sytox Green (0.15μM) (Invitrogen) to label dead cells and bis-benzimide (10μg/mL) to label all cells for 15min in PBS. Imaging was performed on an inverted fluorescence microscope (Olympus IX51). Images were then analyzed using ImageJ software (NIH).

5.9 Measurement of Calcium Retention Capacity

Calcium retention capacity (CRC) was measured as described previously [72]. MEFs were trypsinized, counted, washed with PBS then resuspended in CRC buffer containing 120mM KCl, 10mM Tris at pH 7.4, 1mM KH_2PO_4, and 20μM EDTA at a concentration of $4x10^6$ cells/mL. For each measurement $1x10^6$ cells, 5mM succinate or 5mM glutamate/malate, 1μM Calcium Green 5N (Invitrogen) and 8μM digitonin (Promega) were loaded into a cuvette to a total volume of 1mL. The cuvette was placed in a fluorometer (Vernier) and exposed to 500nm light. After two minutes, pulses of 2.5μM $CaCl_2$ were added every minute until an increase in fluorescence was detected at 530nm consistent with MPT pore opening.

5.10 Measurement of Mitochondrial Respiration

Mitochondrial respiration was determined as previously described [199,200]. Confluent MEFs were washed with PBS, trypsinized, and resuspended at a concentration of $2x10^6$ cells per 0.1mL in buffer containing 137mM NaCl, 5mM KCl, 0.7mM NaH_2PO_4 and 25mM Tris at pH 7.4, and then permeabilized by the addition of 10μg/$1x10^6$ cells digitonin. Mitochondrial respiration was measured using a Clark-type electrode using either 10mM glutamate/malate or succinate. State 3 was initiated by the addition of

200μM ADP to the reaction. State 4 was initiated by the addition of 2μM oligomycin (Alexis Biochemicals).

5.11 Measurement of Mitochondrial Transmembrane Potential ($\Delta\Psi_m$)

$\Delta\Psi_m$ was measured using tetramethylrhodamine (TMRE, Life Technologies) staining in MEFs and NRVMs. Initially, MEFs and NRVMs were treated with H_2O_2 (100μM for 2 hours or 50μM for 0.5 hours, respectively). Cells were loaded with 100nM TMRE for 30min at 37°C in Hank's buffered saline solution (HBSS), washed once with HBSS, then imaged on an inverted fluorescence microscope (Olympus IX51). TMRE fluorescence per cell was calculated using ImageJ (NIH).

5.12 Measurement of Antioxidant Capacity, GSH levels, and ATP levels

MEFs and NRVMs were homogenized in lysis buffer per the manufacturers specifications containing: 5 mM KH_2PO_4, 0.9% NaCl and 0.1% Dextrose then lysed by sonication. Total antioxidant capacity was measured using an Antioxidant Assay Kit (709001, Cayman Chemical), GSH was measured using the GSH-GLO® kit (V6911, Promega), and ATP was measured using the CellTiter-GLO® kit (G7570, Promega). All assays were performed in 96-well plates according to the manufacturers' instructions and measured using a Modulus™ II microplate multimode reader (Promega).

5.13 Quantification of Mitochondrial Content

Total DNA was isolated from MEFs and NRVMs by proteinase-K digestion followed by phenol/chloroform extraction then diluted to a concentration of 5ng/μL. Real time PCR

was performed on 25ng of DNA using a Bio-Rad cycler with Sybr green intercalating dye (Takara SYBR Premix Ex Taq). The mitochondrial 12s rRNA gene (primers: Fw – atttcgtgccagccaccgcgg, Rev - ggctacaccttgacctaacgt) was used as a marker of mtDNA content while the 18s rRNA gene (primers: Fw – ggaataatggaataggaccgcg, Rev - ggacatctaagggcatcacag) was used as a control for nuclear DNA content. Analysis of comparative cycle threshold (C_t) was used for relative quantification of the mtDNA/nucDNA ratio.

5.14 Statistical Analysis

All data are reported as the mean ± S.E.M. A Student's unpaired t-test was used to determine statistical significance between two groups. Statistical significance was set at a p value <0.05.

Chapter 3: Cardiac myocyte specific overexpression of FASTKD1 prevents myocardial infarction induced cardiac rupture

1. Abstract

Aims: The mitochondrial protein FASTKD1 protects cells from oxidative stress induced cell death *in vitro*; however, its role *in vivo* is unknown. Therefore we generated cardiac myocyte specific FASTKD1 overexpressing mice to test the effects of this protein on experimental myocardial infarction (MI).

Methods and Results: Three independent lines of mice with cardiac myocyte specific overexpression of FASTKD1 to varying degrees were obtained. These mice displayed normal cardiac morphology and function at the gross and microscopic levels. Isolated cardiac mitochondria from all transgenic mouse lines showed normal mitochondrial function. Male mice from the highest expressing line were subjected to 8-weeks of permanent coronary ligation with ~40% of non-transgenic mice undergoing left ventricular free wall rupture within 7-days of MI compared to 0% of FASTKD1 overexpressing mice. At 3-days post-MI FASTKD1 overexpression resulted in decreased neutrophils, increased macrophages and elevated levels of the extracellular matrix component periostin at the border and scar regions compared to control mice.

Conclusions: Cardiac specific overexpression of FASTKD1 results in viable mice displaying normal cardiac morphology and function. However, these mice are resistant

to MI-induced cardiac rupture and display altered inflammatory and ECM responses following MI.

2. Introduction

Acute myocardial infarction (MI) is a major cause of mortality worldwide, with approximately 700,000 Americans experiencing their first MI each year[169,201]. Following MI, reactive oxygen species (ROS) are elevated, and the heart begins to heal in a process involving myocytes, non-myocytic cells and the extracellular matrix[169,202]. Elevated post-MI ROS are produced by both mitochondrial and non-mitochondrial sources [203]. As the heart undergoes remodeling following MI, there is a progressive decline in antioxidant activity in the heart[204]. Decreased antioxidant capacity is evidenced by the presence of elevated levels of 3-nitrotyrosine in the infarcted rat heart [205]. These elevated levels of ROS are known to mediate myocyte cell death following MI [206]. Long-term antioxidant therapy is capable of reducing apoptosis following MI, although 100 days of treatment were required for these effects [207]. Oxidative stress-induced cell death therefore presents a promising target for treatment of MI associated cardiac injury. Novel strategies that reduce ROS induced cell death without requiring months of treatment to impact the antioxidant system are needed.

We have previously shown that FAST kinase domain containing protein 1 (FASTKD1) protects cells, including myocytes, from oxidative stress-induced cell death *in vitro*, and this protection is independent of any modulations to the cellular antioxidant sytem (unpublished data). FASTKD1 is a member of the FAST kinase family consisting of

FASTK and FASTKD1 – FASTKD5 [118]. This family of proteins shares two FAST domains, an RNA binding domain and an N-terminal mitochondrial targeting sequence. FASTK has been implicated in many cellular processes, however it was first identified as a negative regulator of apoptosis [119]. Other members of the FASTK family of proteins have been implicated in cell death pathways including FASTKD2, which acts as a pro-apoptotic protein in breast cancer cells [131]. Comparatively little is known about the function of FASTKD1 besides its mitochondrial localization and its ability to bind mRNA [118,124]. FASTKD1 mRNA and protein levels are elevated aspirates from human cases of endometrial carcinoma [127]. Additionally, elevated FASTKD1 expression is indicative of a poor prognosis in lymphocytic leukemia [128]. However, the role that FASTKD1 plays in the healthy heart has not been explored. Importantly, FASTKD1 presents a promising cardioprotective target following MI based on the *in vitro* data showing its ability to protect against ROS.

We therefore set out to test the role of FASTKD1 in the heart *in vivo*. We developed an inducible, cardiac-specific FASTKD1 overexpression mouse model to test the hypothesis that overexpression of FASTKD1 protects the heart from experimental MI induced by permanent coronary ligation. We obtained three transgenic mouse lines that overexpressed FASTKD1 at varying levels without any noxious side effects at baseline. High expressing FASTKD1 mice displayed similar responses to control mice following 8-weeks of experimental MI, however they were resistant to left ventricular rupture. Our data suggest that FASTKD1 presents a novel target to decrease the incidence of post-MI left ventricular rupture.

3. Materials and Methods

3.1 Generation of cardiac specific FASTKD1 overexpressing mice

All animal experiments were approved by the University of Missouri Animal Care and Use Committee and conformed to the NIH guidelines for the use and care of animals. FASTKD1 cDNA containing a C-terminal Myc tag was obtained from Origene and then cloned downstream of a tetracycline responsive minimal αMHC promoter [208]. This transgene was linearized out of the vector with SpeI and injected into fertilized FVB/N oocytes. Resulting TG mice were then crossed with αMHC tTA driver mice to induce expression (DTG) [208]. Experiments were performed at eight to twelve weeks of age on male and female mice and DTG animals were compared to non-transgenic (NTG) controls. Experiments were also performed on a limited number of single-transgenic (TG) and tTA mice to control for the effect of the transgene or tTA driver alone.

3.2 Echocardiography

Echocardiography was performed on eight to twelve week old male mice under 1.6 – 1.8% isoflurane anesthesia primarily using a GE Vivid 1 ultrasound system equipped with a 12-mHz transducer. Analysis was performed offline using GE EchoPAC software. A subset of animals had echocardiography performed at 3 days using a VisualSonics Vevo 2100 system and data was analyzed using VisualSonics VevoLab software.

3.3 Myocardial infarction injury model

Myocardial infarction was performed on 8-12 week old male mice as described previously [209]. Briefly, mice were anesthetized using isoflurane (VetOne), intubated and ventilated using a model "687" mouse ventilator (Harvard Apparatus) with a tidal volume of 250μL at 122 breaths per minute. A left-sided thoracotomy was performed between the third and fourth rib, the pericardium torn and the heart exposed. The anterior descending branch of the left coronary artery was ligated just distal to the atrial appendage using 7-0 Ti-Cron suture (Covidien). Successful ligation of the artery was confirmed by tissue blanching. For sham operations, the suture was passed beneath the coronary artery and not tied. The chest was closed using 6-0 polypropylene monofilament suture (CP Medical), buprenex was administered and the animals were allowed to recover. Animals were subjected to echocardiography at 4- and 8-weeks post MI. Following the 8-week echo, mice were sacrificed and hearts were excised for gravimetric analysis and infarct measurement by planimetry before flash freezing. For the day 3 studies, animals were first subjected to echocardiography and then sacrificed and their hearts perfusion fixated in buffer containing 5mM KCl, 5% dextrose and 4% paraformaldehyde in PBS. Hearts were placed sequentially in 15% then 30% sucrose before embedding in OCT compound (Tissue-Tek). Hearts were subjected to serial sectioning at 1mm intervals throughout the left ventricle and stained with Gomori's Trichrome to determine infarct size.

3.4 Mitochondrial isolation and subcellular fractionation

Heart mitochondria were isolated by differential centrifugation as previously described [63,70,72]. Briefly, hearts were homogenized using a Dounce in a buffer consisting of

250mM sucrose, 10nM Tris pH 7.4 and 1mM EDTA. The crude homogenates were centrifuged at 1,000g for 5 minutes at 4°C. Pelleted material was resuspended in sucrose-Tris buffer (lacking EDTA) and passed through a 40 micron nylon mesh filter (Fisher Scientific) before centrifugation at 1,000g for 5 minutes at 4°C to isolate nuclei. The nuclear pellet was washed twice in sucrose-Tris (lacking EDTA) buffer. The supernatant was removed and spun at 10,000g at 4°C for 10 minutes to separate cytosol from mitochondria. The cytosolic fraction was subjected to further centrifugation at 100,000g for 60 min at 4°C to isolate cellular membranes. The mitochondrial pellet was washed twice in sucrose-Tris buffer (lacking EDTA) before being resuspended in the appropriate assay buffer.

3.5 Measurement of mitochondrial calcium retention capacity and oxygen consumption

Assays on isolated cardiac mitochondria were performed at 22°C as described previously [72]. Briefly, for measurement of calcium retention capacity (CRC), 100μg of mitochondria were suspended in buffer containing 120mM KCl, 10mM Tris pH 7.4, 1mM KH_2PO_4 and 20μM EDTA. Mitochondria were energized with 10mM succinate and extra-mitochondrial Ca^{2+} was measured fluorimetrically with 1mM Calcium Green-5N (Invitrogen) making a final volume of 1mL, which was loaded into a cuvette. The cuvette was placed in a fluorometer (Vernier) emitting 500nm light. After a two-minute incubation and a spike of 10μM $CaCl_2$, 2.5μM pulses of $CaCl_2$ were added every minute until an increase in fluorescence was detected at 530nm indicative of MPT pore opening. For determination of mitochondrial oxygen consumption, 100μg of mitochondria were suspended in a buffer containing 120mM KCl, 10mM Tris pH 7.4, 5mM KH_2PO_4 and

1mM $MgCl_2$ and placed in a Clark-type electrode. Mitochondria were energized with either 5mM glutamate/5mM malate to measure Complex I respiration or 10mM succinate to measure complex II respiration. State 3 respiration was measured after the addition of 200μM ADP to the reaction mixture while state 4 respiration was measured after the addition of 2μM oligomycin (Alexis Biochemicals).

3.6 Western Blotting

Whole tissues and cellular sub fractions were homogenized in a buffer containing 150mM NaCl, 10mM Tris (pH 7.4), 1mM EDTA, 1% Triton-X100, and phosphatase/protease inhibitors (Halt, Thermo Scientific). Lysates were subjected to sonication, followed by centrifugation at 17,000g for 10 min at 4°C to remove debris. Protein concentrations were determined by Bradford assay (Bio-Rad). SDS-PAGE was performed on 10% polyacrylamide gels before transfer to PVDF membranes. Blocking was performed using 10% non-fat milk in TBS-T. Immunoblotting was performed using the following antibodies: FASTKD1 (Custom made by YenZym, 1:1000), Myc (Cell Signaling, 2276S, 1:1000), PiC (Custom made by YenZym, 1:1000), Cyclophilin F (Abcam, ab110324, 1:1000), OxPhos antibody cocktail (Mitosciences, MS604, 1:1000), ANT1/2 (Santa Cruz, Sc-9299, 1:100), VDAC (Abcam, ab14734, 1:1000), ATP5A (Abcam, ab14748, 1:1000) LDH (Abcam, ab52488, 1:1000). BiP (Cell Signaling, C50B12, 1:100), Histone H3 (Cell Signaling, D1H2, 1:100), GAPDH (Millipore, MAB374, 1:1000). After an overnight incubation with primary antibody in blocking solution at 4°C, membranes were incubated with the appropriate alkaline-phosphatase conjugated secondary antibody (Cell Signaling, 1:1000) at room temperature for two

hours in blocking solution. Membranes were imaged by chemiflourescence (ECF, GE Healthcare Life Sciences) using a Bio-Rad Gel Doc XR system.

3.7 Measuremnt of ATP content

ATP content was measured in whole cardiac tissue homogenates using the CellTiter-GLO® kit (G7570, Promega). Assays were performed according to the manufacturers instructions in a 96-well plate. Data were acquired using a Modulus™ II microplate multimode reader (Promega).

3.8 Histology and immunohistochemistry

Histology and immunohistochemistry were performed as described previously [197]. Briefly, fixed hearts embedded in OCT were sectioned using a cryostat. Sections were fluorescently labeled with wheat germ agglutinin and imaged with an inverted fluorescence microscope (Olympus IX51) before planimetric analysis of cell size using ImageJ software (NIH). Gomori's Trichrome staining was performed to assess fibrosis. Serial sections were stained with anti-NIMP (Santa Cruz) and anti F4/80 (AbD Serotec) to label neutrophils and macrophages respectively. Slides were imaged using an Olympus BX60 microscope using Olympus CellSens software and analyzed using ImageJ software (NIH). Periostin was detected by immunofluorescence using a polyclonal antibody (Abcam, ab92460) and the appropriate fluorescence conjugated secondary antibody. Sections were counterstained with bis-benzimide to identify nuclei. Slides were imaged with an inverted fluorescence microscope (Olympus IX51) and analyzed using ImageJ software (NIH).

3.9 Statistical analysis

All data are reported as mean ± S.E.M. Student t-tests were used to compare two groups with statistical significance set at $p < 0.05$. A two–way ANOVA was used to determine the difference between multiple treatments while a one-way ANOVA with a Tukey post-hoc test was used for comparison of multiple groups with statistical significance set at a p value < 0.05. Survival curves were analyzed using a log-rank test with a p value < 0.05.

4. Results

4.1 Development of inducible cardiac-specific FASTKD1 overexpressing mouse lines

To overexpress FASTKD1, myc-tagged FASTKD1 cDNA was cloned downstream of a tetracycline responsive αMHC promoter and crossing the resultant single transgenic (TG) mice with tTA driver mice. Three independent mouse lines were generated with varying levels of FASTKD1 overexpression compared to NTG mice. These mouse lines were classified as line 474, line 473 and line 475. Levels of FASTKD1 protein overexpression were ~1.9, 2.0, and 3.2 times relative to endogenous levels measured in control NTG mice for line 474, line 473 and line 475 respectively (**Figure 9A, 9B**). The product of the transgene ran slightly higher than endogenous FASTKD1 due to the presence of the Myc-tag. To confirm the cardiac specificity of FASTKD1 overexpression, various tissues were collected from NTG and DTG mice from all three lines (**Figure 9C**). FASTKD1 protein overexpression was limited to cardiac tissue as assessed by Western

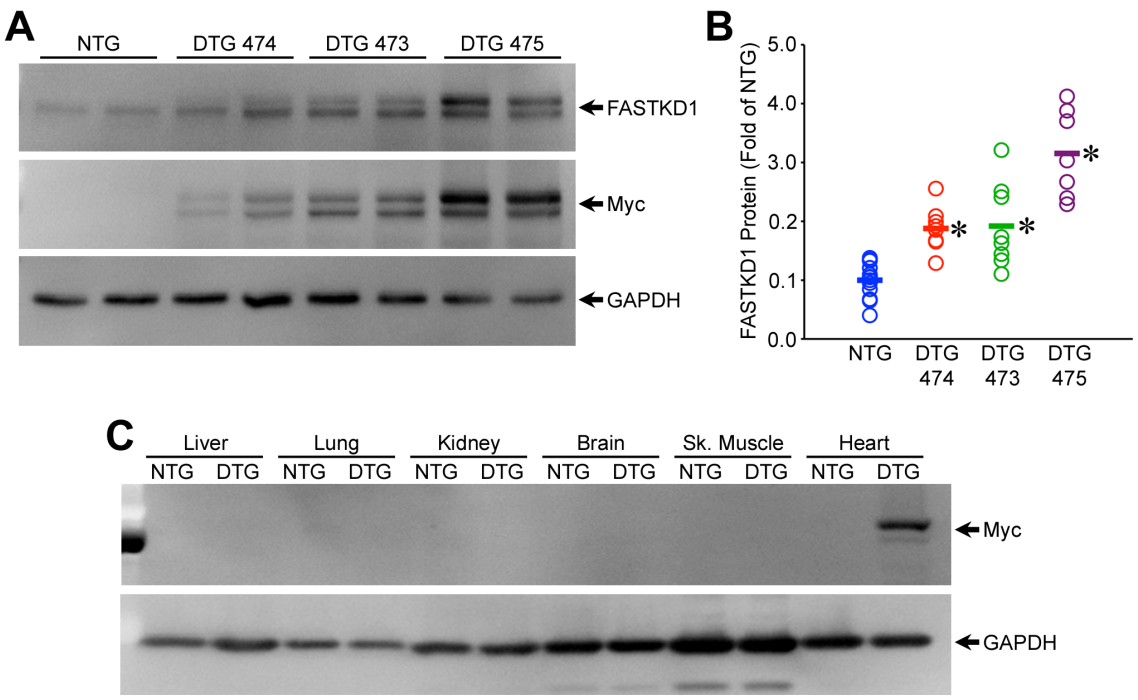

Figure 9. Development of cardiac specific FASTKD1 overexpressing mouse lines.

A. Representative Western blot of whole heart homogenate from NTG and DTG mice from lines 474, 473 and 475. Immunoblotting was performed for FASTKD1, Myc-tagged overexpressed FASTKD1 and GAPDH was used as a loading control. B. Densitometry was performed on NTG and DTG mice from lines 474, 473 and 474 for total FASTKD1 expression (n = 7-14 per group). C. Representative Western blot from line 475 depicting cardiac specific overexpression of Myc-tagged FASTKD1 in DTG whole tissue homogenate compared to NTG control tissue. GAPDH was used as a loading control (n = 3 NTG/DTG pairs per line). *$p<0.05$ versus NTG.

blotting for the Myc-tagged FASTKD1 transgene product in a variety of tissue types (**Figure 9C**).

4.2 Characterization of inducible cardiac-specific FASTKD1 overexpressing mouse lines

The three mouse lines generated were subjected to functional characterization to determine whether FASTKD1 overexpression altered basal cardiac function and morphology. DTG hearts from the three mouse lines displayed normal gross cardiac morphology compared to NTG controls (**Figure 10A**). Gravimetric analysis revealed no difference in HW/BW ratio of DTG mice from all three FASTKD1 overexpressing mouse lines compared to NTG mice (**Figure 10B**). To assess fibrosis in DTG hearts, Gomori trichrome staining was performed on longitudinal-sectioned perfusion fixed mouse hearts. DTG mice did not display any overt fibrotic phenotype compared to NTG mice in all three lines tested (**Figure 10C**). Finally, myocyte cross-sectional (CSA) area was measured in DTG and NTG mice from the three FASTKD1 overexpressing mouse lines by planimetry in wheat-germ agglutinin stained, longitudinal cryo-sections (**Figure 10D, 10E**). Analysis revealed a slight but not significant decrease in myocyte CSA in DTG mice from lines 473 and 475 compared to NTG mice. DTG mice from line 474 displayed similar myocyte CSA compared to NTG mice. Thus FASTKD1 DTG mice appear normal, both morphologically and histologically. To assess cardiac function *in vivo*, NTG and DTG mice from all three FASTKD1 overexpressing lines were subjected to echocardiographic analysis. Increasing levels of FASTKD1 protein as seen in the three transgenic mouse lines did not alter fractional shortening, a measure of cardiac function (**Figure 10F**). Similarly, left ventricular dimensions at end systole and

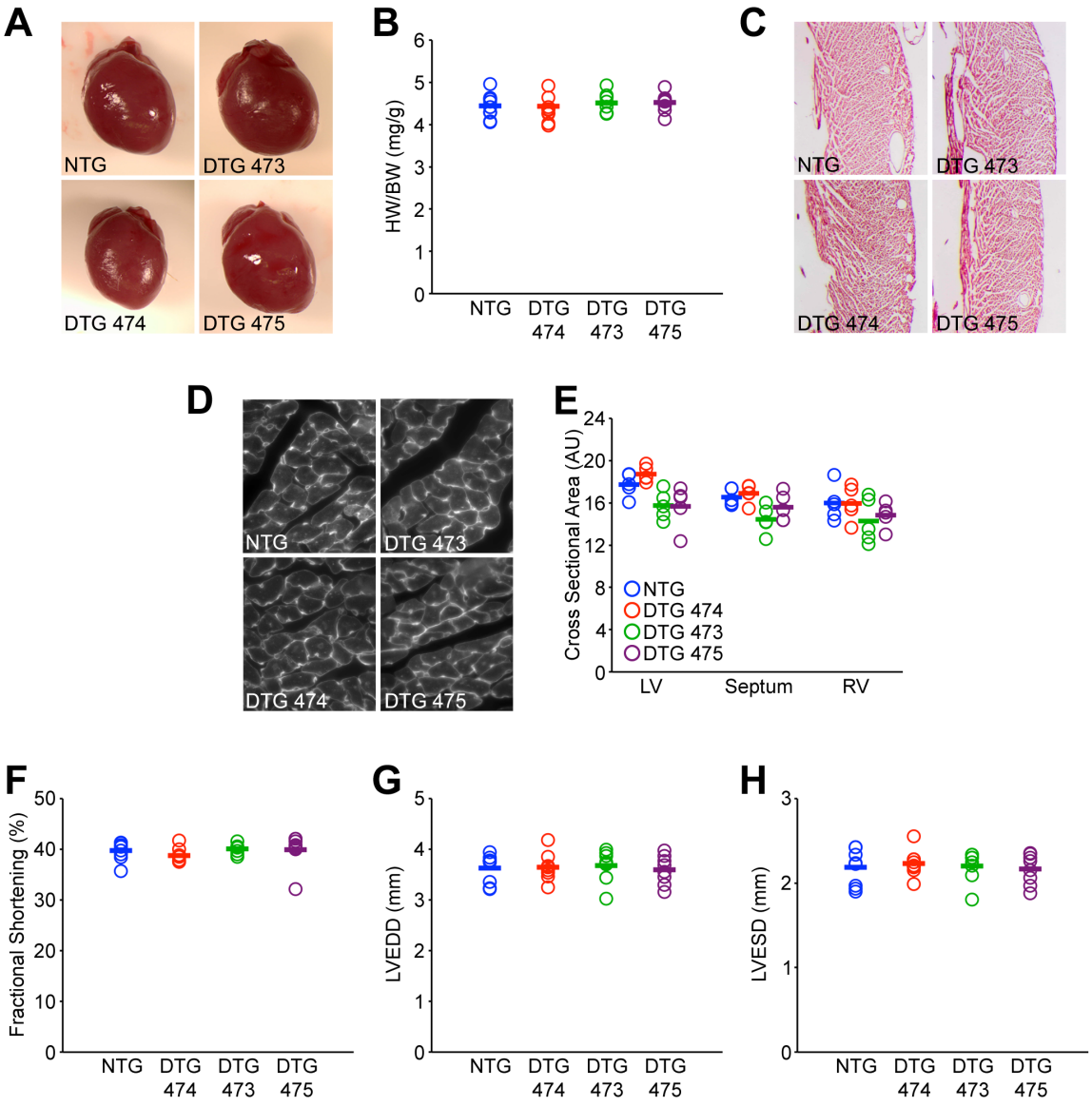

Figure 10. Characterization of cardiac specific FASTKD1 overexpressing mouse lines. A. Representative images of hearts excised from 8-12 week old NTG and DTG mice from lines 474, 473 and 475. B. Calculation of HW/BW ratio of DTG mice from lines 474, 473 and 475 mice compared to NTG controls at 8-12 weeks of age mice (n = 9-12). C. Representative images of trichrome stained heart sections from NTG and DTG mice from lines 474, 473 and 475 perfused and fixed at 8-12 weeks of age (n = 5, imaged at 4.2x magnification). D. Representative images of WGA stained mouse heart sections

from NTG and DTG mice from lines 474, 473 and 475 (n = 5, imaged at 100x magnification). E. Myocyte cross sectional area (CSA) calculated for 8-12 week old NTG and DTG mice from lines 474, 473 and 475 from WGA staining. Myocyte CSA was determined in the left ventricle, septum and right ventricle (n = 5). F. Fractional shortening as determined by echocardiography in male NTG and DTG mice from lines 474, 473 and 475 at 8-12 weeks of age (n = 8-9). G. LVEDD as determined by echocardiography in male NTG and DTG mice from lines 474, 473 and 475 at 8-12 weeks of age (n = 8-9). H. LVESD as determined by echocardiography in male NTG and DTG mice from lines 474, 473 and 475 at 8-12 weeks of age (n = 8-9).

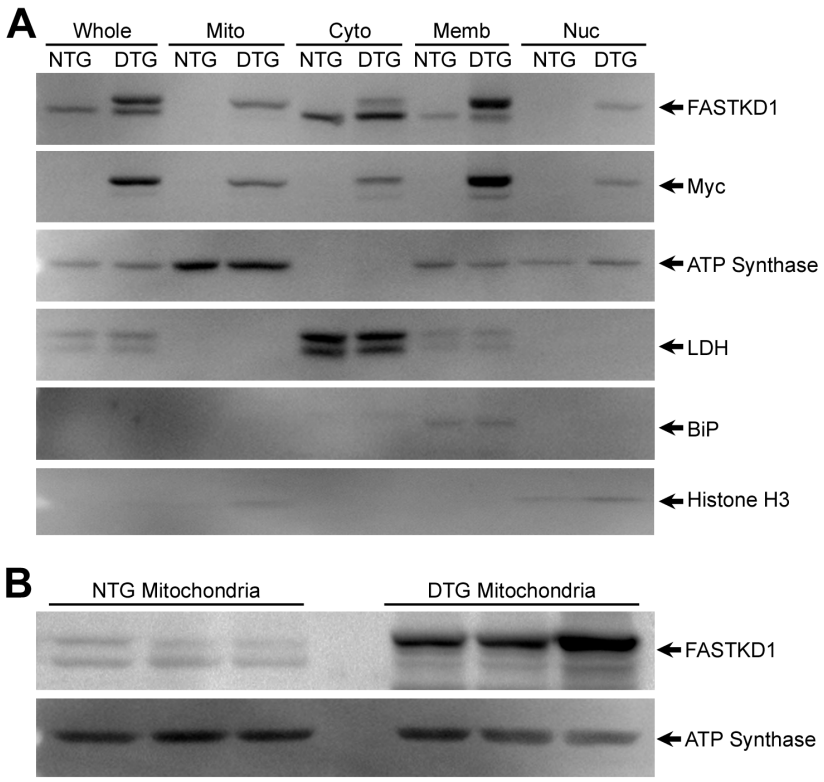

Figure 11. Subcellular localization of FASTKD1 in subfractionated mouse hearts.

A. Representative Western blot image performed on subfractionated mouse hearts from NTG and DTG mice from line 475. Immunoblotting was performed for FASTKD1, Myc-tag, ATP synthase, LDH, BiP and histone H3 (n = 3 NTG/DTG pairs per line). B. Western blot of subfractionated mouse heart mitochondria from NTG and DTG mice from line 475 with immunoblotting performed for FASTKD1 and ATP synthase (n = 3).

end diastole were not altered by manipulation of FASTKD1 protein levels (**Figure 10G, 10H**). These data indicate that FASTKD1 overexpression does not compromise cardiac function at baseline.

4.3 Subcellular Localization of FASTKD1

Overexpressed FASTKD1 has been reported to localize specifically to the mitochondria [118]. Therefore we determined the subcellular localization of both the endogenous and exogenous FASTKD1 (**Figure 11A**). To our surprise, endogenous FASTKD1 was present in the cytosol and membrane cell fractions but not the nuclear or mitochondrial fractions. The transgene was present in all compartments tested (mitochondrial, cytosolic, membrane and nuclear). Similar subcellular distribution of FASTKD1 protein was detected in all three tested mouse lines. Because we did not initially detect endogenous FASTKD1 in the mitochondrial fraction, we performed Western blotting on only mitochondrial isolates from line 475 (**Figure 11B**). Endogenous FASTKD1 was present in the mitochondrial compartment of NTG mice, but at a greatly decreased relative amount compared to DTG mice. This difference in relative abundance could explain our initial failure to identify endogenous FASTKD1 in the mitochondrial compartment of NTG mice. Our transgene shows similar subcellular localization to the endogenous FASTKD1, with a relatively greater abundance of the transgene in the mitochondria.

4.4 FASTKD1 overexpression does not alter mitochondrial respiration or MPT pore function

Because FASTKD1 is known to interact with the known MPT pore sensitizer CypD, we set out to determine if FASTKD1 overexpression modulates MPT pore function *in vivo*. First, to assess whether FASTKD1 overexpression alters protein levels of purported MPT pore components or mitochondrial respiratory components, Western blotting was performed on homogenized cardiac tissue. No significant changes were detected for components of respiratory chain complexes V, III and II, or purported MPT pore components VDAC 1/3, ANT 1/2, PiC or CypD (**Figure 12A, 12B, 12C**). Similar results were obtained in all three mouse lines regardless of FASTKD1 overexpression level. Therefore, FASTKD1 overexpression does not alter expression of a panel of proteins related to mitochondrial respiration or purported MPT pore components. FASTKD1 was previously shown to uncouple Complex I stimulated respiration (unpublished data). Therefore, mitochondrial function was next assessed in isolated cardiac mitochondria. Complex I and II-dependent mitochondrial respiration were measured in isolated cardiac mitochondria from mouse lines 474, 473 and 475. State 2 was defined as basal oxygen consumption without ADP, with state 3 occurring with the addition of ADP and state 4 being measured in the presence of ADP and oligomycin. In the presence of glutamate/malate or succinate, FASTKD1 overexpression did not alter mitochondrial oxygen consumption in states 2, 3 or 4 compared to NTG control mice (**Figure 12D, 12E**). To further study the metabolism of mice overexpressing FASKD1, total cardiac ATP content was elevated in a roughly gene dose-dependent manner with increasing, but not-statistically significant levels of ATP seen in presence of increasing levels of FASTKD1 protein (**Figure 12F**). Next, because we identified FASTKD1 as a novel CypD interacting protein, we tested the effects of FASTKD1 overexpression on MPT

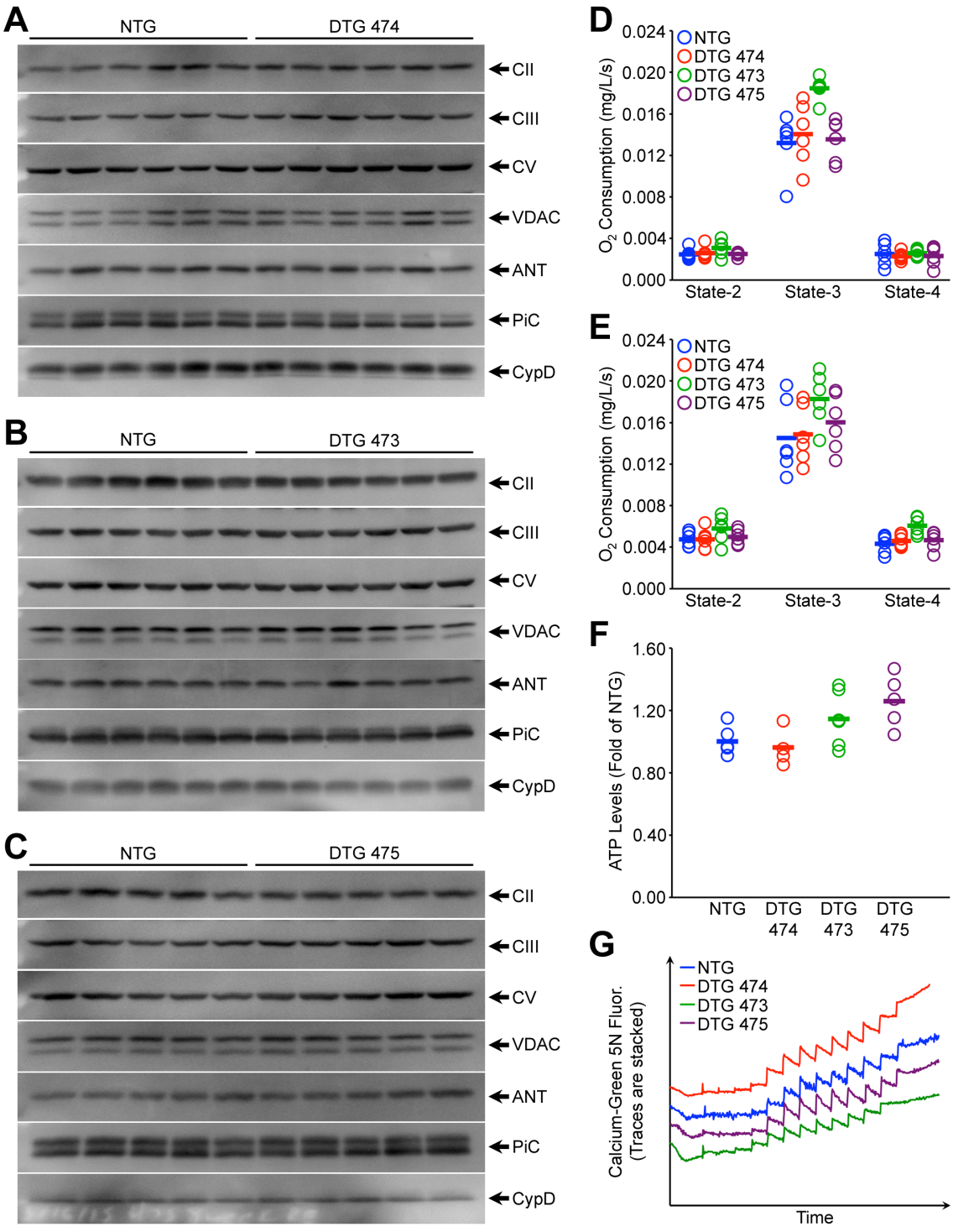

Figure 12. Cardiac myocyte specific overexpression of FASTKD1 does not alter mitochondrial respiration or MPT pore activity. A. Western blotting performed on whole heart homogenates from NTG and DTG mice from line 474 performed on whole

heart homogenate and probed for succinate dehydrogenase B (Complex II), Complex III subunit core 2 (Complex III), ATP synthase subunit alpha (Complex V), Voltage Dependent Anion Channel (VDAC), Adenine nucleotide translocase (ANT), mitochondrial phosphate carrier (PiC) and Cyclophilin D (CypD) (n = 6). B. Western blotting performed on whole heart homogenates from NTG and DTG mice from line 473 performed on whole heart homogenate and probed for Complex II, Complex III, Complex V, VDAC, ANT, PiC and CypD (n = 6). C. Western blotting performed on whole heart homogenates from NTG and DTG mice from line 475 performed on whole heart homogenate and probed for Complex II, Complex III, Complex V, VDAC, ANT, PiC and CypD (n = 5). D. Glutamate/Malate stimulated complex I respiration as measured in isolated from heart mitochondria from NTG and DTG mice from lines 474, 473 and 475 (n = 6). E. Succinate stimulated complex II respiration as measured in isolated from heart mitochondria from NTG and DTG mice from lines 474, 473 and 475 (n = 6). F. Total ATP content from whole heart homogenate from NTG and DTG mice from lines 474, 473 and 475 (n = 4-6). G. Representative fluorescence versus time traces of isolated heart mitochondria from NTG and DTG mice from lines 474, 473 and 475 subjected to calcium retention capacity measurement (n = 6).

pore activity as assessed by calcium retention capacity (CRC) on succinate energized cardiac mitochondria (**Figure 12G**). CRC was not affected by FASTKD1 overexpression in isolated mitochondria in all three lines tested. Thus, FASTKD1 overexpression does not modulate mitochondrial oxygen consumption or MPT pore activity in isolated cardiac mitochondria.

4.5 FASTKD1 overexpression prevents left ventricular free wall rupture in a mouse model of myocardial infarction

Next, because myocardial infarction is associated with elevated ROS, we performed permanent coronary ligation surgeries on the high expressing, line 475 mice [145,170]. Following permanent coronary ligation, mice then had echocardiography performed at 8-weeks post MI, before sacrifice and tissue collection. Eight-week survival was significantly different between NTG (28.57%) and DTG (75%) mice (**Figure 13A**). A majority of this difference was due to left ventricular free wall rupture with ~40% of NTG mice suffering from this fatal event, while no DTG mice experienced this post-surgical complication. Rupture occurred between days 3 and 7 post-MI. Similar rates of rupture were detected in a subset of tTA and TG mice following MI compared to NTG mice (not shown). Ruptures were detected in both the scar and border region and were detected by the presence of blood clots in the chest cavity and a visible defect in the left ventricle (**Figure 13B**). One NTG and one DTG mouse died later than 1-week post-MI. Cause of death in both of these cases was undetermined as no blood or fluid (indicating heart failure) was present in the chest cavity during necropsy. Scar size was not significantly different between NTG and DTG mice subjected to MI 8-

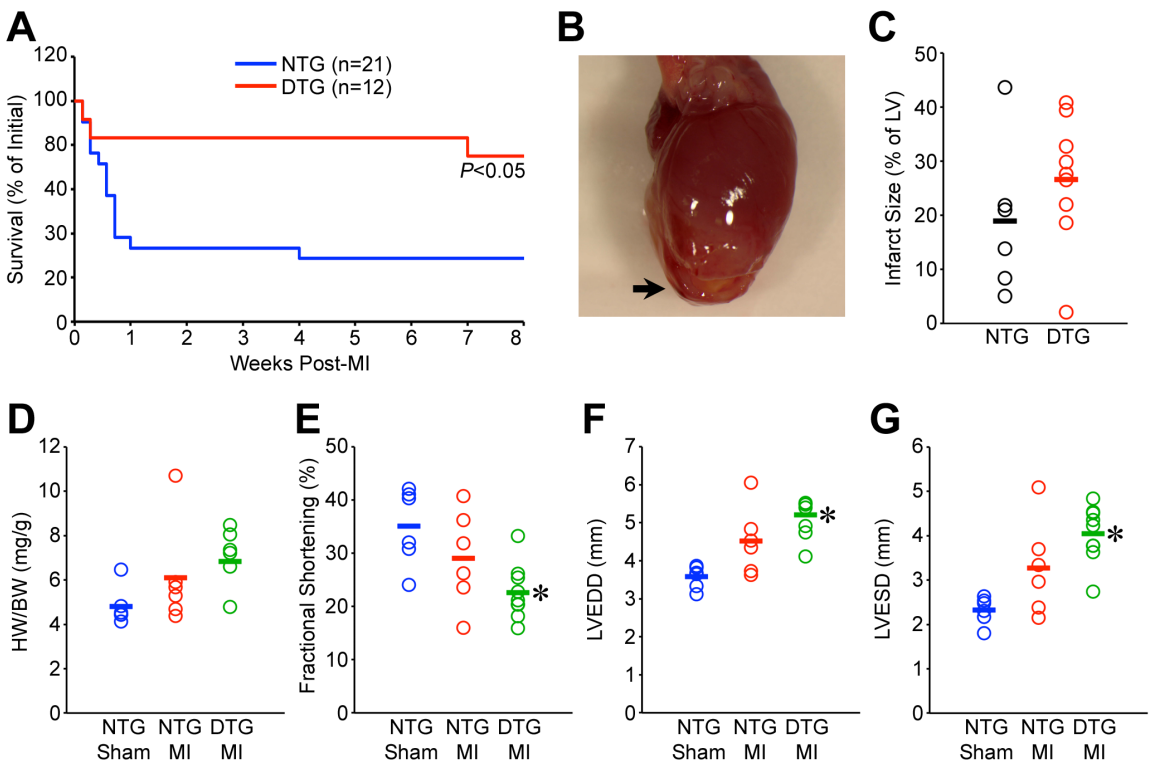

Figure 13. Cardiac myocyte specific overexpression of FASTKD1 in line 475 prevents left ventricular rupture in a mouse model of MI. A. Survival curves for NTG and DTG mice subjected to 8-weeks of permanent coronary ligation. B. Representative image of NTG heart following left ventricular rupture displays compromised LV integrity. Arrow denotes point of rupture. C. Infarct size analysis as determined by LV planometry of NTG and DTG mice following 8-weeks of permanent coronary ligation. D. HW/BW ratio calculated in NTG sham, NTG MI and DTG MI operated mice 8-weeks post-MI. E. Fractional shortening as determined by echocardiography in NTG sham, NTG MI and DTG MI operated mice 8-weeks post-MI. F. LVEDD as determined by echocardiography in NTG sham, NTG MI and DTG MI operated mice 8-weeks post-MI. G. LVESD as determined by echocardiography in NTG sham, NTG MI and DTG MI operated mice 8-weeks post-MI. *p<0.05 vs NTG Sham. NTG Sham n = 6, NTG MI n = 6, DTG MI n = 9 survivors at 8-weeks post MI.

weeks post injury as measured by planimetry of the left ventricle (**Figure 13C**). However, because NTG mice experienced significantly higher rates of left ventricular rupture, it is possible that mice of this genotype with larger infarcts were selected against, and thus did not survive the full 8-week study. DTG mice showed a significant elevation in HW/BW ratio 8-weeks post MI versus NTG sham mice (**Figure 13D**). NTG mice displayed a slight but not statistically significant elevation in HW/BW ratio versus NTG sham mice, which again could be due to selection against larger infarcts in this genotype. MI significantly decreased cardiac function as assessed by echocardiographic measure of fractional shortening in DTG mice compared to NTG sham operated mice 8-weeks after coronary ligation (**Figure 13E**). Echocardiographic measurement of left ventricular dimensions revealed increased systolic and diastolic chamber sizes in DTG MI mice compared to sham operated NTG mice (**Figure 13F, 13G**). Thus FASTKD1 DTG mice demonstrated worse cardiac function and increased chamber dimensions following MI compared to NTG mice. However FASTKD1 completely prevented left ventricular free wall rupture.

Because we observed a significant decrease in cardiac rupture events in DTG mice compared to NTG mice after MI, we sought to explore this phenomenon. An earlier time point of sacrifice was chosen to avoid the confounding variable of rupture and allowed us to dissect the possible mechanisms leading to this fatal complication of MI. Mice were subjected to 3 days of MI followed by echocardiography and sacrifice. This time point corresponded with the onset of left ventricular rupture in NTG mice, in hopes of eliminating any selective effects this event would cause. Infarct size was measured by

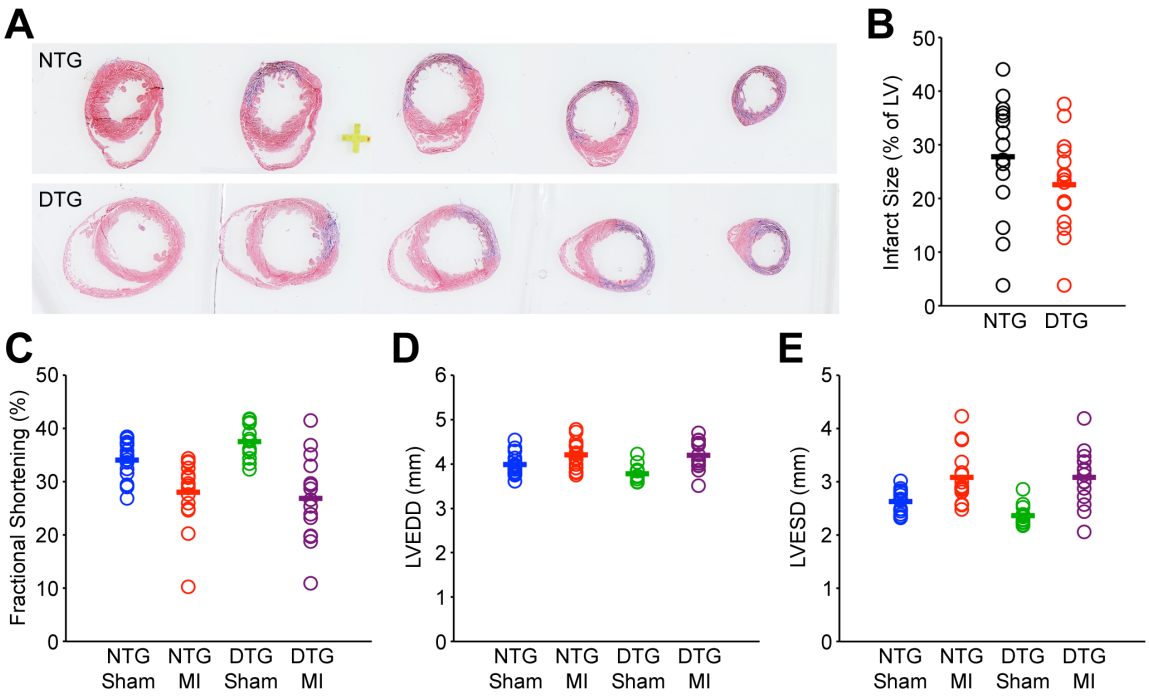

Figure 14. Cardiac myocyte specific overexpression of FASTKD1 in line 475 does not alter scar size or improve cardiac function 3-Days post MI. A. Representative serial heart sections (1 mm apart) subjected to trichrome staining of NTG and DTG following 3 days of permanent coronary occlusion. B. Infarct size as a percent of total LV area determined by trichrome staining of serial sections 3 days after MI in NTG and DTG mice. C. Fractional shortening as determined by echocardiography in NTG sham, NTG MI, DTG sham and DTG MI operated mice 3 days post-MI. D. LVEDD as determined by echocardiography in NTG sham, NTG MI, DTG sham and DTG MI operated mice 3 days post-MI. E. LVESD as determined by echocardiography in NTG sham, NTG MI, DTG sham and DTG MI operated mice 3 days post-MI. NTG Sham n = 15, NTG MI n = 15, DTG Sham n = 13, DTG MI n = 15.

serial sectioning of hearts followed by trichrome staining (**Figure 14A**). Infarct size was not statistically different between NTG and DTG mice 3-days post MI (**Figure 14B**). Functional assessment of fractional shortening by echocardiography revealed similar deficits in NTG and DTG mice compared to respective sham operated controls (**Figure 14C**). Additionally, chamber dilation at both end systole and end diastole was detected in both NTG and DTG mice compared to sham operated controls (**Figure 14D, 14E**). However, none of these MI induced changes reached statistical significance. Thus, three days of coronary ligation induced an equal degree of cardiac dysfunction in NTG and DTG mice, with FASTKD1 failing to provide any significant protections in terms of scar size or function.

To better understand the mechanism by which cardiac myocyte specific overexpression of FASTKD1 protects hearts from MI induced left ventricular rupture, mediators of cardiac wound healing were investigated. A subset of NTG and DTG mice (n=5 per group) that had undergone MI was selected for further immunohistological analysis. These mice displayed similar infarct areas. Because of their important role in mediating early inflammation and repair following MI, neutrophils and macrophages were chosen for analysis. Neutrophils were detected using an anti-NIMP antibody and were present in both the border and scar region of mice following MI (**Figure 15A**). Interestingly, neutrophils were decreased in the border zone and scar in DTG versus NTG mice following MI (**Figure 15B**). Next, macrophages were detected in the border and scar region of NTG and DTG mice following MI using an anti-F4/80 antibody (**Figure 15C**). Elevated levels of macrophages as measured by F4/80 positive cells were found in both

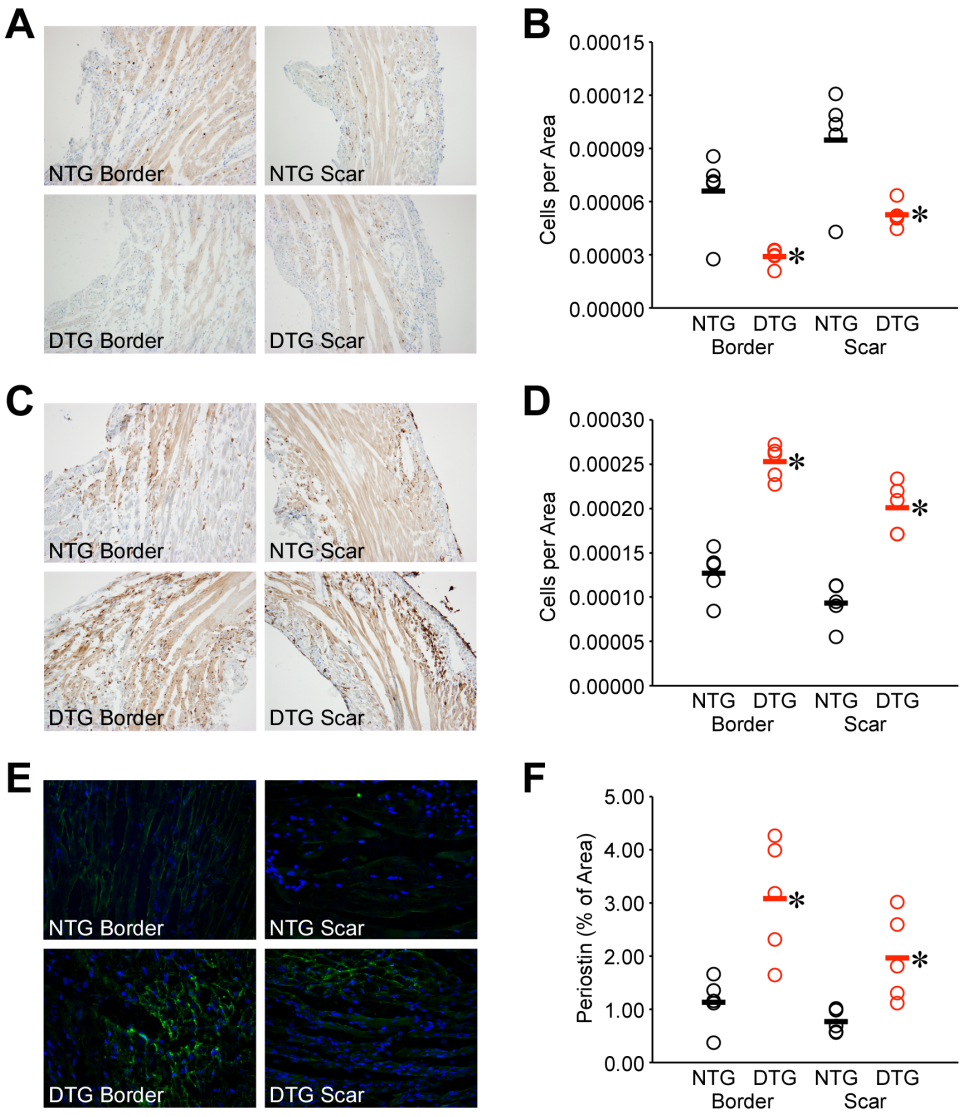

Figure 15. Cardiac myocyte specific overexpression of FASTKD1 in line 475 alters inflammatory cell infiltration and ECM accumulation post-MI. A. Representative images of heart sections from NTG and DTG mice stained for NIMP to identify neutrophils in the border and scar region 3-days post MI (n = 5, imaged at 20x magnification). B. Quantification of neutrophil accumulation in the border and scar region 3-days post MI of NTG and DTG mice (n = 5). C. Representative images of heart sections from NTG and DTG mice stained for F4/80 to identify macrophages in the border and scar region 3-days post MI (n = 5, imaged at 20x magnification). D.

Quantification of macrophage accumulation in the border and scar region 3-days post MI of NTG and DTG mice (n = 5). E. Representative images of heart sections from NTG and DTG mice stained for periostin from the border and scar region following 3-days of MI (n = 5, imaged at 40x magnification). F. Quantification of periostin as a percent of total area in the border and scar region 3-days post MI of NTG and DTG mice (n = 5). *$p<0.05$ versus NTG.

the border zone and scar region in DTG compared to NTG mice following MI (**Figure 15D**). These data indicate that FASKD1 overexpression modulates the response of the inflammatory system to experimental MI, resulting in a decreased presence of neutrophils and an increased presence of macrophages. Inflammatory cells can influence the wound healing process and processing of extracellular matrix (ECM). Because of this, we analyzed levels of the ECM component periostin. Periostin was detected in both the border and scar regions of hearts post-MI in both NTG and DTG mice (**Figure 15E**). However, levels of periostin as assessed by immunohistochemistry were elevated in the border and scar regions of the heart in DTG mice compared to NTG mice 3-days after MI (**Figure 15F**). Consequently, in addition to modulating inflammatory cell recruitment following MI, FASTKD1 overexpression modulates composition of the ECM.

5. Discussion

Heart disease is a major cause of morbidity and mortality worldwide. Novel strategies aimed at reducing cardiac damage in response to this noxious stimulus are critical. Reducing cell death following MI is known to reduce infarct size in mouse models of MI [210]. We have previously shown that FASTKD1 protects cells from oxidative stress-induced cell death *in vitro* (unpublished data). To the best of our knowledge, this is the first study of FASTKD1 function *in vivo*.

The major finding of this study is that cardiac-myocyte specific overexpression of FASTKD1 prevents left ventricular rupture in a mouse model of MI induced by permanent coronary artery occlusion. Although increasingly rare in the post-reperfusion

era, left-ventricular free wall rupture remains a major cause of post-MI mortality [171]. While only roughly 3% of patients will suffer from left ventricular rupture following MI, a staggering 75% of them will die from this complication accounting for 10% – 20% of total MI related deaths [186]. In humans, left ventricular rupture occurs mainly between three and ten days post-MI [172]. In mice, left ventricular rupture occurs during the first ten days following MI, with peak rates at two to six days, with rates reported in FVB/N mice ranging from 3% - 60% [173,174]. Therefore, mice represent a useful model for studying this process. Strategies aimed at reducing the incidence of left ventricular rupture remain important and can significantly reduce the risk of death following MI. MI induced non-significant functional deficits and an elevation in HW/BW ratio as early as 3-days post-MI which reached statistical significance at study termination 8-weeks post-MI. Analysis of survival data revealed that FASTKD1 overexpression completely prevented death due to left ventricular rupture. This finding has very important implications for the interpretation of our findings in the 8-week MI study. We noted that a large percentage of NTG mice underwent left ventricular rupture following MI. This process is known to be at least partially dependent on infarct size [211]. Mice with larger infarcts are known to be more prone to left ventricular rupture compared to mice with relatively smaller infarcts. It is possible that our study selected against mice with relatively larger infarcts in the NTG group, leaving only mice with relatively smaller infarcts 8-weeks post-MI. FASTKD1 overexpression may very well modulate infarct size, however this could not be determined in the current study due to mortality in the NTG mice. In the future the 8-week MI experiment could be repeated using female mice, as these mice have been shown to be more resistant to left ventricular rupture than their male counterparts [180].

However, this may mask any findings involving matrix deposition, remodeling and inflammation as female mice show changes in these parameters compared to male mice and our findings point toward altered inflammatory processes and possible changes in remodeling.

Because our initial MI study resulted in left ventricular rupture in NTG mice and not DTG mice, we undertook a study utilizing a 3-day MI model. While 3-days of MI did induce changes in cardiac function and chamber size as assessed by echocardiography, these changes did not reach statistical significance. This finding was not entirely unexpected as 3-days represents the limit of detection for changes in cardiac function in the FVB/N mouse strain [212]. This time point was chosen based on the finding that the inflammatory response and remodeling are present 3-days post MI in the mouse and this relatively early time point avoids the confounding variable of rupture [185]. The finding that FASTKD1 overexpression resulted in protection from left ventricular rupture was associated with decreased neutrophil and enhanced macrophage infiltration into the ischemic zone points towards a role for FASTKD1 in the post-MI wound healing process. Reductions in oxidative stress are associated with a decreased rate of rupture [185]. It has been previously shown that macrophage recruitment to the site of MI is a critical step for healing. In fact, reduced macrophage recruitment is linked to insufficient neutrophil clearance and an enhanced propensity toward rupture [181]. The data presented herein fit nicely with this finding. Cells of the inflammatory/immune system are crucial for scar formation as they mediate the clearing of necrotic tissue and cell debris and regulate formation and degradation of the extracellular matrix [175]. Macrophages in the infarct

zone are not just important for clearing necrotic cell and tissue debris, but can also mediate healing, matrix deposition and cell survival [213].

Macrophages can be broadly split into M1 inflammatory and M2 reparative subgroups with very different characteristics, however, this could be an oversimplification of the phenotypic characteristics of cardiac macrophages [214]. Interestingly, the switch from M1 to M2 type macrophage can be mediated by the engulfment and digestion of apoptotic neutrophils [215]. Decreased neutrophils present in the NTG hearts could be indicative of enhanced engulfment by elevated number of macrophages and increased M2 polarization resulting in abatement of the inflammatory response and stable scar formation. However, we can only speculate on why there are decreased neutrophils present in the DTG myocardium. This could be a result of decreased recruitment to the site of injury, decreased neutrophil presence in DTG mice at baseline or enhanced neutrophil clearance. Additionally, the hypothesis of macrophage polarization is only speculative as markers of M1 and M2 macrophages were not examined. Also, we cannot definitively state the cause of elevated presence of macrophages observed in the current study in FASTKD1 overexpressing mice following MI. DTG mice may have elevated levels of macrophages at baseline, have enhanced recruitment or even decreased clearance. Although, there are data pointing towards an enhanced inflammatory response leading to left ventricular rupture [211], it is also possible that the altered inflammatory response seen in DTG mice is not responsible for their protection from left ventricular rupture. Reducing the loss of cardiomyocytes following MI has proven an effective tool for decreasing the rate of rupture as partial ablation of p53 prevents left ventricular rupture following MI in a

process independent of inflammatory cell involvement or extracellular matrix alterations [187]. Additionally, partial ablation of p53 exerts its protective effects without modulating overall infarct size. Findings in a rat model of coronary ligation show that caspase inhibition can be protective following MI, however because this model does not show the same propensity for rupture as mice, findings on this complication are unavailable [216].

DTG mice displayed elevated levels of the ECM component periostin compared to NTG mice 3-days after MI. Periostin is an extracellular matrix component secreted by fibroblasts that is critically involved in healing following MI [172]. Importantly, elevated levels of periostin can be detected as early as 3-days post-MI [217]. Mice lacking periostin are more susceptible to left ventricular rupture than control mice following MI [218,219]. Additionally, strategies aimed at protecting the heart and reducing rupture such as overexpression of the chaperone protein melusin are associated with increased periostin expression compared to control mice following MI [174]. FASTKD1 overexpression may result in early recruitment of fibroblasts and enhanced wound healing compared to control mice as evidenced by elevated levels of periostin in the hearts of DTG mice compared to NTG mice following MI.

It is not clear at this point how the cardiac myocyte-restricted FASTKD1 is leading to these altered inflammatory and ECM responses, and hence decreased rupture, in the context of MI. As indicated above, decreased myocyte death would reduce alarmin release, which in turn would influence the inflammatory response and ECM deposition. Members of the FASTK family all contain N-terminal mitochondrial targeting sequences

[118] and FASTKD1 is reported to localize to the mitochondria in both humans and mice [220,221]. Therefore, it is possible that alterations in the myocytes mitochondrial function are cytoprotective. In this regard we found that endogenous cardiac FASTKD1 is localized to the mitochondria. However, endogenous FASTKD1 appeared in the mitochondria at a relatively lower concentration than the transgene, and was nearly undetectable compared to endogenous cytosolic FASTKD1. Moreover, while we initially identified FASTKD1 as a CypD interacting protein, cardiac myocyte specific overexpression did not alter MPT pore function in isolated cardiac mitochondria. Additionally, because FASTKD3 is critical for mitochondrial oxygen consumption, we tested the effects of FASTKD1 overexpression in isolated cardiac mitochondria [118]. However, no effects on mitochondrial oxygen consumption or expression of mitochondrial respiratory chain components were detected in our model, and ATP levels were not significantly altered. Thus altered mitochondrial function appears unlikely to play a role in FASTKD1's effects. Interestingly, non-mitochondrial roles of FASTK family members are plentiful. FASTK, the founding member of this protein family has roles in the cytoplasm and nucleus in addition to the mitochondria [120,121,123,125]. Additionally, mitochondrial localization of FASTKD2 is not required for its pro-apoptotic effects in breast cancer cells [131]. Thus, FASTKD1 may exert its effects outside of the mitochondria. It may be that myocyte death is unaltered *per se* by FASTKD1 overexpression, but the proteomic signature of alarmins released by the dying cells is altered in such a way that the subsequent recruitment of inflammatory cells and ECM deposition is modified to generate a stronger scar that is resistant to rupture. Alternatively FASTKD1 expression may modify the secretion of proteins from intact

myocytes that influence the resident non-myoctic cells. Finally it maybe that release of FASTKD1, either by secretion or during myocyte necrosis, directly mediates these effects. Current studies are underway to test these possibilities.

In summary, here we show for the first time that endogenous FASTKD1 localizes to the mitochondria of the heart *in vivo*, but is not exclusively mitochondrial as has previously proposed in cell culture. Its overexpression does not result in any deleterious effects *in vivo*, and it may function as a novel protective protein. Additionally, the finding of this study that FASTKD1 prevents left ventricular rupture opens up a novel area of study for this mitochondrial protein. The idea that myeloid cells can alter the propensity of a heart to rupture is relatively new with the finding that secreted factors from myocytes can protect the heart from rupture [222]. Further investigations are required to determine the molecular mechanism by which FASTKD1 mediates altered healing in the post-MI heart and whether this protection can be applied to other models of disease.

Chapter 4: Conclusions and Future Directions

We initially identified FASTKD1 as a novel CypD interacting protein that localizes to the mitochondria [118,220,221]. Our initial hypothesis was that FASTKD1 would modulate MPT pore function and therefore cell death due to its interaction with CypD. This hypothesis fits well with the finding that members of the FASTK family of proteins are involved in diverse cellular processes including cell death as both pro- and anti-apoptotic proteins [121,131]. FASTKD1 is elevated in endometrial carcinoma and its elevation is associated with a poor prognosis in lymphocytic leukemia [127,128]. Based on these findings, elevated levels of FASTKD1 could play a protective role in cancer cells, by preventing them from undergoing cell death. Here we show that 1) FASTKD1 overexpression protects and knockdown sensitizes cells to oxidative stress-induced cell death independently of the MPT pore or modulation of the endogenous antioxidant system, 2) FASTKD1 modulates mitochondrial morphology and mitochondrial function, and 3) cardiac myocyte specific FASTKD1 overexpression prevents left ventricular free wall rupture (LVFWR) in a mouse model of MI.

In Aim 1, we investigated the role of FASTKD1 in ROS induced cell death and mitochondrial function *in vitro*. We initially set out to study FASTKD1 as a potential modulator of the MPT pore and therefore cell death. Both ROS and calcium are known to open the MPT pore [58,59]. Cell death in response to both ROS and calcium overload were tested in this study; with FASTKD1 manipulation only modulating ROS induced cell death. Additionally, CypD is a known MPT pore sensitizing protein, and its deletion makes cells resistant to ROS induced cell death [63]. FASTKD1 overexpression further

protected cells lacking CypD from ROS induced cell death. We are the first to identify FASTKD1 as a novel modulator of cell death *in vitro*. Furthermore, because mitochondria are major cellular sources of ROS and have a highly developed antioxidant system, we tested whether manipulation of FASTKD1 levels alters the level of or capacity of the antioxidant system [148]. FASTKD1 does not alter cell death via manipulation of the cellular antioxidant system.

Additionally, mitochondria are dynamic organelles that constantly undergo fission and fusion to maintain cellular homeostasis [193]. Surprisingly, modulation of FASTKD1 expression altered mitochondrial morphology *in vitro*. Overexpression of FASTKD1 was associated with a decrease in Mfn1 expression, which could explain increased mitochondrial fragmentation associated with this treatment. Knockdown of FASTKD1 decreased mitochondrial fragmentation. Interestingly, no change in total mtDNA was seen with FASTKD1 overexpression, indicating that alterations in mitochondrial fragmentation seen in the present study were independent of enhanced mitophagy.

In Aim 2, we tested the role of FASTKD1 overexpression *in vivo*. We performed these experiments using an inducible cardiac myocyte specific overexpression mouse model. Based on *in vitro* results, we hypothesized that FASTKD1 overexpression would protect mice from oxidative stress induced injury, including coronary ligation induced MI.

Cardiac myocyte specific overexpression of FASTKD1 did not result in any overt deleterious effects in our mouse model. FASTKD1 overexpressing mice showed normal cardiac morphology, mitochondrial oxygen consumption and MPT pore function compared to control mice. FASTKD1 overexpression resulted in a relatively small

decrease in myocyte cross-sectional area and did not alter total cardiac ATP content, both of which were not statistically significant. Additionally, FASTKD1 overexpression did not alter basal cardiac function as assessed by echocardiography. FASTKD1 overexpression did prevent LVFWR following MI, which was associated with enhanced macrophage infiltration, and decreased neutrophil infiltration into the MI scar area. Additionally, FASTKD1 overexpressing mice displayed alterations in ECM componentry with enhanced periostin deposition being present 3-days post-MI.

1. Discussion of Initial Hypothesis

1.1 Aim 1 Hypothesis

We initially identified FASTKD1 as a novel CypD interacting protein, and therefore hypothesized that it would modulate cell death via the MPT pore. Our hypothesis was proven correct in that FASTKD1 was demonstrated to modulate cell death. However, the protection seen with overexpression and the sensitization observed with knockdown were limited to ROS oxidative stress-induced cell death. Further study using MEFs showed that FASTKD1 protected cells from ROS induced cell death independently of the MPT pore and even its interaction with CypD. Additional experiments showed that FASTKD1 also did not modulate the cellular antioxidant system. Further experimentation revealed that FASTKD1 overexpression did not modulate basal levels of autophagy (**Appendix Figure 17**). While performing the above studies, we noted that modulation of FASTKD1 levels altered mitochondrial morphology, which we quantified objectively via immunocytochemistry and mitochondrial fragmentation scoring. This modulation of

mitochondrial morphology was independent of CypD, as MEFs lacking CypD still showed altered mitochondrial morphology following modulation of FASTKD1 levels (**Appendix Figure 18**). FASTKD1 also altered mitochondrial function as assessed by mitochondrial oxygen consumption using a Clark type electrode with digitonin permeabilized MEFs. Complex I respiration was significantly uncoupled with FASTKD1 overexpression. Mitochondria showed significant changes in $\Delta\psi_m$ with modulation of FASTKD1 protein levels.

While we cannot identify a mechanism by which FASTKD1 modulates cell death, mitochondrial morphology or mitochondrial function, it is clear that this protein is critical in the mitochondria. It presents a novel target for future manipulation and study in cell death and metabolism.

1.2 Aim 2 Hypothesis

Because FASTKD1 showed promise as a cytoprotective protein *in vitro* we developed an inducible, cardiac specific FASTKD1 overexpression model. We used this model to test our hypothesis in Aim 2 that, cardiac myocyte specific overexpression of FASTKD1 will protect mice from experimental MI induced cardiac dysfunction and cardiac injury.

Contrary to our initial hypothesis, FASTKD1 overexpression did not preserve cardiac function or decrease injury area as assessed by scar size 3-days or 8-weeks following experimental MI induced by coronary ligation. However, FASTKD1 transgenic mice were protected from LVFWR compared to control mice. This protection was associated with enhanced non-myocyte cell infiltration into the scar border region 3-days post-

injury. FASTKD1 overexpression increased macrophage and decreased neutrophil infiltration into the border zone and scar. Additional changes in ECM were detected with enhanced periostin deposition being present in FASTKD1 overexpressing mice 3-days post-MI. It is possible that larger scars were selected against in NTG mice because larger scar size is associated with an enhanced propensity toward LVFWR [211]. FASTKD1 overexpression may indeed decrease scar size but this could not be determined within the design of this study.

While we have not identified the cellular mechanism by which FASTKD1 protects the heart from LVFWR, FASTKD1 overexpression presents a novel mechanism to prevent this deleterious side effect of MI. Additionally, we show that endogenous FASTKD1 localizes to the mitochondria in the heart. Future studies are required to determine FASTKD1's effects as either an immune-modulator or cytoprotective protein *in vivo*.

2. Potential Limitations

The studies presented herein encompass both *in vitro* and *in vivo* methodologies. The use of primary and physiologically relevant cell culture models was an attempt to apply this work directly to human physiology and pathology. Additionally, by performing *in vivo* experiments and testing FASTKD1 overexpression in a physiologically relevant disease model, we attempted to make our results translatable to human disease. However, these studies were not without limitations.

2.1 Time Course and Location of Protein Expression

The methods used to express FASTKD1 *in vitro* and *in vivo* differed in the studies performed. In the cell culture studies, FASTKD1 was transiently overexpressed using an adenovirus. Adenovirus studies lasted a relatively short forty-eight hours, and resulted in overexpressed FASTKD1 protein localizing to the mitochondria. This finding was consistent with previous studies that overexpressed FASTKD1[118]. In the *in vivo* studies, FASTKD1 was constitutively overexpressed. While the system allowed expression to be turned off, we performed our studies under chronic overexpression. Overexpressed protein localized to all four cellular compartments analyzed via Western blotting (cytosol, mitochondria, membrane and nucleus) while endogenous FASTKD1 appeared in all subcellular compartments studied except the nucleus. Endogenous FASTKD1 was present at nearly undetectable levels in the mitochondria using Western blotting. It was only when we performed Western blotting on only mitochondrial lysates at a relatively greater protein concentration that we detected endogenous FASTKD1 in the mitochondria. This was consistent with previous results, as FASTKD1 has been reported as a mitochondrial protein in prior studies [118,220,221]. Previously, endogenous FASTKD1 has only been found in the mitochondria of the liver and large intestine in both humans and mice *in vivo*. In this study, protein localization was only analyzed in mouse hearts under normal conditions. It is unknown if FASTKD1 could translocate to the mitochondria during specific physiological or pathological processes, thus increasing its relative mitochondrial concentration. Differences in the results attained from our studies could arise from the short versus long-time courses studied (i.e. 48 hours vs. 8-12 weeks), or the tissues being studies (cell culture vs. whole hearts).

Knockdown studies were only performed in mouse embryonic fibroblasts and not the more physiologically relevant NRCM model or *in vivo*. This was only a transient treatment for forty-eight hours. FASTKD1 specific siRNA treatment resulted in significant sensitization of cells to H_2O_2 induced cell death. However, it is unknown what percentage of this knockdown was specific to mitochondrial FASTKD1. It would also be instructive to assess the effects of total FASTKD1 knockout, as a relatively small amount of FASTKD1 could still maintain normal cellular functions.

2.2 Induction of Cell Death

Cell death was induced *in vitro* by various mechanisms. Initially, death was induced by exposure to excess oxidative stress in the form of H_2O_2. H_2O_2 is capable of crossing biological membranes, possibly via aquaporins [150]. It is known that H_2O_2 induces necrotic cell death as opposed to apoptosis [223]. β-lapachone is also a known inducer of necrotic cell death via a ROS dependent mechanism [190,224]. Interestingly, this initiation of cell death may be independent of the MPT pore and programmed necrosis. This finding fits nicely with our data showing that FASTKD1 modulates cell death independently of the MPT pore. Finally, the calcium ionophore ionomycin was used to induce calcium dependent necrotic cell death via the MPT pore [77]. These experiments were performed *in vitro* on single cell types. Additionally, ROS are generally produced within a cell, and are not applied externally such as H_2O_2 in these experiments. However, β-lapachone produces ROS internally, and helps overcome this shortcoming. A more physiological relevant method of inducing cell death could be applied in the future such as modeling ischemia reperfusion injury either chemically or by altering incubator conditions to

simulate this event [225]. However, the use of specific inducers of cell death allows for greater control and decreased variability in experiments. By causing death by a specific mechanism, such as calcium overload or ROS exposure, we can better evaluate and untwist the convoluted mechanisms that underpin cell death.

2.3 Mouse Model of MI

Mice are a common model organism in cardiovascular research and are known to undergo ventricular remodeling in response to experimental MI [226]. In terms of their response to coronary ligation, mice are known to be subject to LVFWR similarly to humans [186]. However, the incidence and context of LVFWR differs greatly between mice and humans. In humans, LVFWR has declined as a post MI complication from 2%-6% in the pre-reperfusion era to as little as 0.2% currently [171]. Nevertheless, patients undergoing LVFWR have an in-hospital mortality rate around 80% [227]. In mice, LVFWR is a spontaneous consequence to experimental MI, but its incidence is highly strain and gender dependent. Male mice and mice of certain strains are primarily affected by LVFWR [173,212]. In humans, women of advanced age are the primary sufferers of LVFWR [186]. Many strains of mice undergo LVFWR at a significantly higher rate than humans.

We show a reduced propensity for LVFWR with FASTKD1 overexpression. This is associated an altered inflammatory cell infiltration. Enhanced neutrophil infiltration into the scar is associated with increased incidence of cardiac rupture [181]. FASTKD1 overexpressing mice displayed reduced neutrophil infiltration into the border zone and scar, which could be responsible for reduced rupture propensity. It is unknown if the reduced presence of neutrophils is due to decreased recruitment or enhanced clearance.

Both of which are possible, as FASTKD1 may decrease the inflammatory signal that initially recruits this early mediator of the inflammatory response. Coupled with the finding that FASTKD1 overexpression results in enhanced macrophage infiltration into the scar and border zone, it is possible that macrophages are merely clearing the neutrophils more rapidly. In terms of enhanced macrophage infiltration, it is unknown if this is due to elevated resident macrophage populations in the heart or increased migration from the blood stream to the site of injury. Additionally, the polarization of these macrophages is unknown. Type M1 macrophages are considered inflammatory while type M2 macrophages are considered reparative [214]. Additionally, this study was performed in male FVBN mice. Contrary to data from humans, female mice are at a reduced risk of LVFWR compared to male mice [180]. This study could be repeated in female mice to avoid the confounding variable of LVFWR to determine if FASTKD1 can prevent MI induced cardiac dysfunction. However, differences in inflammation and remodeling could mask any potential FASTKD1 overexpression effects. Additionally, FVBN mice have highly variable reported rates of rupture. This study could be repeated in the 129sv mouse strain, which is known to be highly rupture prone to confirm our reported results [173]. As to how an intracellular protein that is thought to be localized to the mitochondria could be altering the wound healing response, several mechanisms are possible. FASTKD1 could itself be secreted from stressed or dying myocytes as an "alarmin" and may result in an altered inflammatory response and ECM processing (**Figure 16A**). FASTKD1 could be changing what is secreted from cardiac myocytes resulting in the secretion of some factor such as Reg3β resulting in an altered inflammatory response [181] (**Figure 16B**).

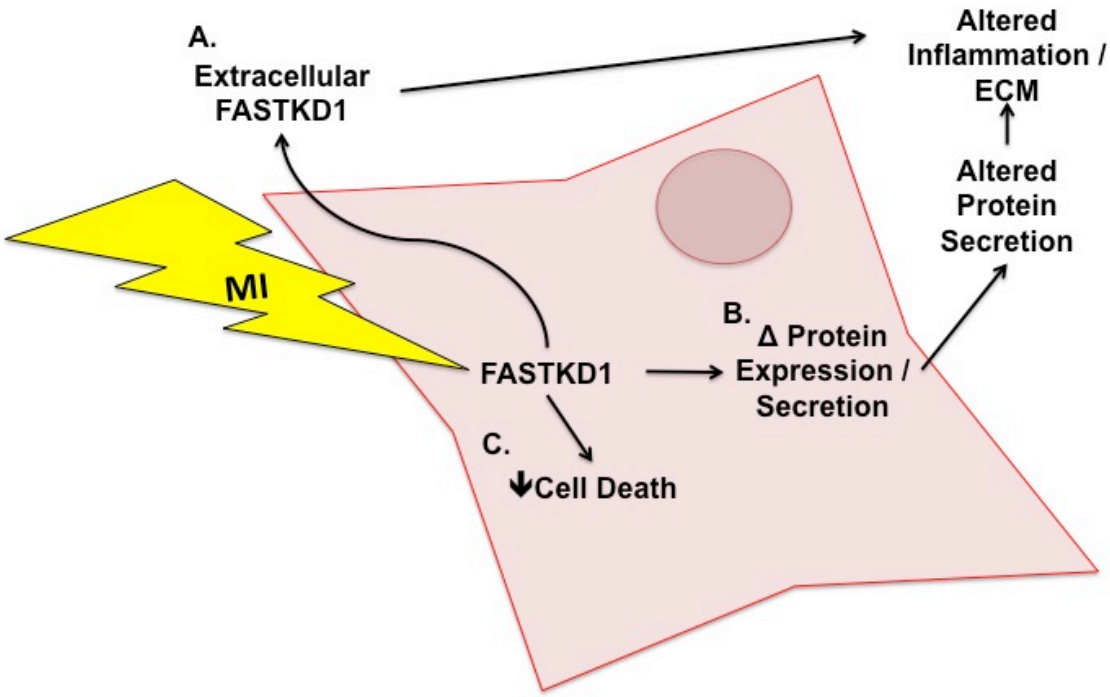

Figure 16. Possible mechanisms by which FASTKD1 prevents LVFWR. Following MI, the heart begins a process of healing. Improper healing can result in LVFWR. FASTKD1 may prevent this fatal complication by multiple possible mechanisms. A. FASTKD1 could be secreted either basally or released following myocyte death. B. FASTKD1 could alter protein expression or secretion. C. FASTKD1 may decrease myocyte death following MI.

FASTKD1 could act as an intracellular chaperone much as melusin and decrease cell death and inflammation through this pathway [174]. Finally, FASTKD1 could simply be limiting cell death in response to MI, which has been shown to decrease incidence of LVFWR; however this process seems to be independent of alterations to the inflammatory response, at least in the case of p53 [187] (**Figure 16C**).

3. Summary

Our studies show that FASTKD1 is a novel cytoprotective protein that protects cells against oxidative stress induced cell death. Because we initially identified FASTKD1 as a CypD interacting protein, we hypothesized that it would modulate cell death via the MPT pore. However this hypothesis was proved only partially correct. FASTKD1 does modulate cell death, but this is independent of the MPT pore, its interaction with CypD, or any other mechanism that we could identify. Additionally, FASTKD1 modulates mitochondrial morphology and function.

We also investigated the role of FASTKD1 *in vivo* using a cardiac myocyte specific overexpression model. Transgenic mice were morphologically and functionally normal at baseline. Based on our *in vitro* data, we hypothesized that these mice would be protected from pathological insults involving elevated levels of ROS. FASTKD1 overexpression did not protect mice from MI induced cardiac dysfunction and scar size was unaltered. However FASTKD1 prevented LVFWR, which was associated with alterations in inflammatory cell infiltration and ECM accumulation in the border zone and scar.

4. Potential Future Directions

In the future, many experiments can be performed to continue elucidating FASTKD1's role in normal physiology and its potential as a cytoprotective target. Both *in vitro* and *in vivo* experiments could be used to further explore and identify FASTKD1's cellular function.

Initially, it would be interesting to determine if mitochondrial localization of FASTKD1 is required in order to exert its cytoprotective properties. FASTKD2 is a pro-apoptotic protein in breast cancer cells, and this action does not require its mitochondrial localization [131]. This could be accomplished by cloning an adenovirus or overexpression mouse model in which the N-terminal mitochondrial targeting sequence of FASTKD1 has been removed. Studies measuring cell death and mitochondrial function could be performed to assess if mitochondrial localization of overexpressed FASTKD1 is required for its protective abilities. Mutational studies of FASTKD1 could also be performed. Overexpression studies could be performed using FASTKD1 with different mutations including removal of FAST or RNA binding domains. This could provide information regarding which function of FASTKD1 is responsible for its cytoprotective effects, and therefore help to delineate the mechanism by which FASTKD1 exerts its protective effects.

In a similar fashion, it would be interesting to determine if FASTKD1's cytoprotective properties are dependent on its effects on mitochondrial morphology. Mfn1 has been implicated in cell death, as its deletion leads to cells being protected from

oxidative stress-induced cell death[116]. Because FASTKD1 overexpression is associated with decreased levels of Mfn1, it would be useful to perform a rescue experiment using Mfn1 overexpression to return this protein to normal levels of expression. It is possible that FASTKD1's effects on mitochondrial morphology are independent of its pro-survival effects. Additionally, future studies could be performed to determine the mechanism by which FASTKD1 alters mitochondrial morphology. Initially, immunoprecipitation could be used to determine if FASTKD1 directly interacts with mitochondrial fission/fusion machinery.

Studies depleting cells of FASTKD1 were only performed transiently in mouse embryonic fibroblasts. It would be informative to test long-term knockdown of FASTKD1 as mediated by a stable transfection with a small-hairpin RNA containing plasmid. This could further deplete FASTKD1 levels *in vitro*. Additionally, generating a FASTKD1 knockout mouse could help to further explore the role of this protein *in vivo*. Based on our current findings, testing this model in response to MI would be an important study. It would be interesting to see if FASTKD1 knockout mice are more prone to LVFWR than normal controls, as this would show that FASTKD1 is not just sufficient but also necessary to prevent LVFWR. Additionally, the polarization of macrophages recruited to the scar needs to be further studied. This could be accomplished using flow cytometry to sort for specific markers of macrophage polarization (i.e. the membrane receptor CD206) [181].

To determine if FASTKD1 overexpression results in a difference in protein secretion that could account for the differences seen in the inflammatory response to MI, a proteomic approach could be utilized. Cardiac myocytes could be infected with an

adenovirus to overexpress FASTKD1 and the media could be compared for protein content compared to control infected cells. Additionally, this same study could be performed after induction of ROS dependent cell death or ischemia to look at differences in secreted proteins following cellular injury. Media from these cells could also be used to treat macrophage cultures to assess cell polarization if differences in this parameter are shown to be important *in vivo*. Additionally, the coronary effluent of NTG versus DTG hearts could be compared following *ex vivo* ischemia as this approach has been previously employed to identify proteins released by pathological stimuli [228,229].

The FASTKD1 overexpression model needs to be tested in a variety of pathological states. This could initially be accomplished using a model of cardiac ischemia reperfusion. This process is known to involve excess ROS generation [92]. This could be accomplished *in vivo* or *ex vivo* using a Langendorf-based approach [230]. This experiment could show a direct cytoprotective effect for FASTKD1 in a more physiological relevant model than the cell culture based approaches used in our studies.

The overexpression mouse model that we generated could be used in an inducible fashion. FASTKD1 overexpression could be suppressed until the time of an injury to mimic more closely a pharmacological intervention that activates FASTKD1. Transient FASTKD1 overexpression might more closely resemble the results from *in vitro* studies, showing effects on mitochondrial function.

References

1 Lalaoui, N., Lindqvist, L. M., Sandow, J. J. & Ekert, P. G. The molecular relationships between apoptosis, autophagy and necroptosis. *Seminars in cell & developmental biology*, doi:10.1016/j.semcdb.2015.02.003 (2015).

2 Kerr, J. F., Wyllie, A. H. & Currie, A. R. Apoptosis: a basic biological phenomenon with wide-ranging implications in tissue kinetics. *British journal of cancer* **26**, 239-257 (1972).

3 Cairrão, F. & Domingos, P. M. in *eLS* (John Wiley & Sons, Ltd, 2001).

4 Pisetsky, D. Cell death in the pathogenesis of immune-mediated diseases: the role of HMGB1 and DAMP-PAMP complexes. *Swiss medical weekly* **141**, w13256, doi:10.4414/smw.2011.13256 (2011).

5 Yamaguchi, Y. & Miura, M. Programmed Cell Death in Neurodevelopment. *Developmental cell* **32**, 478-490, doi:10.1016/j.devcel.2015.01.019 (2015).

6 Green, D. R., Galluzzi, L. & Kroemer, G. Cell biology. Metabolic control of cell death. *Science* **345**, 1250256, doi:10.1126/science.1250256 (2014).

7 Green, D. R. & Levine, B. To be or not to be? How selective autophagy and cell death govern cell fate. *Cell* **157**, 65-75, doi:10.1016/j.cell.2014.02.049 (2014).

8 Hamasaki, M., Shibutani, S. T. & Yoshimori, T. Up-to-date membrane biogenesis in the autophagosome formation. *Current opinion in cell biology* **25**, 455-460, doi:10.1016/j.ceb.2013.03.004 (2013).

9 Karch, J. *et al.* Bax and Bak function as the outer membrane component of the mitochondrial permeability pore in regulating necrotic cell death in mice. *eLife* **2**, e00772, doi:10.7554/eLife.00772 (2013).

10 Siu, W. P., Pun, P. B., Latchoumycandane, C. & Boelsterli, U. A. Bax-mediated mitochondrial outer membrane permeabilization (MOMP), distinct from the mitochondrial permeability transition, is a key mechanism in diclofenac-induced hepatocyte injury: Multiple protective roles of cyclosporin A. *Toxicology and applied pharmacology* **227**, 451-461, doi:10.1016/j.taap.2007.11.030 (2008).

11 Hu, Y., Benedict, M. A., Ding, L. & Nunez, G. Role of cytochrome c and dATP/ATP hydrolysis in Apaf-1-mediated caspase-9 activation and apoptosis. *The EMBO journal* **18**, 3586-3595, doi:10.1093/emboj/18.13.3586 (1999).

12 Yuan, S. & Akey, C. W. Apoptosome structure, assembly, and procaspase activation. *Structure* **21**, 501-515, doi:10.1016/j.str.2013.02.024 (2013).

13 Liu, Y. & Levine, B. Autosis and autophagic cell death: the dark side of autophagy. *Cell death and differentiation* **22**, 367-376, doi:10.1038/cdd.2014.143 (2015).

14 Taylor, R. C., Cullen, S. P. & Martin, S. J. Apoptosis: controlled demolition at the cellular level. *Nature reviews. Molecular cell biology* **9**, 231-241, doi:10.1038/nrm2312 (2008).

15 Baines, C. P. How and when do myocytes die during ischemia and reperfusion: the late phase. *Journal of cardiovascular pharmacology and therapeutics* **16**, 239-243, doi:10.1177/1074248411407769 (2011).

16 Kockara, A. & Kayatas, M. Renal cell apoptosis and new treatment options in sepsis-induced acute kidney injury. *Renal failure* **35**, 291-294, doi:10.3109/0886022X.2012.744040 (2013).

17 Yao, R. Q. *et al.* Quercetin attenuates cell apoptosis in focal cerebral ischemia rat brain via activation of BDNF-TrkB-PI3K/Akt signaling pathway. *Neurochemical research* **37**, 2777-2786, doi:10.1007/s11064-012-0871-5 (2012).

18 Fulda, S. & Kogel, D. Cell death by autophagy: emerging molecular mechanisms and implications for cancer therapy. *Oncogene* **34**, 5105-5113, doi:10.1038/onc.2014.458 (2015).

19 Chen, Y., McMillan-Ward, E., Kong, J., Israels, S. J. & Gibson, S. B. Oxidative stress induces autophagic cell death independent of apoptosis in transformed and cancer cells. *Cell death and differentiation* **15**, 171-182, doi:10.1038/sj.cdd.4402233 (2008).

20 Liu, Y. *et al.* Autosis is a Na+,K+-ATPase-regulated form of cell death triggered by autophagy-inducing peptides, starvation, and hypoxia-ischemia. *Proceedings of the National Academy of Sciences of the United States of America* **110**, 20364-20371, doi:10.1073/pnas.1319661110 (2013).

21 Meijer, A. J. & Klionsky, D. J. Vps34 is a phosphatidylinositol 3-kinase, not a phosphoinositide 3-kinase. *Autophagy* **7**, 563-564 (2011).

22 Ohsumi, Y. Molecular dissection of autophagy: two ubiquitin-like systems. *Nature reviews. Molecular cell biology* **2**, 211-216, doi:10.1038/35056522 (2001).

23 Ikeda, Y. *et al.* Molecular mechanisms mediating mitochondrial dynamics and mitophagy and their functional roles in the cardiovascular system. *Journal of molecular and cellular cardiology* **78**, 116-122, doi:10.1016/j.yjmcc.2014.09.019 (2015).

24 Ishihara, N., Fujita, Y., Oka, T. & Mihara, K. Regulation of mitochondrial morphology through proteolytic cleavage of OPA1. *The EMBO journal* **25**, 2966-2977, doi:10.1038/sj.emboj.7601184 (2006).

25 Feng, D., Liu, L., Zhu, Y. & Chen, Q. Molecular signaling toward mitophagy and its physiological significance. *Experimental cell research* **319**, 1697-1705, doi:10.1016/j.yexcr.2013.03.034 (2013).

26 Eura, Y., Ishihara, N., Yokota, S. & Mihara, K. Two mitofusin proteins, mammalian homologues of FZO, with distinct functions are both required for mitochondrial fusion. *Journal of biochemistry* **134**, 333-344 (2003).

27 Chen, H. *et al.* Mitofusins Mfn1 and Mfn2 coordinately regulate mitochondrial fusion and are essential for embryonic development. *The Journal of cell biology* **160**, 189-200, doi:10.1083/jcb.200211046 (2003).

28 Olichon, A. *et al.* Loss of OPA1 perturbates the mitochondrial inner membrane structure and integrity, leading to cytochrome c release and apoptosis. *The Journal of biological chemistry* **278**, 7743-7746, doi:10.1074/jbc.C200677200 (2003).

29 Ishihara, N., Otera, H., Oka, T. & Mihara, K. Regulation and physiologic functions of GTPases in mitochondrial fusion and fission in mammals. *Antioxidants & redox signaling* **19**, 389-399, doi:10.1089/ars.2012.4830 (2013).

30 Chen, Y. & Dorn, G. W., 2nd. PINK1-phosphorylated mitofusin 2 is a Parkin receptor for culling damaged mitochondria. *Science* **340**, 471-475, doi:10.1126/science.1231031 (2013).

31 Frank, M. *et al.* Mitophagy is triggered by mild oxidative stress in a mitochondrial fission dependent manner. *Biochimica et biophysica acta* **1823**, 2297-2310, doi:10.1016/j.bbamcr.2012.08.007 (2012).

32 Christofferson, D. E., Li, Y. & Yuan, J. Control of Life-or-Death Decisions by RIP1 Kinase. *Annual review of physiology*, doi:10.1146/annurev-physiol-021113-170259 (2013).

33 Galluzzi, L., Kepp, O., Krautwald, S., Kroemer, G. & Linkermann, A. Molecular mechanisms of regulated necrosis. *Seminars in cell & developmental biology*, doi:10.1016/j.semcdb.2014.02.006 (2014).

34 Vanden Berghe, T., Linkermann, A., Jouan-Lanhouet, S., Walczak, H. & Vandenabeele, P. Regulated necrosis: the expanding network of non-apoptotic cell death pathways. *Nature reviews. Molecular cell biology* **15**, 135-147, doi:10.1038/nrm3737 (2014).

35 Van Herreweghe, F., Festjens, N., Declercq, W. & Vandenabeele, P. Tumor necrosis factor-mediated cell death: to break or to burst, that's the question. *Cellular and molecular life sciences : CMLS* **67**, 1567-1579, doi:10.1007/s00018-010-0283-0 (2010).

36 Hsu, H., Xiong, J. & Goeddel, D. V. The TNF receptor 1-associated protein TRADD signals cell death and NF-kappa B activation. *Cell* **81**, 495-504 (1995).

37 Ermolaeva, M. A. *et al.* Function of TRADD in tumor necrosis factor receptor 1 signaling and in TRIF-dependent inflammatory responses. *Nature immunology* **9**, 1037-1046, doi:10.1038/ni.1638 (2008).

38 Hsu, H., Huang, J., Shu, H. B., Baichwal, V. & Goeddel, D. V. TNF-dependent recruitment of the protein kinase RIP to the TNF receptor-1 signaling complex. *Immunity* **4**, 387-396 (1996).

39 Hsu, H., Shu, H. B., Pan, M. G. & Goeddel, D. V. TRADD-TRAF2 and TRADD-FADD interactions define two distinct TNF receptor 1 signal transduction pathways. *Cell* **84**, 299-308 (1996).

40 Tada, K. *et al.* Critical roles of TRAF2 and TRAF5 in tumor necrosis factor-induced NF-kappa B activation and protection from cell death. *The Journal of biological chemistry* **276**, 36530-36534, doi:10.1074/jbc.M104837200 (2001).

41 McComb, S. *et al.* cIAP1 and cIAP2 limit macrophage necroptosis by inhibiting Rip1 and Rip3 activation. *Cell death and differentiation* **19**, 1791-1801, doi:10.1038/cdd.2012.59 (2012).

42 Cho, Y. S. *et al.* Phosphorylation-driven assembly of the RIP1-RIP3 complex regulates programmed necrosis and virus-induced inflammation. *Cell* **137**, 1112-1123, doi:10.1016/j.cell.2009.05.037 (2009).

43 He, S. *et al.* Receptor interacting protein kinase-3 determines cellular necrotic response to TNF-alpha. *Cell* **137**, 1100-1111, doi:10.1016/j.cell.2009.05.021 (2009).

44 Zhang, D. W. *et al.* RIP3, an energy metabolism regulator that switches TNF-induced cell death from apoptosis to necrosis. *Science* **325**, 332-336, doi:10.1126/science.1172308 (2009).

45 Newton, K. *et al.* Activity of protein kinase RIPK3 determines whether cells die by necroptosis or apoptosis. *Science* **343**, 1357-1360, doi:10.1126/science.1249361 (2014).

46 Murphy, J. M. *et al.* The pseudokinase MLKL mediates necroptosis via a molecular switch mechanism. *Immunity* **39**, 443-453, doi:10.1016/j.immuni.2013.06.018 (2013).

47 Sun, L. *et al.* Mixed lineage kinase domain-like protein mediates necrosis signaling downstream of RIP3 kinase. *Cell* **148**, 213-227, doi:10.1016/j.cell.2011.11.031 (2012).

48 Zhao, J. *et al.* Mixed lineage kinase domain-like is a key receptor interacting protein 3 downstream component of TNF-induced necrosis. *Proceedings of the National Academy of Sciences of the United States of America* **109**, 5322-5327, doi:10.1073/pnas.1200012109 (2012).

49 Chen, X. *et al.* Translocation of mixed lineage kinase domain-like protein to plasma membrane leads to necrotic cell death. *Cell research* **24**, 105-121, doi:10.1038/cr.2013.171 (2014).

50 Wang, Z., Jiang, H., Chen, S., Du, F. & Wang, X. The mitochondrial phosphatase PGAM5 functions at the convergence point of multiple necrotic death pathways. *Cell* **148**, 228-243, doi:10.1016/j.cell.2011.11.030 (2012).

51 Moriwaki, K. *et al.* The Mitochondrial Phosphatase PGAM5 Is Dispensable for Necroptosis but Promotes Inflammasome Activation in Macrophages. *Journal of immunology* **196**, 407-415, doi:10.4049/jimmunol.1501662 (2016).

52 Cai, Z. *et al.* Plasma membrane translocation of trimerized MLKL protein is required for TNF-induced necroptosis. *Nature cell biology* **16**, 55-65, doi:10.1038/ncb2883 (2014).

53 Dondelinger, Y. *et al.* MLKL compromises plasma membrane integrity by binding to phosphatidylinositol phosphates. *Cell reports* **7**, 971-981, doi:10.1016/j.celrep.2014.04.026 (2014).

54 Wang, H. *et al.* Mixed lineage kinase domain-like protein MLKL causes necrotic membrane disruption upon phosphorylation by RIP3. *Molecular cell* **54**, 133-146, doi:10.1016/j.molcel.2014.03.003 (2014).

55 Tait, S. W. *et al.* Widespread mitochondrial depletion via mitophagy does not compromise necroptosis. *Cell reports* **5**, 878-885, doi:10.1016/j.celrep.2013.10.034 (2013).

56 Karch, J. *et al.* Necroptosis Interfaces with MOMP and the MPTP in Mediating Cell Death. *PloS one* **10**, e0130520, doi:10.1371/journal.pone.0130520 (2015).

57 Halestrap, A. P. & Richardson, A. P. The mitochondrial permeability transition: A current perspective on its identity and role in ischaemia/reperfusion injury. *Journal of molecular and cellular cardiology*, doi:10.1016/j.yjmcc.2014.08.018 (2014).

58 Liang, H. L., Sedlic, F., Bosnjak, Z. & Nilakantan, V. SOD1 and MitoTEMPO partially prevent mitochondrial permeability transition pore opening, necrosis, and

mitochondrial apoptosis after ATP depletion recovery. *Free radical biology & medicine* **49**, 1550-1560, doi:10.1016/j.freeradbiomed.2010.08.018 (2010).

59 Shintani-Ishida, K., Inui, M. & Yoshida, K. Ischemia-reperfusion induces myocardial infarction through mitochondrial Ca(2)(+) overload. *Journal of molecular and cellular cardiology* **53**, 233-239, doi:10.1016/j.yjmcc.2012.05.012 (2012).

60 Bonora, M. *et al.* Molecular mechanisms of cell death: central implication of ATP synthase in mitochondrial permeability transition. *Oncogene* **0**, doi:10.1038/onc.2014.96 (2014).

61 Baines, C. P. The cardiac mitochondrion: nexus of stress. *Annual review of physiology* **72**, 61-80, doi:10.1146/annurev-physiol-021909-135929 (2010).

62 Gomez, L. *et al.* Inhibition of mitochondrial permeability transition improves functional recovery and reduces mortality following acute myocardial infarction in mice. *American journal of physiology. Heart and circulatory physiology* **293**, H1654-1661, doi:10.1152/ajpheart.01378.2006 (2007).

63 Baines, C. P. *et al.* Loss of cyclophilin D reveals a critical role for mitochondrial permeability transition in cell death. *Nature* **434**, 658-662, doi:10.1038/nature03434 (2005).

64 Singh, D., Chander, V. & Chopra, K. Cyclosporine protects against ischemia/reperfusion injury in rat kidneys. *Toxicology* **207**, 339-347, doi:10.1016/j.tox.2004.09.018 (2005).

65 Schinzel, A. C. *et al.* Cyclophilin D is a component of mitochondrial permeability transition and mediates neuronal cell death after focal cerebral ischemia.

Proceedings of the National Academy of Sciences of the United States of America **102**, 12005-12010, doi:10.1073/pnas.0505294102 (2005).

66 Itoh, T. *et al.* Cytoprotective regulation of the mitochondrial permeability transition pore is impaired in type 2 diabetic Goto-Kakizaki rat hearts. *Journal of molecular and cellular cardiology* **53**, 870-879, doi:10.1016/j.yjmcc.2012.10.001 (2012).

67 Gharanei, M., Hussain, A., Janneh, O. & Maddock, H. L. Doxorubicin induced myocardial injury is exacerbated following ischaemic stress via opening of the mitochondrial permeability transition pore. *Toxicology and applied pharmacology* **268**, 149-156, doi:10.1016/j.taap.2012.12.003 (2013).

68 Reutenauer, J., Dorchies, O. M., Patthey-Vuadens, O., Vuagniaux, G. & Ruegg, U. T. Investigation of Debio 025, a cyclophilin inhibitor, in the dystrophic mdx mouse, a model for Duchenne muscular dystrophy. *British journal of pharmacology* **155**, 574-584, doi:10.1038/bjp.2008.285 (2008).

69 Millay, D. P. *et al.* Genetic and pharmacologic inhibition of mitochondrial-dependent necrosis attenuates muscular dystrophy. *Nature medicine* **14**, 442-447, doi:10.1038/nm1736 (2008).

70 Baines, C. P., Kaiser, R. A., Sheiko, T., Craigen, W. J. & Molkentin, J. D. Voltage-dependent anion channels are dispensable for mitochondrial-dependent cell death. *Nature cell biology* **9**, 550-555, doi:10.1038/ncb1575 (2007).

71 Kokoszka, J. E. *et al.* The ADP/ATP translocator is not essential for the mitochondrial permeability transition pore. *Nature* **427**, 461-465, doi:10.1038/nature02229 (2004).

72 Gutierrez-Aguilar, M. *et al.* Genetic manipulation of the cardiac mitochondrial phosphate carrier does not affect permeability transition. *Journal of molecular and cellular cardiology* **72**, 316-325, doi:10.1016/j.yjmcc.2014.04.008 (2014).

73 Kwong, J. Q. *et al.* Genetic deletion of the mitochondrial phosphate carrier desensitizes the mitochondrial permeability transition pore and causes cardiomyopathy. *Cell death and differentiation* **21**, 1209-1217, doi:10.1038/cdd.2014.36 (2014).

74 Giorgio, V. *et al.* Dimers of mitochondrial ATP synthase form the permeability transition pore. *Proceedings of the National Academy of Sciences of the United States of America* **110**, 5887-5892, doi:10.1073/pnas.1217823110 (2013).

75 Bonora, M. *et al.* Role of the c subunit of the FO ATP synthase in mitochondrial permeability transition. *Cell cycle* **12**, 674-683, doi:10.4161/cc.23599 (2013).

76 Carraro, M. *et al.* Channel formation by yeast F-ATP synthase and the role of dimerization in the mitochondrial permeability transition. *The Journal of biological chemistry* **289**, 15980-15985, doi:10.1074/jbc.C114.559633 (2014).

77 Alavian, K. N. *et al.* An uncoupling channel within the c-subunit ring of the F1FO ATP synthase is the mitochondrial permeability transition pore. *Proceedings of the National Academy of Sciences of the United States of America* **111**, 10580-10585, doi:10.1073/pnas.1401591111 (2014).

78 Nakagawa, T. *et al.* Cyclophilin D-dependent mitochondrial permeability transition regulates some necrotic but not apoptotic cell death. *Nature* **434**, 652-658,

doi:http://www.nature.com/nature/journal/v434/n7033/suppinfo/nature03317_S1.html (2005).

79 Basso, E. *et al.* Properties of the permeability transition pore in mitochondria devoid of Cyclophilin D. *The Journal of biological chemistry* **280**, 18558-18561, doi:10.1074/jbc.C500089200 (2005).

80 Nguyen, T. T. *et al.* Cysteine 203 of cyclophilin D is critical for cyclophilin D activation of the mitochondrial permeability transition pore. *The Journal of biological chemistry* **286**, 40184-40192, doi:10.1074/jbc.M111.243469 (2011).

81 Tanno, M. *et al.* Translocation of GSK-3beta, a Trigger of Permeability Transition, Is Kinase Activity-dependent and Mediated by Interaction with VDAC2. *The Journal of biological chemistry*, doi:10.1074/jbc.M114.563924 (2014).

82 Rasola, A. *et al.* Activation of mitochondrial ERK protects cancer cells from death through inhibition of the permeability transition. *Proceedings of the National Academy of Sciences of the United States of America* **107**, 726-731, doi:10.1073/pnas.0912742107 (2010).

83 Vaseva, A. V. *et al.* p53 opens the mitochondrial permeability transition pore to trigger necrosis. *Cell* **149**, 1536-1548, doi:10.1016/j.cell.2012.05.014 (2012).

84 Shanmughapriya, S. *et al.* SPG7 Is an Essential and Conserved Component of the Mitochondrial Permeability Transition Pore. *Molecular cell* **60**, 47-62, doi:10.1016/j.molcel.2015.08.009 (2015).

85 Bernardi, P. & Forte, M. Commentary: SPG7 is an essential and conserved component of the mitochondrial permeability transition pore. *Frontiers in physiology* **6**, 320, doi:10.3389/fphys.2015.00320 (2015).

86 Pan, X. *et al.* The physiological role of mitochondrial calcium revealed by mice lacking the mitochondrial calcium uniporter. *Nature cell biology* **15**, 1464-1472, doi:10.1038/ncb2868 (2013).

87 Crompton, M. & Costi, A. A heart mitochondrial Ca2(+)-dependent pore of possible relevance to re-perfusion-induced injury. Evidence that ADP facilitates pore interconversion between the closed and open states. *The Biochemical journal* **266**, 33-39 (1990).

88 Crompton, M., Costi, A. & Hayat, L. Evidence for the presence of a reversible Ca2+-dependent pore activated by oxidative stress in heart mitochondria. *The Biochemical journal* **245**, 915-918 (1987).

89 Haworth, R. A. & Hunter, D. R. The Ca2+-induced membrane transition in mitochondria. II. Nature of the Ca2+ trigger site. *Archives of biochemistry and biophysics* **195**, 460-467 (1979).

90 Elrod, J. W. *et al.* Cyclophilin D controls mitochondrial pore-dependent Ca(2+) exchange, metabolic flexibility, and propensity for heart failure in mice. *The Journal of clinical investigation* **120**, 3680-3687, doi:10.1172/JCI43171 (2010).

91 Korge, P. *et al.* Protective role of transient pore openings in calcium handling by cardiac mitochondria. *The Journal of biological chemistry* **286**, 34851-34857, doi:10.1074/jbc.M111.239921 (2011).

92 Saotome, M. *et al.* Transient opening of mitochondrial permeability transition pore by reactive oxygen species protects myocardium from ischemia-reperfusion injury. *American journal of physiology. Heart and circulatory physiology* **296**, H1125-1132, doi:10.1152/ajpheart.00436.2008 (2009).

93 Roca, F. J. & Ramakrishnan, L. TNF dually mediates resistance and susceptibility to mycobacteria via mitochondrial reactive oxygen species. *Cell* **153**, 521-534, doi:10.1016/j.cell.2013.03.022 (2013).

94 Lim, S. Y., Davidson, S. M., Mocanu, M. M., Yellon, D. M. & Smith, C. C. The cardioprotective effect of necrostatin requires the cyclophilin-D component of the mitochondrial permeability transition pore. *Cardiovascular drugs and therapy / sponsored by the International Society of Cardiovascular Pharmacotherapy* **21**, 467-469, doi:10.1007/s10557-007-6067-6 (2007).

95 Kaiser, W. J. *et al.* RIP3 mediates the embryonic lethality of caspase-8-deficient mice. *Nature* **471**, 368-372, doi:10.1038/nature09857 (2011).

96 Ch'en, I. L., Tsau, J. S., Molkentin, J. D., Komatsu, M. & Hedrick, S. M. Mechanisms of necroptosis in T cells. *The Journal of experimental medicine* **208**, 633-641, doi:10.1084/jem.20110251 (2011).

97 Linkermann, A. *et al.* Two independent pathways of regulated necrosis mediate ischemia-reperfusion injury. *Proceedings of the National Academy of Sciences of the United States of America* **110**, 12024-12029, doi:10.1073/pnas.1305538110 (2013).

98 Ong, S. B., Hall, A. R. & Hausenloy, D. J. Mitochondrial dynamics in cardiovascular health and disease. *Antioxidants & redox signaling* **19**, 400-414, doi:10.1089/ars.2012.4777 (2013).

99 Li, J., Zhou, J., Li, Y., Qin, D. & Li, P. Mitochondrial fission controls DNA fragmentation by regulating endonuclease G. *Free radical biology & medicine* **49**, 622-631, doi:10.1016/j.freeradbiomed.2010.05.021 (2010).

100 Chen, H., Chomyn, A. & Chan, D. C. Disruption of fusion results in mitochondrial heterogeneity and dysfunction. *The Journal of biological chemistry* **280**, 26185-26192, doi:10.1074/jbc.M503062200 (2005).

101 Rehman, J. *et al.* Inhibition of mitochondrial fission prevents cell cycle progression in lung cancer. *FASEB journal : official publication of the Federation of American Societies for Experimental Biology* **26**, 2175-2186, doi:10.1096/fj.11-196543 (2012).

102 Santel, A. & Fuller, M. T. Control of mitochondrial morphology by a human mitofusin. *Journal of cell science* **114**, 867-874 (2001).

103 Park, Y. Y. & Cho, H. Mitofusin 1 is degraded at G2/M phase through ubiquitylation by MARCH5. *Cell division* **7**, 25, doi:10.1186/1747-1028-7-25 (2012).

104 Song, Z., Ghochani, M., McCaffery, J. M., Frey, T. G. & Chan, D. C. Mitofusins and OPA1 mediate sequential steps in mitochondrial membrane fusion. *Molecular biology of the cell* **20**, 3525-3532, doi:10.1091/mbc.E09-03-0252 (2009).

105 Chang, C. R. & Blackstone, C. Dynamic regulation of mitochondrial fission through modification of the dynamin-related protein Drp1. *Annals of the New*

York Academy of Sciences **1201**, 34-39, doi:10.1111/j.1749-6632.2010.05629.x (2010).

106 Otera, H. *et al.* Mff is an essential factor for mitochondrial recruitment of Drp1 during mitochondrial fission in mammalian cells. *The Journal of cell biology* **191**, 1141-1158, doi:10.1083/jcb.201007152 (2010).

107 Ishihara, N. *et al.* Mitochondrial fission factor Drp1 is essential for embryonic development and synapse formation in mice. *Nature cell biology* **11**, 958-966, doi:10.1038/ncb1907 (2009).

108 Strappazzon, F. & Cecconi, F. The multifaceted mitochondrion: An attractive candidate for therapeutic strategies. *Pharmacological Research*, doi:http://dx.doi.org/10.1016/j.phrs.2015.03.007.

109 Kasahara, A. & Scorrano, L. Mitochondria: from cell death executioners to regulators of cell differentiation. *Trends in cell biology*, doi:10.1016/j.tcb.2014.08.005 (2014).

110 Cassidy-Stone, A. *et al.* Chemical inhibition of the mitochondrial division dynamin reveals its role in Bax/Bak-dependent mitochondrial outer membrane permeabilization. *Developmental cell* **14**, 193-204, doi:10.1016/j.devcel.2007.11.019 (2008).

111 Montessuit, S. *et al.* Membrane remodeling induced by the dynamin-related protein Drp1 stimulates Bax oligomerization. *Cell* **142**, 889-901, doi:10.1016/j.cell.2010.08.017 (2010).

112 Sugioka, R., Shimizu, S. & Tsujimoto, Y. Fzo1, a protein involved in mitochondrial fusion, inhibits apoptosis. *The Journal of biological chemistry* **279**, 52726-52734, doi:10.1074/jbc.M408910200 (2004).

113 Frezza, C. *et al.* OPA1 controls apoptotic cristae remodeling independently from mitochondrial fusion. *Cell* **126**, 177-189, doi:10.1016/j.cell.2006.06.025 (2006).

114 Remijsen, Q. *et al.* Depletion of RIPK3 or MLKL blocks TNF-driven necroptosis and switches towards a delayed RIPK1 kinase-dependent apoptosis. *Cell death & disease* **5**, e1004, doi:10.1038/cddis.2013.531 (2014).

115 Moujalled, D. M., Cook, W. D., Murphy, J. M. & Vaux, D. L. Necroptosis induced by RIPK3 requires MLKL but not Drp1. *Cell death & disease* **5**, e1086, doi:10.1038/cddis.2014.18 (2014).

116 Papanicolaou, K. N. *et al.* Cardiomyocyte deletion of mitofusin-1 leads to mitochondrial fragmentation and improves tolerance to ROS-induced mitochondrial dysfunction and cell death. *American journal of physiology. Heart and circulatory physiology* **302**, H167-179, doi:10.1152/ajpheart.00833.2011 (2012).

117 Papanicolaou, K. N. *et al.* Mitofusin-2 maintains mitochondrial structure and contributes to stress-induced permeability transition in cardiac myocytes. *Molecular and cellular biology* **31**, 1309-1328, doi:10.1128/MCB.00911-10 (2011).

118 Simarro, M. *et al.* Fast kinase domain-containing protein 3 is a mitochondrial protein essential for cellular respiration. *Biochemical and biophysical research communications* **401**, 440-446, doi:10.1016/j.bbrc.2010.09.075 (2010).

119 Tian, Q., Taupin, J., Elledge, S., Robertson, M. & Anderson, P. Fas-activated serine/threonine kinase (FAST) phosphorylates TIA-1 during Fas-mediated apoptosis. *The Journal of experimental medicine* **182**, 865-874 (1995).

120 Li, W. *et al.* FAST is a BCL-X(L)-associated mitochondrial protein. *Biochemical and biophysical research communications* **318**, 95-102, doi:10.1016/j.bbrc.2004.03.188 (2004).

121 Li, W., Simarro, M., Kedersha, N. & Anderson, P. FAST is a survival protein that senses mitochondrial stress and modulates TIA-1-regulated changes in protein expression. *Molecular and cellular biology* **24**, 10718-10732, doi:10.1128/MCB.24.24.10718-10732.2004 (2004).

122 Simarro, M. *et al.* Fas-activated serine/threonine phosphoprotein (FAST) is a regulator of alternative splicing. *Proceedings of the National Academy of Sciences of the United States of America* **104**, 11370-11375, doi:10.1073/pnas.0704964104 (2007).

123 Izquierdo, J. M. & Valcarcel, J. Fas-activated serine/threonine kinase (FAST K) synergizes with TIA-1/TIAR proteins to regulate Fas alternative splicing. *The Journal of biological chemistry* **282**, 1539-1543, doi:10.1074/jbc.C600198200 (2007).

124 Castello, A. *et al.* Insights into RNA biology from an atlas of mammalian mRNA-binding proteins. *Cell* **149**, 1393-1406, doi:10.1016/j.cell.2012.04.031 (2012).

125 Jourdain, A. A. *et al.* A Mitochondria-Specific Isoform of FASTK Is Present In Mitochondrial RNA Granules and Regulates Gene Expression and Function. *Cell reports* **10**, 1110-1121, doi:10.1016/j.celrep.2015.01.063 (2015).

126 Simarro, M. *et al.* Fas-activated serine/threonine phosphoprotein promotes immune-mediated pulmonary inflammation. *Journal of immunology* **184**, 5325-5332, doi:10.4049/jimmunol.1000104 (2010).

127 Colas, E. *et al.* Molecular markers of endometrial carcinoma detected in uterine aspirates. *International journal of cancer. Journal international du cancer* **129**, 2435-2444, doi:10.1002/ijc.25901 (2011).

128 Wang, J. *et al.* A six gene expression signature defines aggressive subtypes and predicts outcome in childhood and adult acute lymphoblastic leukemia. *Oncotarget* **6**, 16527-16542, doi:10.18632/oncotarget.4113 (2015).

129 Ghezzi, D. *et al.* FASTKD2 nonsense mutation in an infantile mitochondrial encephalomyopathy associated with cytochrome c oxidase deficiency. *American journal of human genetics* **83**, 415-423, doi:10.1016/j.ajhg.2008.08.009 (2008).

130 Antonicka, H. & Shoubridge, E. A. Mitochondrial RNA Granules Are Centers for Posttranscriptional RNA Processing and Ribosome Biogenesis. *Cell reports*, doi:10.1016/j.celrep.2015.01.030 (2015).

131 Yeung, K. T. *et al.* A novel transcription complex that selectively modulates apoptosis of breast cancer cells through regulation of FASTKD2. *Molecular and cellular biology* **31**, 2287-2298, doi:10.1128/MCB.01381-10 (2011).

132 Wolf, A. R. & Mootha, V. K. Functional genomic analysis of human mitochondrial RNA processing. *Cell reports* **7**, 918-931, doi:10.1016/j.celrep.2014.03.035 (2014).

133 Nickel, A., Kohlhaas, M. & Maack, C. Mitochondrial reactive oxygen species production and elimination. *Journal of molecular and cellular cardiology* **73**, 26-33, doi:10.1016/j.yjmcc.2014.03.011 (2014).

134 Rich, P. R. & Marechal, A. The mitochondrial respiratory chain. *Essays in biochemistry* **47**, 1-23, doi:10.1042/bse0470001 (2010).

135 Chaban, Y., Boekema, E. J. & Dudkina, N. V. Structures of mitochondrial oxidative phosphorylation supercomplexes and mechanisms for their stabilisation. *Biochimica et biophysica acta* **1837**, 418-426, doi:10.1016/j.bbabio.2013.10.004 (2014).

136 Turrens, J. F. Mitochondrial formation of reactive oxygen species. *The Journal of physiology* **552**, 335-344, doi:10.1113/jphysiol.2003.049478 (2003).

137 Li, B. *et al.* Inhibition of complex I regulates the mitochondrial permeability transition through a phosphate-sensitive inhibitory site masked by cyclophilin D. *Biochimica et biophysica acta* **1817**, 1628-1634, doi:10.1016/j.bbabio.2012.05.011 (2012).

138 Chen, Y. R., Chen, C. L., Yeh, A., Liu, X. & Zweier, J. L. Direct and indirect roles of cytochrome b in the mediation of superoxide generation and NO catabolism by mitochondrial succinate-cytochrome c reductase. *The Journal of biological chemistry* **281**, 13159-13168, doi:10.1074/jbc.M513627200 (2006).

139 Chen, Y. R. & Zweier, J. L. Cardiac mitochondria and reactive oxygen species generation. *Circulation research* **114**, 524-537, doi:10.1161/CIRCRESAHA.114.300559 (2014).

140 Kussmaul, L. & Hirst, J. The mechanism of superoxide production by NADH:ubiquinone oxidoreductase (complex I) from bovine heart mitochondria. *Proceedings of the National Academy of Sciences of the United States of America* **103**, 7607-7612, doi:10.1073/pnas.0510977103 (2006).

141 Lambert, A. J. & Brand, M. D. Inhibitors of the quinone-binding site allow rapid superoxide production from mitochondrial NADH:ubiquinone oxidoreductase (complex I). *The Journal of biological chemistry* **279**, 39414-39420, doi:10.1074/jbc.M406576200 (2004).

142 Lambert, A. J. & Brand, M. D. Superoxide production by NADH:ubiquinone oxidoreductase (complex I) depends on the pH gradient across the mitochondrial inner membrane. *The Biochemical journal* **382**, 511-517, doi:10.1042/BJ20040485 (2004).

143 Ohnishi, S. T., Shinzawa-Itoh, K., Ohta, K., Yoshikawa, S. & Ohnishi, T. New insights into the superoxide generation sites in bovine heart NADH-ubiquinone oxidoreductase (Complex I): the significance of protein-associated ubiquinone and the dynamic shifting of generation sites between semiflavin and semiquinone radicals. *Biochimica et biophysica acta* **1797**, 1901-1909, doi:10.1016/j.bbabio.2010.05.012 (2010).

144 Yankovskaya, V. *et al.* Architecture of succinate dehydrogenase and reactive oxygen species generation. *Science* **299**, 700-704, doi:10.1126/science.1079605 (2003).

145 Prabu, S. K. *et al.* Protein kinase A-mediated phosphorylation modulates cytochrome c oxidase function and augments hypoxia and myocardial ischemia-

related injury. *The Journal of biological chemistry* **281**, 2061-2070, doi:10.1074/jbc.M507741200 (2006).

146 Edmondson, D. E., Mattevi, A., Binda, C., Li, M. & Hubalek, F. Structure and mechanism of monoamine oxidase. *Current medicinal chemistry* **11**, 1983-1993 (2004).

147 Akhmedov, A. T., Rybin, V. & Marin-Garcia, J. Mitochondrial oxidative metabolism and uncoupling proteins in the failing heart. *Heart failure reviews* **20**, 227-249, doi:10.1007/s10741-014-9457-4 (2015).

148 Kowaltowski, A. J., de Souza-Pinto, N. C., Castilho, R. F. & Vercesi, A. E. Mitochondria and reactive oxygen species. *Free radical biology & medicine* **47**, 333-343, doi:10.1016/j.freeradbiomed.2009.05.004 (2009).

149 Lustgarten, M. S. *et al.* Complex I generated, mitochondrial matrix-directed superoxide is released from the mitochondria through voltage dependent anion channels. *Biochemical and biophysical research communications* **422**, 515-521, doi:10.1016/j.bbrc.2012.05.055 (2012).

150 Bienert, G. P., Schjoerring, J. K. & Jahn, T. P. Membrane transport of hydrogen peroxide. *Biochimica et biophysica acta* **1758**, 994-1003, doi:10.1016/j.bbamem.2006.02.015 (2006).

151 Radi, R. *et al.* Detection of catalase in rat heart mitochondria. *The Journal of biological chemistry* **266**, 22028-22034 (1991).

152 Lu, L. Y., Ou, N. & Lu, Q. B. Antioxidant induces DNA damage, cell death and mutagenicity in human lung and skin normal cells. *Scientific reports* **3**, 3169, doi:10.1038/srep03169 (2013).

153 Groeger, G., Quiney, C. & Cotter, T. G. Hydrogen peroxide as a cell-survival signaling molecule. *Antioxidants & redox signaling* **11**, 2655-2671, doi:10.1089/ARS.2009.2728 (2009).

154 Mailloux, R. J. & Harper, M. E. Uncoupling proteins and the control of mitochondrial reactive oxygen species production. *Free radical biology & medicine* **51**, 1106-1115, doi:10.1016/j.freeradbiomed.2011.06.022 (2011).

155 Circu, M. L. & Aw, T. Y. Reactive oxygen species, cellular redox systems, and apoptosis. *Free radical biology & medicine* **48**, 749-762, doi:10.1016/j.freeradbiomed.2009.12.022 (2010).

156 Ricci, C. *et al.* Mitochondrial DNA damage triggers mitochondrial-superoxide generation and apoptosis. *American journal of physiology. Cell physiology* **294**, C413-422, doi:10.1152/ajpcell.00362.2007 (2008).

157 Kagan, V. E. *et al.* Cytochrome c acts as a cardiolipin oxygenase required for release of proapoptotic factors. *Nature chemical biology* **1**, 223-232, doi:10.1038/nchembio727 (2005).

158 Lin, Y. *et al.* Tumor necrosis factor-induced nonapoptotic cell death requires receptor-interacting protein-mediated cellular reactive oxygen species accumulation. *The Journal of biological chemistry* **279**, 10822-10828, doi:10.1074/jbc.M313141200 (2004).

159 Vanlangenakker, N. *et al.* cIAP1 and TAK1 protect cells from TNF-induced necrosis by preventing RIP1/RIP3-dependent reactive oxygen species production. *Cell death and differentiation* **18**, 656-665, doi:10.1038/cdd.2010.138 (2011).

160 Ardestani, S., Deskins, D. L. & Young, P. P. Membrane TNF-alpha-activated programmed necrosis is mediated by Ceramide-induced reactive oxygen species. *Journal of molecular signaling* **8**, 12, doi:10.1186/1750-2187-8-12 (2013).

161 Goossens, V., Stange, G., Moens, K., Pipeleers, D. & Grooten, J. Regulation of tumor necrosis factor-induced, mitochondria- and reactive oxygen species-dependent cell death by the electron flux through the electron transport chain complex I. *Antioxidants & redox signaling* **1**, 285-295 (1999).

162 Schulze-Osthoff, K. *et al.* Cytotoxic activity of tumor necrosis factor is mediated by early damage of mitochondrial functions. Evidence for the involvement of mitochondrial radical generation. *The Journal of biological chemistry* **267**, 5317-5323 (1992).

163 Davis, C. W. *et al.* Nitration of the mitochondrial complex I subunit NDUFB8 elicits RIP1- and RIP3-mediated necrosis. *Free radical biology & medicine* **48**, 306-317, doi:10.1016/j.freeradbiomed.2009.11.001 (2010).

164 Temkin, V., Huang, Q., Liu, H., Osada, H. & Pope, R. M. Inhibition of ADP/ATP exchange in receptor-interacting protein-mediated necrosis. *Molecular and cellular biology* **26**, 2215-2225, doi:10.1128/MCB.26.6.2215-2225.2006 (2006).

165 Kushnareva, Y. E. & Sokolove, P. M. Prooxidants open both the mitochondrial permeability transition pore and a low-conductance channel in the inner mitochondrial membrane. *Archives of biochemistry and biophysics* **376**, 377-388, doi:10.1006/abbi.2000.1730 (2000).

166 Lotscher, H. R., Winterhalter, K. H., Carafoli, E. & Richter, C. Hydroperoxide-induced loss of pyridine nucleotides and release of calcium from rat liver mitochondria. *The Journal of biological chemistry* **255**, 9325-9330 (1980).

167 Thygesen, K. *et al.* Third universal definition of myocardial infarction. *Global heart* **7**, 275-295, doi:10.1016/j.gheart.2012.08.001 (2012).

168 Tian, X. F., Cui, M. X., Yang, S. W., Zhou, Y. J. & Hu, D. Y. Cell death, dysglycemia and myocardial infarction. *Biomedical reports* **1**, 341-346, doi:10.3892/br.2013.67 (2013).

169 Heusch, G. *et al.* Cardiovascular remodelling in coronary artery disease and heart failure. *Lancet* **383**, 1933-1943, doi:10.1016/S0140-6736(14)60107-0 (2014).

170 Frangogiannis, N. G. The inflammatory response in myocardial injury, repair, and remodelling. *Nature reviews. Cardiology* **11**, 255-265, doi:10.1038/nrcardio.2014.28 (2014).

171 Bajaj, A., Sethi, A., Rathor, P., Suppogu, N. & Sethi, A. Acute Complications of Myocardial Infarction in the Current Era: Diagnosis and Management. *Journal of investigative medicine : the official publication of the American Federation for Clinical Research* **63**, 844-855, doi:10.1097/JIM.0000000000000232 (2015).

172 Gao, X. M., White, D. A., Dart, A. M. & Du, X. J. Post-infarct cardiac rupture: recent insights on pathogenesis and therapeutic interventions. *Pharmacology & therapeutics* **134**, 156-179, doi:10.1016/j.pharmthera.2011.12.010 (2012).

173 Gao, X. M., Xu, Q., Kiriazis, H., Dart, A. M. & Du, X. J. Mouse model of post-infarct ventricular rupture: time course, strain- and gender-dependency, tensile

strength, and histopathology. *Cardiovascular research* **65**, 469-477, doi:10.1016/j.cardiores.2004.10.014 (2005).

174 Unsold, B. *et al.* Melusin protects from cardiac rupture and improves functional remodelling after myocardial infarction. *Cardiovascular research* **101**, 97-107, doi:10.1093/cvr/cvt235 (2014).

175 Ertl, G. & Frantz, S. Healing after myocardial infarction. *Cardiovascular research* **66**, 22-32, doi:10.1016/j.cardiores.2005.01.011 (2005).

176 Frantz, S., Bauersachs, J. & Ertl, G. Post-infarct remodelling: contribution of wound healing and inflammation. *Cardiovascular research* **81**, 474-481, doi:10.1093/cvr/cvn292 (2009).

177 Willis, M. S., Homeister, J. W. & Stone, J. R. *Cellular and molecular pathobiology of cardiovascular disease*.

178 Vinten-Johansen, J. Involvement of neutrophils in the pathogenesis of lethal myocardial reperfusion injury. *Cardiovascular research* **61**, 481-497, doi:10.1016/j.cardiores.2003.10.011 (2004).

179 Litt, M. R., Jeremy, R. W., Weisman, H. F., Winkelstein, J. A. & Becker, L. C. Neutrophil depletion limited to reperfusion reduces myocardial infarct size after 90 minutes of ischemia. Evidence for neutrophil-mediated reperfusion injury. *Circulation* **80**, 1816-1827 (1989).

180 Fang, L. *et al.* Differences in inflammation, MMP activation and collagen damage account for gender difference in murine cardiac rupture following myocardial infarction. *Journal of molecular and cellular cardiology* **43**, 535-544, doi:10.1016/j.yjmcc.2007.06.011 (2007).

181 Lorchner, H. *et al.* Myocardial healing requires Reg3beta-dependent accumulation of macrophages in the ischemic heart. *Nature medicine* **21**, 353-362, doi:10.1038/nm.3816 (2015).

182 Willems, I. E., Havenith, M. G., De Mey, J. G. & Daemen, M. J. The alpha-smooth muscle actin-positive cells in healing human myocardial scars. *The American journal of pathology* **145**, 868-875 (1994).

183 Whittaker, P., Boughner, D. R. & Kloner, R. A. Role of collagen in acute myocardial infarct expansion. *Circulation* **84**, 2123-2134 (1991).

184 Hofmann, U. *et al.* Activation of CD4+ T lymphocytes improves wound healing and survival after experimental myocardial infarction in mice. *Circulation* **125**, 1652-1663, doi:10.1161/CIRCULATIONAHA.111.044164 (2012).

185 Baysa, A. *et al.* The p66ShcA adaptor protein regulates healing after myocardial infarction. *Basic research in cardiology* **110**, 13, doi:10.1007/s00395-015-0470-0 (2015).

186 Sane, D. C., Mozingo, W. S. & Becker, R. C. Cardiac rupture after myocardial infarction: new insights from murine models. *Cardiology in review* **17**, 293-299, doi:10.1097/CRD.0b013e3181bf4ab4 (2009).

187 Matsusaka, H. *et al.* Targeted deletion of p53 prevents cardiac rupture after myocardial infarction in mice. *Cardiovascular research* **70**, 457-465, doi:10.1016/j.cardiores.2006.02.001 (2006).

188 Wolf, Ashley R. & Mootha, Vamsi K. Functional Genomic Analysis of Human Mitochondrial RNA Processing. *Cell reports* **7**, 918-931, doi:http://dx.doi.org/10.1016/j.celrep.2014.03.035 (2014).

189 Ahn, K. J., Lee, H. S., Bai, S. K. & Song, C. W. Enhancement of radiation effect using beta-lapachone and underlying mechanism. *Radiation oncology journal* **31**, 57-65, doi:10.3857/roj.2013.31.2.57 (2013).

190 Bey, E. A. *et al.* An NQO1- and PARP-1-mediated cell death pathway induced in non-small-cell lung cancer cells by beta-lapachone. *Proceedings of the National Academy of Sciences of the United States of America* **104**, 11832-11837, doi:10.1073/pnas.0702176104 (2007).

191 Barbour, J. A. & Turner, N. Mitochondrial stress signaling promotes cellular adaptations. *International journal of cell biology* **2014**, 156020, doi:10.1155/2014/156020 (2014).

192 Christians, E. S. & Benjamin, I. J. Proteostasis and REDOX state in the heart. *American journal of physiology. Heart and circulatory physiology* **302**, H24-37, doi:10.1152/ajpheart.00903.2011 (2012).

193 Hom, J. & Sheu, S. S. Morphological dynamics of mitochondria--a special emphasis on cardiac muscle cells. *Journal of molecular and cellular cardiology* **46**, 811-820, doi:10.1016/j.yjmcc.2009.02.023 (2009).

194 Dorn, G. W., 2nd. Mitochondrial dynamics in heart disease. *Biochimica et biophysica acta* **1833**, 233-241, doi:10.1016/j.bbamcr.2012.03.008 (2013).

195 Kim, I. & Lemasters, J. J. Mitochondrial degradation by autophagy (mitophagy) in GFP-LC3 transgenic hepatocytes during nutrient deprivation. *American journal of physiology. Cell physiology* **300**, C308-317, doi:10.1152/ajpcell.00056.2010 (2011).

196 Schramm, C., Fine, D. M., Edwards, M. A., Reeb, A. N. & Krenz, M. The PTPN11 loss-of-function mutation Q510E-Shp2 causes hypertrophic cardiomyopathy by dysregulating mTOR signaling. *American journal of physiology. Heart and circulatory physiology* **302**, H231-243, doi:10.1152/ajpheart.00665.2011 (2012).

197 McCommis, K. S., Douglas, D. L., Krenz, M. & Baines, C. P. Cardiac-specific hexokinase 2 overexpression attenuates hypertrophy by increasing pentose phosphate pathway flux. *Journal of the American Heart Association* **2**, e000355, doi:10.1161/JAHA.113.000355 (2013).

198 McGee, A. M. & Baines, C. P. Complement 1q-binding protein inhibits the mitochondrial permeability transition pore and protects against oxidative stress-induced death. *The Biochemical journal* **433**, 119-125, doi:10.1042/BJ20101431 (2011).

199 Gautier, C. A. *et al.* Regulation of mitochondrial permeability transition pore by PINK1. *Molecular neurodegeneration* **7**, 22, doi:10.1186/1750-1326-7-22 (2012).

200 Giaime, E., Yamaguchi, H., Gautier, C. A., Kitada, T. & Shen, J. Loss of DJ-1 does not affect mitochondrial respiration but increases ROS production and mitochondrial permeability transition pore opening. *PloS one* **7**, e40501, doi:10.1371/journal.pone.0040501 (2012).

201 Mozaffarian, D. *et al.* Heart Disease and Stroke Statistics-2016 Update: A Report From the American Heart Association. *Circulation* **133**, e38-e360, doi:10.1161/CIR.0000000000000350 (2016).

202 Ide, T. *et al.* Mitochondrial DNA damage and dysfunction associated with oxidative stress in failing hearts after myocardial infarction. *Circulation research* **88**, 529-535 (2001).

203 Jugdutt, B. I. & Dhalla, N. S. *Cardiac remodeling : molecular mechanisms*.

204 Hill, M. F. & Singal, P. K. Antioxidant and oxidative stress changes during heart failure subsequent to myocardial infarction in rats. *The American journal of pathology* **148**, 291-300 (1996).

205 Lu, L., Quinn, M. T. & Sun, Y. Oxidative stress in the infarcted heart: role of de novo angiotensin II production. *Biochemical and biophysical research communications* **325**, 943-951, doi:10.1016/j.bbrc.2004.10.106 (2004).

206 Li, P. F., Dietz, R. & von Harsdorf, R. Superoxide induces apoptosis in cardiomyocytes, but proliferation and expression of transforming growth factor-beta1 in cardiac fibroblasts. *FEBS letters* **448**, 206-210 (1999).

207 Sia, Y. T. *et al.* Beneficial effects of long-term use of the antioxidant probucol in heart failure in the rat. *Circulation* **105**, 2549-2555 (2002).

208 Sanbe, A. *et al.* Reengineering inducible cardiac-specific transgenesis with an attenuated myosin heavy chain promoter. *Circulation research* **92**, 609-616, doi:10.1161/01.RES.0000065442.64694.9F (2003).

209 Krenz, M. & Robbins, J. Impact of beta-myosin heavy chain expression on cardiac function during stress. *Journal of the American College of Cardiology* **44**, 2390-2397, doi:10.1016/j.jacc.2004.09.044 (2004).

210 Chiong, M. *et al.* Cardiomyocyte death: mechanisms and translational implications. *Cell death & disease* **2**, e244, doi:10.1038/cddis.2011.130 (2011).

211 Gao, X. M. *et al.* Infarct size and post-infarct inflammation determine the risk of cardiac rupture in mice. *International journal of cardiology* **143**, 20-28, doi:10.1016/j.ijcard.2009.01.019 (2010).

212 van den Borne, S. W. *et al.* Mouse strain determines the outcome of wound healing after myocardial infarction. *Cardiovascular research* **84**, 273-282, doi:10.1093/cvr/cvp207 (2009).

213 Frangogiannis, N. G. Emerging roles for macrophages in cardiac injury: cytoprotection, repair, and regeneration. *The Journal of clinical investigation* **125**, 2927-2930, doi:10.1172/JCI83191 (2015).

214 Fujiu, K., Wang, J. & Nagai, R. Cardioprotective function of cardiac macrophages. *Cardiovascular research* **102**, 232-239, doi:10.1093/cvr/cvu059 (2014).

215 Ortega-Gomez, A., Perretti, M. & Soehnlein, O. Resolution of inflammation: an integrated view. *EMBO molecular medicine* **5**, 661-674, doi:10.1002/emmm.201202382 (2013).

216 Chandrashekhar, Y., Sen, S., Anway, R., Shuros, A. & Anand, I. Long-term caspase inhibition ameliorates apoptosis, reduces myocardial troponin-I cleavage, protects left ventricular function, and attenuates remodeling in rats with myocardial infarction. *Journal of the American College of Cardiology* **43**, 295-301 (2004).

217 McCurdy, S. M. *et al.* SPARC mediates early extracellular matrix remodeling following myocardial infarction. *American journal of physiology. Heart and circulatory physiology* **301**, H497-505, doi:10.1152/ajpheart.01070.2010 (2011).

218 Oka, T. *et al.* Genetic manipulation of periostin expression reveals a role in cardiac hypertrophy and ventricular remodeling. *Circulation research* **101**, 313-321, doi:10.1161/CIRCRESAHA.107.149047 (2007).

219 Shimazaki, M. *et al.* Periostin is essential for cardiac healing after acute myocardial infarction. *The Journal of experimental medicine* **205**, 295-303, doi:10.1084/jem.20071297 (2008).

220 Calvo, S. E., Clauser, K. R. & Mootha, V. K. MitoCarta2.0: an updated inventory of mammalian mitochondrial proteins. *Nucleic acids research* **44**, D1251-1257, doi:10.1093/nar/gkv1003 (2016).

221 Pagliarini, D. J. *et al.* A mitochondrial protein compendium elucidates complex I disease biology. *Cell* **134**, 112-123, doi:10.1016/j.cell.2008.06.016 (2008).

222 Shinde, A. V. & Frangogiannis, N. G. Mediators secreted by myeloid cells may protect and repair the infarcted myocardium. *Circulation research* **117**, 10-12, doi:10.1161/CIRCRESAHA.115.306283 (2015).

223 Marshall, K. D., Edwards, M. A., Krenz, M., Davis, J. W. & Baines, C. P. Proteomic mapping of proteins released during necrosis and apoptosis from cultured neonatal cardiac myocytes. *American journal of physiology. Cell physiology* **306**, C639-647, doi:10.1152/ajpcell.00167.2013 (2014).

224 Douglas, D. L. & Baines, C. P. PARP1-mediated necrosis is dependent on parallel JNK and Ca(2)(+)/calpain pathways. *Journal of cell science* **127**, 4134-4145, doi:10.1242/jcs.128009 (2014).

225 Kurian, G. A. & Pemaih, B. Standardization of in vitro Cell-based Model for Renal Ischemia and Reperfusion Injury. *Indian journal of pharmaceutical sciences* **76**, 348-353 (2014).

226 Patten, R. D. *et al.* Ventricular remodeling in a mouse model of myocardial infarction. *The American journal of physiology* **274**, H1812-1820 (1998).

227 Lopez-Sendon, J. *et al.* Factors related to heart rupture in acute coronary syndromes in the Global Registry of Acute Coronary Events. *European heart journal* **31**, 1449-1456, doi:10.1093/eurheartj/ehq061 (2010).

228 Cordwell, S. J. *et al.* Release of tissue-specific proteins into coronary perfusate as a model for biomarker discovery in myocardial ischemia/reperfusion injury. *Journal of proteome research* **11**, 2114-2126, doi:10.1021/pr2006928 (2012).

229 Jacquet, S. *et al.* Identification of cardiac myosin-binding protein C as a candidate biomarker of myocardial infarction by proteomics analysis. *Molecular & cellular proteomics : MCP* **8**, 2687-2699, doi:10.1074/mcp.M900176-MCP200 (2009).

230 Rossello, X., Hall, A. R., Bell, R. M. & Yellon, D. M. Characterization of the Langendorff Perfused Isolated Mouse Heart Model of Global Ischemia-Reperfusion Injury: Impact of Ischemia and Reperfusion Length on Infarct Size and LDH Release. *Journal of cardiovascular pharmacology and therapeutics*, doi:10.1177/1074248415604462 (2015).

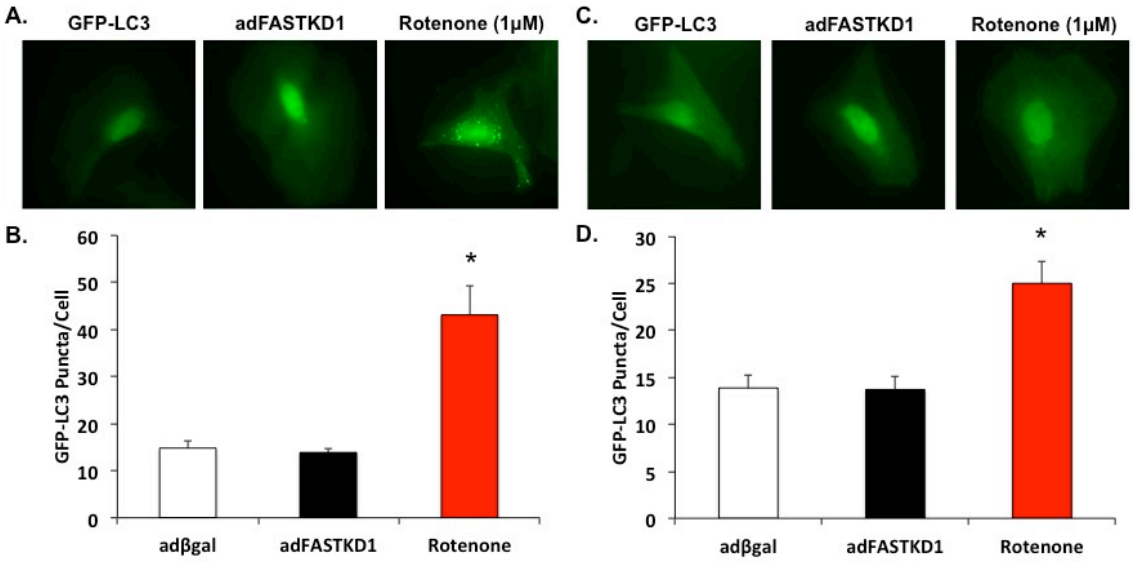

Figure 17. FASTKD1 overvexpression does not induce autophagy in MEFs or NRVMs. (A) Representative images of MEFs co-infected with adenovirus expressing βGal and LC3-GFP or FASTKD1-Myc and LC3-GFP or infected with βGal and treated with rotenone to induce autophagy. (B) GFP-LC3 puncta per cell were counted in MEFs. (C) Representative images of NRVMs co-infected with adenovirus expressing βGal and LC3-GFP or FASTKD1-Myc and LC3-GFP or infected with βGal and treated with rotenone to induce autophagy. (D) GFP-LC3 puncta per cell were counted in NRVMs. Error bars indicate s.e.m. with **P*<0.05 vs. βGal.

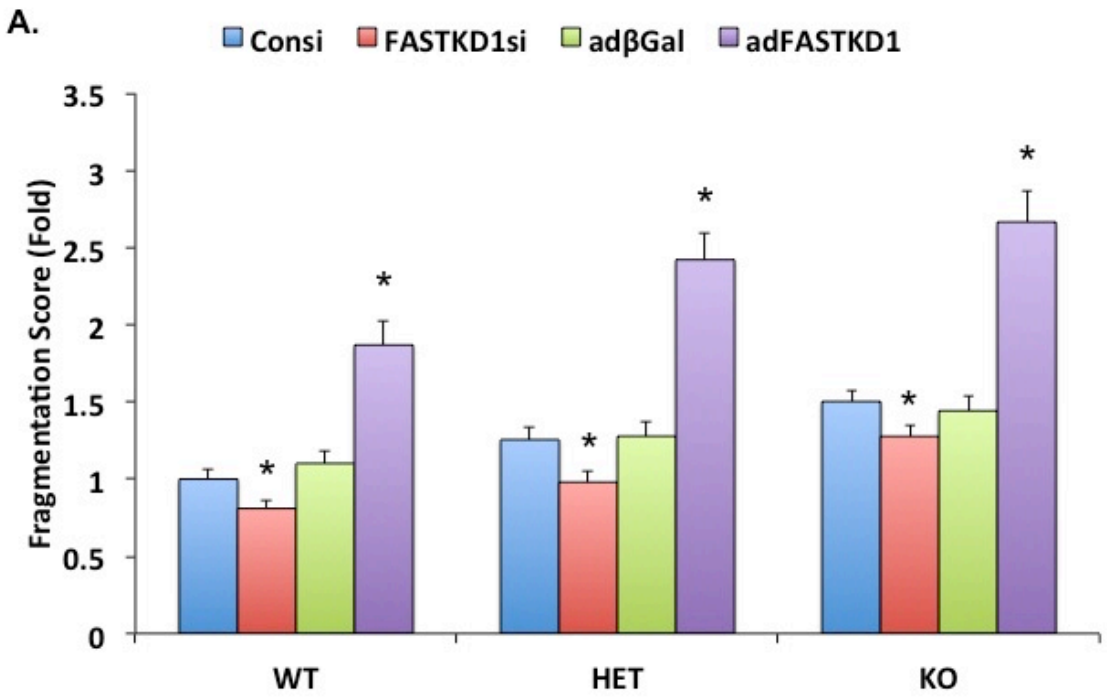

Figure 18. FASTKD1 modulates mitochondrial morphology independently of CypD in MEFs. (A) Quantification of mitochondrial fragmentation scores from WT, *Ppif*$^{/+}$ and *Ppif*$^{/-}$ MEFs either infected with βGal or FASTKD1-Myc adenoviruses or transfected with CONsi or FASTKD1si. Error bars indicate s.e.m. with **P*<0.05 vs. Consi or βGal.

Vita

Kurt Daniel Marshall was born in Austin, Texas on April 13th, 1986 to Bruce and Robin Marshall. He was raised in Louisville, Colorado. Kurt earned his Bachelor of Science degree in Biology from the University of Virginia and his Master of Science degree in Integrative Physiology from the University of Colorado at Boulder. Before relocating to Columbia, Missouri to start work on his PhD, Kurt worked in the biotech industry. After entering the PhD program in Biomedical Sciences in August 2011, Kurt joined the lab of Dr. Christopher Baines in April 2012 where he performed the studies leading to his dissertation. Kurt currently resides in Columbia, Missouri with his wife Jennifer Marshall and their three cats.